

# THE INTEGRATION OF DISTRIBUTED ENERGY RESOURCES INTO ELECTRIC POWER SYSTEMS

A THESIS SUBMITTED TO



FOR THE DEGREE OF  
DOCTOR OF PHILOSOPHY

MOHAMMED JASIM MOHAMMED AL ESSA

SCHOOL OF ENGINEERING  
CARDIFF UNIVERSITY

2017

## Contents

<b>Contents</b> .....	i
<b>List of Tables</b> .....	iv
<b>List of Figures</b> .....	v
<b>Abstract</b> .....	ix
<b>Declaration</b> .....	x
<b>Copyright</b> .....	xi
<b>Acknowledgements</b> .....	xii
<b>List of Publications</b> .....	xiii
<b>List of Abbreviations</b> .....	xiv
<b>1. Introduction</b> .....	1
1.1 Thesis Objectives .....	2
1.2 Thesis Contributions .....	2
1.3 Thesis Structure .....	3
<b>2. A Review of Distributed Energy Recourses in Power Systems</b> .....	5
2.1 Introduction .....	5
2.2 Impacts of Distributed Energy Resources on Future Demand .....	6
2.2.1 Thesis Contribution to Estimate Future Demand with DER Units .....	7
2.3 Impacts of Distributed Energy Resources on Distribution Networks .....	8
2.3.1 Deterministic Studies .....	8
2.3.2 Stochastic Studies .....	10
2.3.3 Real-World Studies .....	11
2.3.4 Thesis Contribution to Study DER Impact on Distribution Networks .....	12
2.4 Coordination Algorithms of EV Charging Loads .....	13
2.4.1 Thesis Contribution to Coordinate EV Charging Loads .....	16
2.5 Demand Side Management Schemes .....	16
2.5.1 Demand Management Schemes in Smart Grids .....	18
2.5.2 Centralized Demand Management Schemes .....	18
2.5.3 Decentralized Demand Management Schemes .....	19
2.5.4 Thesis Contribution to Implement Demand Management Scheme .....	20
2.6 Conclusions .....	21

<b>3. Impacts of Distributed Energy Resources on Future Demand</b> .....	22
3.1 Introduction .....	22
3.2 Methodology .....	22
3.2.1 Historic Demand Measurements .....	23
3.2.2 Synthesized Power of Distributed Energy Resources .....	25
3.3 Demand Predictions with Distributed Energy Resources .....	29
3.4 Simulation Results.....	31
3.5 Conclusions .....	35
<b>4. Impacts of Distributed Energy Resources on Distribution Networks</b> .....	37
4.1 Introduction .....	37
4.2 Methodology of Deterministic Studies.....	37
4.2.1 The Network under Deterministic Studies.....	38
4.2.2 Deterministic Case Studies .....	40
4.3 Simulation Results of Deterministic Studies.....	41
4.4 Methodology of Stochastic Studies .....	44
4.4.1 The Network under Stochastic Studies .....	44
4.4.2 Individual Loads of Residential Customers .....	45
4.4.3 Individual Loads of Electric Vehicles.....	47
4.4.4 Modelled Loads of Heat Pumps.....	48
4.4.5 Modelled Power of Photovoltaic Arrays.....	49
4.4.6 Stochastic Case Studies.....	50
4.5 Simulation Results of Stochastic Studies .....	51
4.6 Conclusions .....	55
<b>5. Centralized Load Allocation of Electric Vehicles in Distribution Networks.</b> 56	
5.1 Introduction .....	56
5.2 Methodology .....	56
5.2.1 The Proposed Objective Function.....	57
5.2.2 The Centralized Control Algorithm .....	59
5.3 Non-iterative Unbalanced Power Flow Calculations .....	60
5.4 Configurations of the System under Study.....	64
5.4.1 The Network under Study .....	64
5.4.2 Synthesizing loads of Residential Customers .....	66
5.4.3 Synthesizing Loads of Electric Vehicles.....	67

5.5	Simulation Results.....	69
5.5.1	Voltage Magnitudes and Voltage Unbalances .....	69
5.5.2	Limitations of Network Components.....	72
5.6	Conclusions .....	76
<b>6.</b>	<b>Decentralized Load Adjustment of Electric Vehicles and Heat Pumps .....</b>	<b>77</b>
6.1	Introduction .....	77
6.2	Methodology .....	77
6.2.1	Mathematical Model of Electric Vehicles.....	79
6.2.2	Mathematical Model of Heat Pumps.....	79
6.2.3	Synthesized Time-varying Tariffs.....	81
6.2.4	Objective Functions .....	82
6.3	The Network under Study .....	86
6.4	Simulation Results.....	90
6.5	Conclusions .....	98
<b>7.</b>	<b>Conclusions and Recommendations for Further Work .....</b>	<b>99</b>
7.1	Conclusions .....	99
7.1.1	Impacts of Distributed Energy Resources on Future Demand.....	99
7.1.2	Impacts of Distributed Energy Resources on Distribution Networks	100
7.1.3	Centralized Load Allocation of Electric Vehicles in Distribution Networks.....	101
7.1.4	Decentralized Load Adjustment of Electric Vehicles and Heat Pumps .....	102
7.2	Recommendations for Further Work.....	103
7.2.1	Demand Predictions .....	103
7.2.2	Impact Assessments .....	104
7.2.3	Centralized Controller.....	104
7.2.4	Decentralized Controller .....	104
	<b>References .....</b>	<b>105</b>
	<b>Appendix A: The Top-Level Code of Future Demand Predictions.....</b>	<b>117</b>
	<b>Appendix B: The Model of the UK Generic Distribution Network .....</b>	<b>118</b>
	<b>Appendix C: The Top-Level Code of Stochastic Studies.....</b>	<b>119</b>
	<b>Appendix D: The Top-Level Codes of the Centralized Controller .....</b>	<b>120</b>
	<b>Appendix E: The Top-Level Code of the Decentralized Controller.....</b>	<b>122</b>

## List of Tables

Table 2.1: A prediction of EV numbers across different countries by 2020 (UK figure from [6], others from [10]).	6
Table 2.2: An executive summary of a number of reviewed publications.	15
Table 2.3: Similarities and differences between DSM and DR strategies based on a number of reviewed publications.	17
Table 3.1: The maximum values of the UK total demand and other DER power over the forthcoming years using “Consumer Power” scenario by National Grid [20].	29
Table 3.2: Maximum and minimum values of the UK residential demand over the next two decades based on the proposed prediction calculations.	35
Table 4.1: The considered deterministic case studies.	41
Table 6.1: The numerical values of considered HP parameters.	81
Table D.1: Answer report of centralized controller using generalized reduced gradient.	121

## List of Figures

Figure 1.1: The framework of the thesis. ....	4
Figure 3.1: The workflow of the proposed long-term prediction tool. ....	23
Figure 3.2: The percentages of the UK residential demand contribution relative to the UK demand over a day of half-hourly time steps, as reported by National Grid [20]. .....	24
Figure 3.3: The UK total demand and the UK residential demand over a day of half-hourly time steps in 2014 for (a) January, (b) April, (c) July, and (d) October (data from [114])......	24
Figure 3.4: The UK total demand and the UK residential demand over the year of 2014 at half-hourly time steps (data from [114])......	25
Figure 3.5: Seasonal mean values of EV charging loads (data from [115]). ....	26
Figure 3.6: Seasonal mean values of PV power generation (data from [115]). ....	26
Figure 3.7: (a) Mean values of 133 EV loads (January-2014) based on CLNR trials. (b) Disaggregating. (c) Filtering. (d) Comparing (i.e. a diagnostic correlation).....	27
Figure 3.8: The synthesized mean values of power over a half-hourly year of (a) EV charging loads and (b) PV generation. ....	28
Figure 3.9: The flowchart of the proposed steps to predict the UK residential demand over the next two decades. ....	30
Figure 3.10: A prediction of the UK residential demand with residential EVs, HPs, and PV arrays over a year of half-hourly time steps in 2035 for each scenario. (a) “Gone Green”. (b) “Slow Progression”. (c) “No Progression”. (d) “Consumer Power”. ....	31
Figure 3.11: The UK seasonal residential demand with residential EVs, HPs, and PV arrays over a day of half-hourly time steps in 2035 of (a) January, (b) April, (c) July, and (d) October. ....	32
Figure 3.12: A prediction range of the UK residential demand over the next two decades using “Gone Green” scenario. ....	33
Figure 3.13: A prediction range of the UK residential demand over the next two decades using “No Progression” scenario. ....	33
Figure 4.1: The workflow of deterministic case studies. ....	38
Figure 4.2: The schematic diagram of the network under deterministic studies with EVs. ....	38

Figure 4.3: Mean values of active power of 8,000 residential customers and 133 EVs (power data from [115]).	39
Figure 4.4: The aggregated loads of residential customers and EVs over a day of half-hourly time steps at the distribution transformer of the UKGDN for each case study.	42
Figure 4.5: RMS phase current flows of the cable segment between node 0 and node 1 for each case study over a day of half-hourly steps (a) Case-1, (b) Case-2, (c) Case-3, and (d) Case-4.	42
Figure 4.6: RMS voltage magnitudes over a day of half-hourly time steps at node 4 for each case study (a) Case-1, (b) Case-2, (c) Case-3, and (d) Case-4.	43
Figure 4.7: The percentages of voltage unbalance factors over a day of half-hourly time steps, as recorded at node 4 for each case study.	43
Figure 4.8: The workflow of stochastic case studies.	44
Figure 4.9: The network under stochastic studies (adapted from [120]).	45
Figure 4.10: The flowchart of stochastically generating residential load profiles.	46
Figure 4.11: Daily demand means of stochastically generated residential loads relative to the actual residential demand mean (real).	46
Figure 4.12: The mean values of synthesized EV charging loads of 135 EVs.	48
Figure 4.13: HP loads over 135 days of minute-by-minute time steps.	49
Figure 4.14: PV generations over 135 days of minute-by-minute time steps.	50
Figure 4.15: In Case 1, histograms of the network under study. (a) Voltage magnitudes. (b) Voltage unbalance factors. (c) Transformer’s loading. (d) Current flow through cables.	52
Figure 4.16: In Case 2, histograms of the network under study. (a) Voltage magnitudes. (b) Voltage unbalance factors. (c) Transformer’s loading. (d) Current flow through cables.	52
Figure 4.17: In Case 3, histograms of the network under study. (a) Voltage magnitudes. (b) Voltage unbalance factors. (c) Transformer’s loading. (d) Current flow through cables.	53
Figure 4.18: In Case 4, histograms of the network under study. (a) Voltage magnitudes. (b) Voltage unbalance factors. (c) Transformer’s loading. (d) Current flow through cables.	54

Figure 4.19: In Case 5, histograms of the network under study. (a) Voltage magnitudes. (b) Voltage unbalance factors. (c) Transformer’s loading. (d) Current flow through cables.....	54
Figure 5.1: The workflow of re-allocating EV charging loads.....	57
Figure 5.2: The flowchart of the centralized control algorithm.....	60
Figure 5.3: The proposed architecture of the centralized controller.....	65
Figure 5.4: Profiles of, (a) the aggregated load of 384 customers for each low voltage (LV) transformer, (b) the daily mean of real and generated loads.....	66
Figure 5.5: The daily mean profiles of the real/synthesized electric vehicle (EV) charging loads.....	68
Figure 5.6: The pattern of the synthesized 384 EV charging loads during a day.....	68
Figure 5.7: UKGDN daily profiles of Scenario I with (a) RMS voltages at each node of the MV feeder; (b) voltage unbalance at each node of the MV feeder.....	70
Figure 5.8: UKGDN daily profiles of Scenario I with (a) phase voltages at node 18; (b) voltage unbalance at node 18.....	71
Figure 5.9: UKGDN daily profiles of Scenario II with (a) phase voltage at node 18; (b) voltage unbalance at node 18.....	72
Figure 5.10: UKGDN daily load profiles at the main substations (the MV transformers) for Scenario I and II, respectively.....	73
Figure 5.11: Scenario I UKGDN daily profiles (a) phase currents of the underground cable between nodes 17 and 18; (b) loading power of the transformer T8.....	74
Figure 5.12: Scenario II UKGDN daily profiles (a) phase currents of the underground cable between node 17 and node 18; (b) loading power of the transformer T8.....	75
Figure 6.1: The workflow of the decentralized control algorithm of EVs and HPs.....	78
Figure 6.2: The proposed steps of the decentralized control algorithm.....	85
Figure 6.3: The real LV distribution network under study (adapted from [120], [140]). The thicknesses of network feeders and service cables are not to scale.....	86
Figure 6.4: (a) Daily 82 HP heating demands. (b) Daily CoP values of these 82 HPs.....	87
Figure 6.5: (a) Daily indoor temperatures of 82 HP houses and their histogram. (b) A sample of 1 HP house daily heating demand along with its daily CoP value and its daily temperature.....	88
Figure 6.6: (a) Daily 82 EV charging loads. (b) BSoC levels of 82 EVs.....	89
Figure 6.7: A sample of two EV charging loads along with their BSoC levels.....	90

Figure 6.8: Daily 330 RMS voltages at each connection point of the network under study along with their histogram (Case 1). .....	91
Figure 6.9: Heat map of daily 330 RMS current flows through feeder segments across adjacent connection points (Case 1).....	92
Figure 6.10: Daily 330 voltage unbalance factors at each connection point of the network under study along with their histogram (Case 1). .....	92
Figure 6.11: Daily 330 RMS voltages at each connection point of the network under study along with their histogram (Case 2). .....	93
Figure 6.12: Heat map of daily 330 RMS current flows through feeder segments across adjacent connection points (Case 2).....	94
Figure 6.13: Daily 330 voltage unbalance factors at each connection point of the network under study along with their histogram (Case 2). .....	94
Figure 6.14: Optimized 82 EV daily charging loads and their average charging loads (Case 2). .....	95
Figure 6.15: The daily BSoC levels of the optimized 82 EVs (Case 2). .....	95
Figure 6.16: Optimized 82 HP daily heating loads and their average heating demands (Case 2). .....	96
Figure 6.17: The indoor temperatures of 82 HP houses optimized along with their histogram (Case 2). .....	97
Figure 6.18: The electricity bill reduction of EV users in Case 2 relative to Case 1. 97	
Figure 6.19: The electricity bill reduction of HP users in Case 2 relative to Case 1. 98	
Figure B.1: The high level of the UK generic distribution network (UKGDN) model (i.e. low voltage section) using Matlab/Simulink/SimPowerSystem.....	118
Figure B.2: The components of the UKGDN Subsystems. ....	119

## Abstract

Small-scale, residential, and distributed energy resources (DER), which are electric vehicles (EVs), heat pumps (HPs), and photovoltaic (PV) arrays, were studied to evaluate their impact on the UK future residential demand and their impact on UK distribution networks. Centralized and decentralized controllers were planned in order to defer reinforcement, while connecting DER units to distribution networks. The centralized controller allocates EV charging durations considering network constraints. The decentralized controller adjusts EV and HP loads based on consumer satisfaction, network constraints, and electricity prices.

Normal probability distribution and median filter were used to predict aggregated power of EVs, HPs, and PV arrays on a half-hourly basis over a year. Because of an expected surplus of PV power generation, a considerable demand reduction followed by a sharp demand increase will occur with these residential DER units during summer days in 2035.

A low voltage section of test network was used to study the impact of uncontrolled EV charging loads on a three-phase four-wire system. Different combinations of EVs, HPs, and PV arrays were used to investigate their uncertainties in a low voltage section of real network. Real-world trials were used to generate the individual power of residential customers and DER units. Results of unbalanced power flow indicated that network constraints exceeded their limits with a high number of these low carbon technologies.

Using an extended section of the test network, the central controller maintains voltage magnitudes, voltage unbalance factors, and power flows within their limits, by re-allocating EV charging durations accordingly.

The decentralized controller was designed to minimize electricity bills of EV and HP users. This controller adjusts EV and HP loads to maintain consumer satisfaction and network constraints within their specified boundaries. Consumer satisfaction was determined using mathematical models of EV battery state-of-charge levels and the indoor temperatures of HP houses. The decentralized controller was used to connect predicted numbers of EVs and HPs to a real distribution network, while overcoming the need for network reinforcement, third parties (aggregators), and extensive communication systems.

## Declaration

### DECLARATION

This work has not previously been accepted in substance for any degree and is not concurrently submitted in candidature for any degree.

Signed. .... (candidate) Date .....

### STATEMENT 1

This thesis is being submitted in partial fulfilment of the requirements for the degree of PhD.

Signed. .... (candidate) Date .....

### STATEMENT 2

This thesis is the result of my own independent work/investigation, except where otherwise stated. Other sources are acknowledged by explicit references.

Signed. .... (candidate) Date .....

### STATEMENT 3

I hereby give consent for my thesis, if accepted, to be available for photocopying and for inter-library loan, and for the title and summary to be made available to outside organisations.

Signed. .... (candidate) Date .....

## **Copyright**

Copyright in text of this thesis rests with the Author. Copies (by any process) either in full, or of extracts, may be made only in accordance with instructions given by the Author and lodged in the Library of Cardiff University. Details may be obtained from the Librarian. This page must form part of any such copies made. Further copies (by any process) of copies made in accordance with such instructions may not be made without the permission (in writing) of the Author. The ownership of any intellectual property rights which may be described in this thesis is vested with the author, subject to any prior agreement to the contrary, and may not be made available for use by third parties without his written permission, which will prescribe the terms and conditions of any agreement.

## **Acknowledgements**

I would like to gratefully acknowledge the financial support of Ministry of Higher Education and Scientific Research of Iraq, and University of Kufa for my PhD study at Cardiff University.

I would like to express my gratitude to a number of people who provided encouragement during my PhD study.

I would like to thank Dr Liana M. Cipcigan for her advice, guidance, and support. I am grateful for her overall supervision.

I would like to express my thankfulness to Professor Nick Jenkins for his support and guidance throughout my PhD study. I am most grateful for all efforts that he has offered to improve my work. I sincerely thank him for his persistent advice.

I would like to thank my family and friends who helped me selflessly over the time of this study.

## List of Publications

The following papers were published based on a part of the work described in this thesis.

1. Al Essa, M. and Cipcigan, L., “Reallocating charging loads of electric vehicles in distribution networks”, *Appl. Sci.*, 6 (2), 53, <http://dx.doi.org/10.3390/app6020053>, 2016.
2. Al Essa, M. and Cipcigan, L., “Effects of randomly charging electric vehicles on voltage unbalance in micro grids”, in *50th International Universities Power Engineering Conference (UPEC)*, Stoke-on-Trent, UK, 1-4 September 2015, <http://dx.doi.org/10.1109/UPEC.2015.7339906>.
3. Al Essa, M. and Cipcigan, L., “Integration of renewable resources into low voltage grids stochastically”, in *International Energy Conference (ENERGYCON)*, Leuven, Belgium, 4-8 April 2016, <http://dx.doi.org/10.1109/ENERGYCON.2016.7514134>.

The paper below is not included in this project.

4. Shariff, N., Al Essa, M. and Cipcigan, L., “Probabilistic analysis of electric vehicles charging load impact on residential Distributions Networks”, in *International Energy Conference (ENERGYCON)*, Leuven, Belgium, 4-8 April 2016, <http://dx.doi.org/10.1109/ENERGYCON.2016.7513943>.

## List of Abbreviations

AC	Alternating Current
Amp	Ampere
BSoC	Battery State-of-Charge
CBT	Customer Behaviour Trials
CLNR	Customer-Led Network Revolution
CoP	Coefficient of Performance
DC	Direct Current
DER	Distributed Energy Resources
DNO	Distribution Network Operator
DR	Demand Response
DSM	Demand Side Management
DTI	Department of Trade and Industry
ENA	Electricity Network Association
EPRI	Electrical Power Research Institute
ESS	Energy Storage Systems
EVs	Electric Vehicles
GRG	Generalized Reduced Gradient
GW	Giga Watt
HPs	Heat Pumps
ICT	Information and Communication Technology
IEEE	Institute for Electrical and Electronic Engineering
J	Joule
K	Kelvin

kVA	kilo Volt Ampere
kW	kilo Watt
LCL	Low Carbon London
LCNF	Low Carbon Networks Fund
LV	Low Voltage
mCHPs	micro Combined Heat and Power
MCS	Monte Carlo Simulation
MV	Medium Voltage
NP	Non-deterministic Polynomial
NTS	National Travel Survey
Ofgem	Office for Gas and Electricity Market
PHEVs	Plug-in Hybrid Electric Vehicles
pu	Per Unit
PV	Photovoltaic
RES	Renewable Energy Sources
RMS	Root Mean Square
ToU	Time-of-Use
UK	United Kingdom
UKGDN	United Kingdom Generic Distribution Network
V	Volt
VUF	Voltage Unbalance Factor
W	Watt

# CHAPTER 1

## 1. Introduction

As long as many countries use fossil fuels to generate electricity, carbon dioxide emissions will increase. Alternatively, carbon-free distributed energy resources (DER) and renewable energy sources (RES) can be locally used to generate electricity in a clean renewable manner. If high numbers of DER units are connected using a “fit-and-forget” approach, current policies will need to be adjusted [1]. Policymakers and network operators play an essential role in amending their current policies. These amendments will create opportunities and challenges, entering a new era of generating and distributing electricity [2].

According to Ref. [3], DER units refer to distributed generators, energy storage systems, and flexible demands. The Electrical Power Research Institute (EPRI) [4] investigated the impact of DER units on the operation of power systems, considering a cost-effective investment to modernize networks. A successful integration of DER units relies on the existing grids, because the networks can only contain a certain number of DER units without exceeding their limits [4].

Therefore, existing power networks were not designed to accommodate high numbers of DER units. However, network components can only tolerate certain numbers of these low carbon technologies without immediate reinforcement.

This thesis poses the following main questions:

- How the predicted numbers of electric vehicles (EVs), heat pumps (HPs), and photovoltaic (PV) arrays will affect the UK overall residential demand?
- What is the impact of the integration of EVs, HPs, and PV arrays on power distribution networks considering voltage magnitudes, voltage unbalance factors, and other network constraints?
- Is it possible to connect high numbers of EV units to power distribution networks without further network reinforcement?
- How can EV and HP users adjust their demand in a decentralized manner while maintaining the use of EVs and HPs?

## 1.1 Thesis Objectives

The impacts of DER integration on power distribution networks were studied to determine the hosting capacity of existing networks. This capacity was evaluated by monitoring voltage magnitudes, voltage unbalance factors, and other network constraints. The main objective of this thesis was the development of coordination algorithms, which were used to connect EVs and HPs to existing networks in order to defer network reinforcement. The thesis objectives are:

1. Predicting the UK overall residential demand based on future scenarios of aggregated power of EVs, HPs, and PV arrays.
2. Simulating test and real networks with EVs, HPs, and PV arrays. Residential and EV loads were synthesized using real trials. HP loads were modelled using ambient temperature, whereas PV power was modelled using solar irradiance.
3. Coordinating high EV charging loads using a centralized controller, while considering network constraints. A three-phase unbalanced power flow was developed to achieve this aim.
4. Adjusting EV and HP loads using a decentralized controller based on a modelled time-varying tariff. Consumer comforts and network constraints were considered with the decentralized controller. The satisfaction of EV user was monitored using EV battery state-of-charge (BSoC) levels. The comfort of HP user was monitored using the indoor temperatures of HP premises.

## 1.2 Thesis Contributions

Thesis contributions are summarized as follows:

1. Prediction techniques were proposed to estimate the UK overall residential demand with EVs, HPs, and PV arrays.
2. Deterministic and stochastic modelling tools were developed to assess the impact of EVs, HPs, and PV arrays on distribution networks.
3. A centralized control algorithm was implemented to coordinate EV charging loads in distribution networks. EV charging loads were re-allocated using the control algorithm to defer further network reinforcement.
4. A decentralized control algorithm was planned to adjust EV and HP loads using mixed integer linear programming. Current flows through cables were reduced

using the decentralized control algorithm, while considering consumer satisfaction of EV and HP users.

### 1.3 Thesis Structure

This thesis is organized as follows:

**Chapter 2** reviews related work using a proposed classification of previous studies. Reviewed publications were mainly classified into deterministic and stochastic studies. The relevant publications were categorized based on studied EVs, HPs, and PV arrays. Surveyed impact studies of DER units were presented using voltage levels, energy losses, and reinforcement costs. Reviewed demand management schemes with DER units were categorized into centralized and decentralized strategies.

**Chapter 3** predicts the UK overall residential demand with residential EVs, HPs, and PV arrays. The power of residential DER units was firstly synthesized over a year of half-hourly time steps based on Customer-Led Network Revolution trials. Then, the UK overall residential demand was predicted over the next two decades, considering National Grid and GridWatch databases.

**Chapter 4** explains the impact of residential DER units on power networks using deterministic and stochastic methods. Deterministic outcomes were presented using four case studies of uncontrolled EV charging loads with a generic low voltage network, which was adapted from Department of Trade and Industry. Meanwhile, stochastic results were shown with different combinations of EVs, HPs, and PV arrays using a real distribution network of Electricity North West.

**Chapter 5** presents the centralized control algorithm to coordinate high EV charging loads considering network constraints. The central controller was developed to maintain existing network components within their limits, while charging high numbers of EVs.

**Chapter 6** describes the decentralized control algorithm to adjust EV and HP loads using mixed integer linear programming. EV and HP loads were modelled based on their operational characteristics over a day of quarter-hourly time steps. Consumer satisfaction and network constraints were considered while developing the proposed algorithm. Simulations results were presented using another real low voltage distribution network of Electricity North West.

**Chapter 7** gives conclusions and recommendations for further work.

Figure 1.1 shows the framework of the thesis chapters.

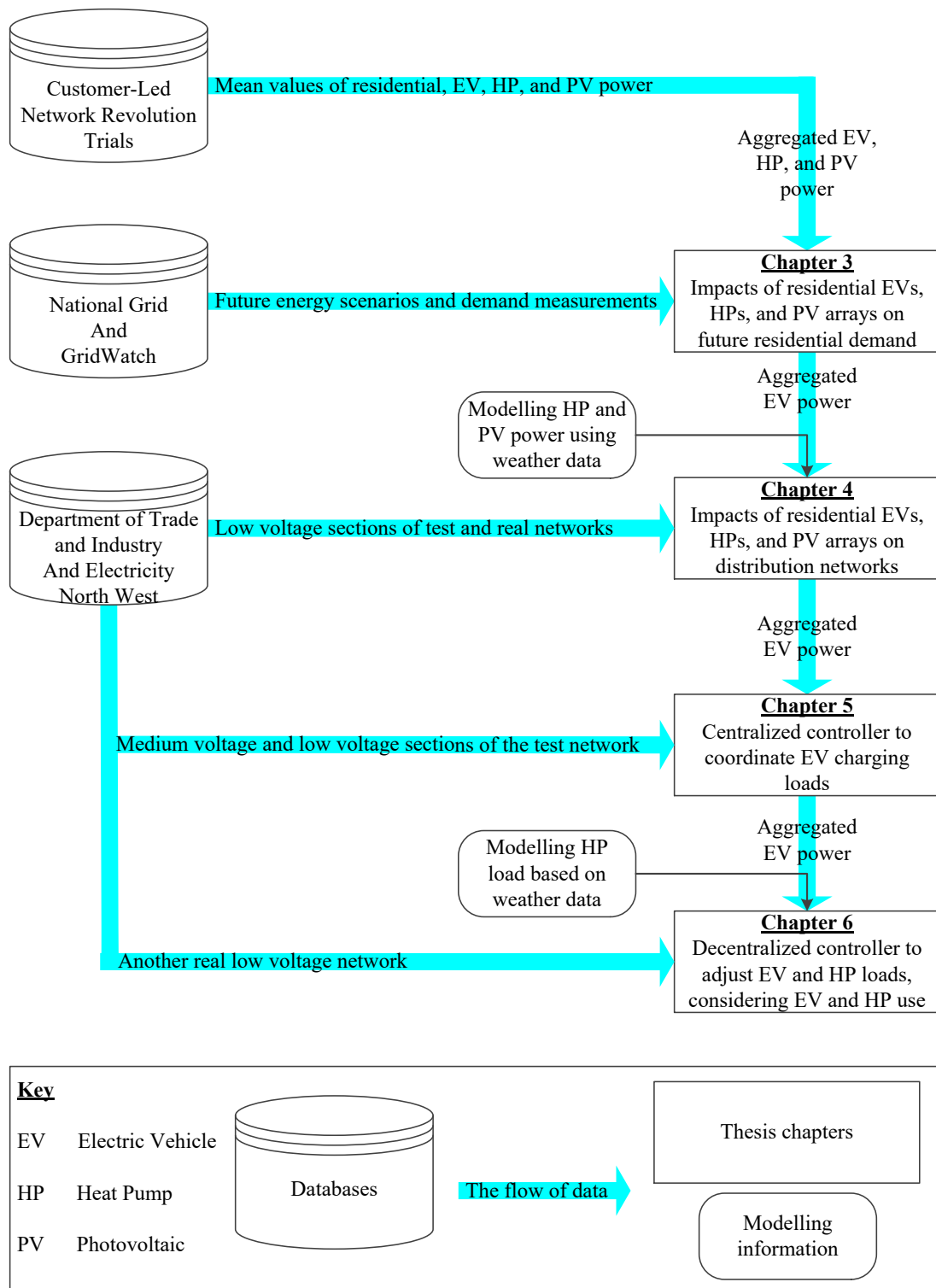


Figure 1.1: The framework of the thesis.

## CHAPTER 2

### 2. A Review of Distributed Energy Recourses in Power Systems

#### 2.1 Introduction

This review presents the literature that discussed the connection of distributed energy resources (DER) to electric power systems. Residential units of electric vehicles (EVs), heat pumps (HPs), and photovoltaic (PV) arrays are mainly considered in this literature survey, concentrating on some of their environmental benefits, technical challenges, and methodological considerations.

The energy consumption of residential sector was reported to be responsible for a 25% of carbon dioxide emissions in the UK [5]. Objectives were adjusted to reduce UK emissions below their level in 1990 as follows: a 34% cut of emissions by 2020, a 60% cut of emissions by 2030, and an 80% cut of emissions by 2050 [5], [6].

The use of carbon-free DER units in residential sectors can reduce carbon dioxide emissions to a certain level. Renewable energy sources (RES) were estimated to supply a 15% of the UK demand by 2020, accommodating a 30-45% of the UK energy consumption by 2030 [7]. National Grid [8] identified that, a 25% of heat and transport sectors should be decarbonized to accomplish an economic pathway of using renewables by 2030. HPs are able to decarbonize UK heat networks, offering a potential reduction of carbon dioxide emissions [9]. EVs were suggested to support the UK long-term objective of reducing carbon dioxide emissions [10]. The current emphasis of the UK government on greening the private and commercial vehicles can help in decarbonizing a substantial part of the transport sector [10], [11].

Carbon dioxide emissions from transport sectors were rising, as compared to these emissions from other sectors. European countries have agreed to reduce greenhouse gas emissions by 20% by 2020 (i.e. relative to 1990 levels) [12]. The regulations of European commission can increase the number of EVs to reduce carbon dioxide emissions over the next years. European countries have adopted a set of mandatory targets to cut these emissions in accordance with legislative Acts in 2009, including penalties of noncompliance with these objectives for new cars [12]. The use of EVs

was investigated in Ref. [13] to underpin a “green energy economy” based on several EV studies of national and regional levels by 2030, considering barriers and drivers of governing the use of EVs in transport sectors.

Currently, EVs account a small share of private cars but this share is anticipated to increase over the coming years. Table 2.1 illustrates a prediction of EV numbers across different countries by 2020.

Table 2.1: A prediction of EV numbers across different countries by 2020 (UK figure from [6], others from [10]).

Country	The number of electric vehicles
China	5,000,000
Spain	2,500,000
United States	2,488,320
France	2,000,000
Germany	1,000,000
South Korea	1,000,000
Japan	800,000
United Kingdom	763,944
Canada	500,000
Austria	250,000
Ireland	230,000
Portugal	200,000
Netherlands	200,000

## 2.2 Impacts of Distributed Energy Resources on Future Demand

Office for gas and electricity market (Ofgem) [14] assessed the risk of electricity supply in the UK over winter seasons between 2014/15 and 2018/19 based on future energy scenarios by National Grid. A significant demand reduction has started since 2013 because of the connection of distributed generators to electricity networks [14]. Ofgem also demonstrated that, demand reductions of non-residential customers over peak hours have caused further overall demand reduction.

Future demand can follow a predictable pattern over a day if specific aspects are unchanged (e.g. electrification of transport and heat sectors). Future loads of Britain

and Germany were predicted over the year of 2050 at hourly time steps by scaling overall demands, considering low carbon loads of EVs and HPs [15].

National Grid [16] has anticipated that, a considerable amount of intermittent renewable energy will be connected to the UK transmission system by 2020. High numbers of DER units will affect the UK residential demand by 2030 as follows. Residential loads will increase by 48% above the current value of demand, as reported in Ref. [11]. The average ratio of residential demand in winter days relative to summer days will increase by 22% by 2030, as compared to its value in 2010 [11].

A scenario-based approach was used in Ref. [17] to integrate RES units into German electricity systems based on a prediction of solar and wind energies by 2050. The future trend of RES integration was estimated considering several RES uptakes and economic benefits. Thereafter, economic and technical parameters of German energy system were estimated by 2050 [17]. In Finland [18], nuclear power plants and wind energies were modelled to predict Finish future energy profiles, considering HPs in heating systems. The maximum share from intermittent wind energy was evaluated with nuclear power plants using a “wind-nuclear compromise chart”. The chart was used to study different scenarios, illustrating carbon dioxide emissions, power exchanges, and total energy costs. It was concluded that nuclear energy generation can limit the maximum value of variable wind energy [18]. Several methods were proposed in Ref. [19] to maintain reliable energy systems with intermittent renewable energy resources using the roles of the following elements: demands, energy markets, energy storages, smart grids, and institutional policies.

### **2.2.1 Thesis Contribution to Estimate Future Demand with DER Units**

It can be seen that, distributed generators such as PV arrays were only considered in Ref. [14], whereas the impact of EV and HP technologies on the UK future demand was investigated in Ref. [15]. Although future energy scenarios by National Grid [8], [20] predicted the UK future demand with DER units, the shape of the UK annual demand was not presented over the forthcoming years.

Therefore, a simultaneous impact of residential DER units on the UK future demand is required, considering a long-term interval (e.g. two decades ahead). In Chapter 3 of this thesis, a long-term prediction model is developed to estimate the impact of residential EV, HP, and PV arrays on the UK residential demand over half-

hourly time steps. This tool can help system operators to acquire an estimate of future domestic demand, while connecting residential DER units to UK electricity networks.

### 2.3 Impacts of Distributed Energy Resources on Distribution Networks

The impacts of DER units on electric power systems were assessed in transmission and distribution levels [21]. Temporal attributes (e.g. EV charging durations) and spatial attributes (e.g. EV locational connections) were analysed using medium voltage (MV) networks to study uncontrolled and controlled charging of EVs [21], [22]. Deterministic power flows were used in Ref. [23] to evaluate the hosting capacity of existing networks with the integration of RES units. The power of DER units was estimated in Ref. [24] using stochastic methods. Deterministic and stochastic analyses were used in Ref. [25] to evaluate the impact of DER integration on existing networks. Moreover, both of stochastic and deterministic methods were presented in Ref. [26] to model controlled and uncontrolled charging of EVs. Uncontrolled EV charging loads were reported to have a remarkable impact on network components [26]. The impact of EV charging loads on distribution networks was studied in Ref. [27] using a three-phase power flow, monitoring voltage magnitudes and current flows. Stochastic and deterministic approaches were also compared in Ref. [27] using 13-bus and 25-bus networks.

#### 2.3.1 Deterministic Studies

Deterministic methods, which use non-randomized numbers of DER units, were presented in Refs. [28], [29] to study the impact of DER units on distribution networks. It was concluded in Ref. [23] that the hosting capacity of low voltage (LV) networks with RES units can be calculated by performing power flows.

According to the Institute for Electrical and Electronic Engineering (IEEE) [30], residential customers are typically connected to main feeders via single-phase lines. The combination of DER power and residential demand will produce unbalanced loads, causing unbalanced voltages across the three phases. Consequently, three-phase equipment (e.g. induction motors) can be overheated due to voltage unbalance [30]. High residential charging loads of EVs will increase the aggregated residential demand. The aggregated demand can cause a violation of steady-state operational limits such as voltage unbalance factors and voltage magnitudes. Voltage unbalance

factors were evaluated in Refs. [31], [32] to study the impact of EV charging loads on radial distribution networks. The impact of EV charging loads on a distribution network was evaluated by monitoring voltage fluctuations and voltage unbalance factors [33]. An IEEE 13-bus network was used in Ref. [34] to study the impact of EV charging loads on voltage unbalance factors. A lithium-ion battery was modelled in Ref. [34] based on the characteristics of Tesla-Roadster EVs.

The technical challenges of EV charging loads were reviewed in Ref. [35] with different LV distribution networks. The impacts of EV charging loads on electricity networks were quantified based on EV numbers, EV charging time durations, EV driving patterns, and EV charging features [35]. It was observed that, voltage deviations and other network constraints exceeded their limits with relatively moderate charging loads of uncoordinated EVs in an existing LV network [28]. The impacts of EV charging loads on meshed and radial networks were studied in Ref. [36] based on voltage fluctuations and energy losses.

It was shown that, existing distribution networks could frequently exceed their limits with high numbers of EVs [37], [38]. For example, thermal ageing of distribution transformers can significantly deteriorate with high levels of EV charging loads [38]. In Ref. [39], a number of EVs were connected to real distribution networks to assess their effect on energy losses and reinforcement costs. It has been concluded that grid reinforcement may reach up to 15% of the grid cost, as compared to a case without EV integration [39].

The technical issues of connecting high numbers of PV arrays to residential feeders were addressed in Ref. [40] using unbalanced power flows. Load flow results demonstrated that, voltage magnitudes with high numbers of PV arrays were slightly increased [40]. The impact of PV arrays on a real residential network was presented in Ref. [41] considering a single-phase connection of PV panels to the grid. Unbalanced phase voltages were observed to occur at the weak feeder (i.e. a long radial feeder of high impedance) [41]. Voltage issues were alleviated along LV feeders using a cooperative voltage control, connecting PV and EV units to the same part of distribution networks [42].

The impacts of charging loads of plug-in hybrid electric vehicles (PHEVs) on distribution networks were also investigated in the literature. The capacity of a PHEV battery was typically small, as compared to the capacity of an EV one. Consequently, the impacts of EV/PHEV charging loads on distribution networks have accordingly

varied. In Ref. [43], several modelling tools were reviewed to study the impact of PHEV charging loads on different distribution networks, considering the following aspects: uptakes, driving patterns, charging durations, and charging properties. PHEV charging loads were noticed to have an impact on distribution transformers over peak hours [44]. The impacts of PHEV charging loads on distribution networks were mitigated in Refs. [45]–[48] using different techniques such as: on-line coordination methods [45], centralized controllers [46], and decentralized controllers [48].

### 2.3.2 Stochastic Studies

Stochastic methods were used to address uncertainties of DER units in distribution networks (e.g. EV charging time durations). Monte Carlo Simulation (MCS) techniques were widely used in stochastic studies to address different scenarios using a proposed randomness of DER integration.

Voltage fluctuations and energy losses were studied in an existing LV network considering a stochastic method to simulate uncertainties of EV charging loads [49]. The impact of EV charging loads on a typical LV network was investigated using a stochastic approach to model the uncertainties of EV charging locations and EV charging durations [50]. A stochastic method was used to study the impact of EV charging loads on UK distribution networks based on real datasets that were acquired using smart meters of real trials [51]. It was suggested that uncertainties of EV charging loads can be reduced using a cooperative framework, which incorporates aggregators and distribution network operators (DNOs) [51].

The impacts of EV charging loads and PV power generations on distribution transformers were studied using a probabilistic approach of MCS methods with an IEEE, 123-bus, and modified network [52]. A number of 100 power flows were simulated to study the impact of EVs, HPs, PV arrays, and micro combined heat and power (mCHP) units on 128 residential feeders [24]. Stochastic results were suggested in Ref. [24] to be interpreted into lookup tables by DNOs to evaluate the hosting capacity of residential feeders with these low carbon technologies. The integration of the DER units into real LV feeders was also studied in Ref. [53] using OpenDSS over a day of 5 minutes time steps, considering DER operational characteristics.

Stochastic modelling and optimization methods of future electricity networks were surveyed in Ref. [54], considering the contribution of DER units in micro-grids.

It was concluded that, stochastic modelling and optimization methods require additional statistics and extensive computations, as compared to deterministic methods [54].

### 2.3.3 Real-World Studies

Real electricity networks can experience additional uncertainties with DER integration. For example, the aggregated load of EVs and HPs will increase peak-hour demand. DER integration might affect both of electricity suppliers and electricity consumers in different levels of electricity systems. Therefore, quality and reliability of electricity should be maintained within their limits, while accommodating more DER units [55].

In the UK [56], [57], Customer-Led Network Revolution (CLNR) project was initiated to study the impact of residential DER units on UK distribution networks using smart metered power data [56], [57]. The CLNR project is a cooperative framework between commercial and academic partners. The commercial partners are Northern Powergrid operator, North East and Yorkshire operator, Ofgem, British Gas, Electricity Network Association (ENA) Technology, and low carbon networks fund (LCNF). The LCNF project was replaced with Electricity Network Innovation Competition [8]. The academic partners of the CLNR project are Durham University and Newcastle University.

The CLNR project developed cost-effective solutions to tackle high numbers of DER connection to distribution networks. The CLNR project focuses on residential EVs, HPs, PV arrays, and mCHP units [56]. Useful reports were published during the CLNR trials to illustrate the outcomes of this project. For example, the impact of PV arrays and HPs on UK distribution networks was investigated over a year of half-hourly time steps [29]. The Irish Customer Behaviour Trials (CBT) [58] were initiated to provide a statistical insight of using residential smart meters. CBT results have shown that, the use of smart meters and time-varying tariffs could reduce residential demand. The Low Carbon London (LCL) project [59] was launched to study the effect of DER units on future low carbon networks. LCL studies have focused on the following topics: power quality issues with DER integration, demand response schemes with dynamic time-varying tariffs, and economic opportunities with demand response strategies.

In the Netherlands [60], energy losses and voltage levels were assessed using real power data of residential customers in connection with EV and PV integration. The program (Livelab) of the network operator (Al-liander) was used to perform stochastic three-phase power flow simulations. These simulations were recorded based on real-world residential loads with random locations of EV and PV units using a MCS approach. The hosting capacity of the considered network was determined based on different connections of EVs and PV arrays [60].

In Sweden [61], the impact of EV charging loads was analysed using a steady-state power flow in a local MV/LV distribution network of Gothenburg. Commercial and residential areas were simulated for a worst case scenario by charging all EVs during peak-hour time intervals. Transformers and cables were overloaded because of simultaneous EV charging loads during peak hours. Voltage fluctuations were recorded to be within their acceptable values at EV charging locations [61].

#### **2.3.4 Thesis Contribution to Study DER Impact on Distribution Networks**

In Chapter 4 of this thesis, the impacts of EVs, HPs, and PV arrays on test and real networks were simultaneously studied, whereas the impacts of EV charging loads on distribution networks were separately studied in Refs. [28], [37], [49], [50]. Deterministic evaluations were implemented in Refs. [28], [37] to study the impact of EV charging loads on LV networks using snapshot values of load flows. Daily unbalanced power flows were calculated in Chapter 4 to investigate the impact of EV charging loads on LV networks. The impacts of EV charging loads on distribution networks were just considered in Refs. [49], [50] using stochastic techniques. Meanwhile, studies [24], [53] investigated the impact of EVs, HPs, and PV arrays on LV feeders based on a stochastic method, including their effect on distribution transformers.

Therefore, Chapter 4 uses both of stochastic and deterministic studies to study the impacts of EVs, HPs, and PV arrays on test and real networks, considering real-world datasets of the DER units. The impacts of these low carbon units on LV networks were monitored by recording voltage unbalance factors, voltage magnitudes, and power flows through transformers and cables. Real-world mean values of the power of the low carbon technologies were used to synthesize their individual power over a day of minute-by-minute time steps. This approach presents a near real-time impact of the

DER units on distribution networks. Moreover, Chapter 4 of this thesis is designated to evaluate the number of EVs that can be accommodated in existing networks without exceeding network limits using unbalanced power flow.

#### 2.4 Coordination Algorithms of EV Charging Loads

In Ref. [62], dumb charging was proposed to charge EVs considering the ability of EV owners to recharge their EVs whenever they need without restrictions or incentives. However, dumb charging can cause technical and operational issues. Meanwhile, smart charging was suggested to shift EV charging loads towards off-peak hours using time-of-use (ToU) tariffs [62].

Network reinforcement can be used to strengthen the existing networks; however, a widespread adoption of infrastructure upgrades would be very expensive. Alternatively, smartening the distribution networks have the potential to develop an efficient use of the network components. Responsive loads such as EVs can be used to achieve an optimal energy matching by reshaping the energy demand. Rescheduling strategies of charging and discharging EV batteries were presented in Refs. [63]–[66] based on different constraints, considering other DER units. Coordination algorithms were implemented using several optimization methods. Numerical optimization techniques have been reviewed in Refs. [67], [68] for optimal scheduling of EV charging loads, discussing dynamic programming, linear programming, and non-linear programming. Meta-heuristic methods have also been presented in Refs. [67], [68] to illustrate multi-objective scheduling problems while charging and discharging EVs.

In one study [69], an adaptive controller was proposed to coordinate EV charging schedules. The on-line adaptive controller was used to reduce the impact of EV charging loads on distribution networks, considering EV charging costs, EV owner preferences, voltage magnitudes, and voltage unbalance factors. A direct current (DC) power flow was used in the optimization process, whereas an alternating current (AC) power flow has been performed to validate the results.

In another study [70], a control method was developed to coordinate EV charging loads within a five-minute time resolution. The cost of the energy generation was decreased to achieve the coordination of EV charging loads considering energy losses, voltage fluctuations, and overloads. This cost of energy was further reduced by finding a better solution using fuzzy theory [71]. An on-line fuzzy coordination algorithm was

used for EV charging loads in a smart network with distributed wind generators. The control algorithm reduced the total cost of energy generation based on dynamic energy prices, including power losses. EV users were prioritized according to their preferred charging times. It was ensured that voltage profiles cannot exceed their limits when EVs were charged using the on-line fuzzy coordination algorithm [71].

In yet another study [72], EVs were optimally recharged considering EV battery state-of-charge (BSoC) levels and network constraints. EV charging loads were simulated in Ref. [72] using a real unbalanced distribution network over a day of 5 minute time steps. Meanwhile, EV charging loads were simulated in Ref. [73] over a day of hourly time steps to minimize the following values: transformer overloads, energy losses, and operational costs. A three-phase unbalanced distribution network was used in Ref. [73] to test the performance of the proposed framework based on an optimal power flow. High EV charging loads were scheduled based on heuristic algorithms to reduce peak loads [74], considering voltage deviations and network limitations. However, heuristic algorithms cannot guarantee the accuracy of optimal solutions, because they merely help in detecting the best possible solution of all feasible ones [75].

High numbers of EVs were controlled in a distribution network using a multi-objective algorithm, considering distributed generators. Local network operators were suggested to use a genetic algorithm to mitigate the impact of EV charging loads on distribution networks [76]. The approach proposed in Ref. [76] was updated in another Ref. [77] using integer nonlinear programming. According to Ref. [78], the capacity of distribution transformer was used to determine the maximum number of EVs, which can be connected to an existing network. An optimal charging strategy was proposed in Ref. [78] to maximize the power of EVs accommodated.

EV charging loads have been coordinated using agent-based strategies to mitigate their effect on distribution networks [79]–[81]. A multi-agent system was experimentally implemented in Refs. [79], [81] for a smart charging of EVs. The agent-based controller was tested in an LV network using a search method based on neural networks. EV charging loads were coordinated to follow a low electricity price, while maintaining grid constraints within their limits [81]. Agent-based strategies were reviewed in Ref. [82], while presenting a number of software packages of modelling EV charging loads in smart grids. A number of 125 software packages were surveyed in Ref. [83] to identify relevant simulation tools for modelling and controlling loads of

charging EVs, describing two thirds of these packages briefly. The software packages were related to EV impact studies, EV charging schedules, and EV traffic simulations [83]. Table 2.2 shows an executive summary of a number of reviewed publications.

Table 2.2: An executive summary of a number of reviewed publications.

References	[24]	[21]	[22]	[78]	[51]	[79]	[80]	[81]	[82]	[26]	[27]	[39]	[83]
Deterministic or stochastic methods of studying distributed energy resources (DER)													
Deterministic													
Stochastic													
Electric Vehicles (EVs), Heat Pumps (HPs), and Photovoltaic (PV) arrays													
EVs													
HPs													
PV arrays													
The impact of EVs, HPs, and PV arrays on													
Voltages													
Power losses													
Transformers													
Cables													
Costs													
Medium Voltage (MV) and Low Voltage (LV) levels													
MV													
LV													
Demand Side Management Strategies													
Centralized													
Decentralized													
Programming tools													
MATLAB													
OpenDSS													
MATSim													
IPSA													
PSCAD													
Others									8				125
Publication date	2 0 1 6	2 0 1 2	2 0 1 4	2 0 1 5	2 0 1 5	2 0 1 3	2 0 1 5	2 0 1 4	2 0 1 6	2 0 1 1	2 0 1 4	2 0 1 1	2 0 1 6
Key		These cells represent the aspects considered in each publication											

### 2.4.1 Thesis Contribution to Coordinate EV Charging Loads

The use of ToU tariffs to coordinate EV charging loads may lead to a new peak of aggregated demand over the time intervals of low electricity prices. Therefore, a centralized controller, which can re-allocate charging loads of high numbers of EVs without exceeding the network constraints, is important. In Chapter 5 of this thesis, a centralized controller is implemented to re-allocate EV charging loads, considering network constraints over a day of minute-by-minute time steps.

The centralized controller of Chapter 5 differs from the controllers proposed in Refs. [70]–[73], as it controls EV charging loads regardless electricity prices. Although the controllers presented in Refs. [70]–[73] maintained network constraints within their limits, controlling additional EV charging loads using these controllers may lead to another peak of demand over the hours of low electricity prices.

## 2.5 Demand Side Management Schemes

Similarities and differences between demand response (DR) and demand side management (DSM) mechanisms are presented in Table 2.3. DSM schemes were reviewed in Ref. [84] based on optimization methods with residential customers. The contrasts of defining DSM schemes were highlighted in Ref. [84] using the following aspects: individual versus aggregated users, deterministic versus stochastic methods, and day-ahead versus real-time intervals. DSM and DR schemes can be modelled using centralized or decentralized approaches of control, as shown in Table 2.3.

DR strategies represent the end-user ability of modifying energy consumption by responding to an external signal (e.g. electricity price). DSM techniques can be designed based on load shedding or ToU pricing, as presented in Ref. [85]. A load management method can be used to connect high numbers of DER units to power systems, while considering economic and environmental benefits.

A number of demand management prospects were discussed in Ref. [85] such as: DSM techniques (e.g. load shedding), DSM challenges (e.g. the lack of communication systems), and DSM advantages (e.g. the reduction of operating and planning costs).

Table 2.3: Similarities and differences between DSM and DR strategies based on a number of reviewed publications.

<b>Demand Side Management (DSM)</b>	<b>Demand Response (DR)</b>
A pre-planned action	An immediate action
With or without external signals	With external signals (e.g. electricity price)
Load shedding or ToU pricing (i.e. examples of DSM/DR techniques)	
Centralized or decentralized control (i.e. examples of DSM/DR approaches)	
A postpone of network reinforcement or a reduction of operational cost (i.e. examples of DSM/DR advantages)	
Linear programming, mixed integer linear programming, nonlinear programming, dynamic programming, and quadratic programming (i.e. examples of DSM/DR modelling tools)	

According to Ref. [86], a DR strategy is used to match supply with demand, considering demand reduction over peak-hour time intervals. Commercial and industrial customers obtain a significant contribution of DR by switching their loads on and off. Residential customers can participate in DR schemes using the technical role of smart meters. The use of DR strategies has the potential to reduce generation costs, electricity bills, and carbon dioxide emissions [86].

Thirty trials were reviewed in Ref. [87] to show a number of DR schemes in different contraries, considering different seasons. Domestic energy management systems were reviewed in Ref. [88] to evaluate cost reductions and efficiency improvements, illustrating their functional structure with mixed renewable energy resources. Several studies were reviewed in Ref. [89] to demonstrate the use of optimization methods in different geographical locations of disparate RES types.

Smart EV charging and DSM strategies were presented in Ref. [90] to mitigate the impact of DER units (e.g. EVs and mCHP units) on MV/LV network components. A demand management strategy was investigated in Ref. [91] to reduce EV operating costs using mCHP energy generation. EV charging loads were rescheduled in Ref. [91] based on driving patterns, considering mCHP operating intervals over different weather conditions.

### 2.5.1 Demand Management Schemes in Smart Grids

The environmental challenges of using fossil fuels will encourage further connection of carbon-free DER units to distribution networks. Technical and operational issues of DER integration can be mitigated using a smart grid [92].

The smart grid is a conceivable control of an electric network to decrease operating and planning costs, serving responsive customers efficiently [93]. DR schemes can reduce capital costs by deferring network reinforcement. Information and communication technologies (ICT), smart meters, and energy controllers were presented as important assets of the smart grid, as compared to the conventional one [93]. DSM and DR strategies were highlighted as essential tools in the smart grid to increase the level of automation in distribution networks [94].

Smart grids were reviewed in Ref. [95] considering their economic and environmental benefits. It was shown that, the assessments of smart grids have varied across different studies. Economic and environmental advantages with smart grids were summarized to indicate the origin of these variations. It was concluded that, smart grids might achieve both of economic and environmental benefits to a certain level. Standardized assumptions and standardized methodologies were recommended to acquire a consistent assessment of smart grids [95].

Smart meters and energy prices were demonstrated in Ref. [96] to estimate their roles and advantages in smart grids, while implementing DSM schemes. EV charging loads were controlled considering the participation of EV aggregators in the electricity market, and the limitation of network components. The proposed strategy was assumed to be managed by EV aggregators and network operators. Energy difference between the energy bought and the overall charging demand was minimized to solve operational issues with high numbers of EVs [97].

### 2.5.2 Centralized Demand Management Schemes

DER integration can significantly change an aggregated demand, causing prediction errors. Voltage deviation, voltage unbalance, and frequency fluctuation can occur with DER integration. In addition, variations of solar irradiance and wind speed require a flexible generation capacity. Therefore, DR schemes can help in bringing flexibility, efficiency, and reliability to power systems [98].

In Ref. [99], supply and demand were matched using an energy management system, considering an increase of PV uptakes. A short-term prediction of HP and PV power was used to enhance the performance of the proposed management scheme. Ten probability distributions were examined over a one-year time interval to increase the prediction accuracy. This accurate model of prediction was used to match HP load with PV power generation [99]. Operational challenges were investigated in Ref. [100] using different probability distributions of solar irradiance and wind speed. A demand management strategy was implemented in Ref. [100] to minimize the operational costs considering residential, commercial, and industrial customers. Moreover, the loads of smart appliances were re-scheduled in Ref. [101] based on different probability distributions, investigating the impact of their information delay.

A proposed DR strategy was used to coordinate additional RES power using an aggregation of EV and PHEV energy, while maintaining power systems within acceptable levels of safety and reliability [102]. According to Ref. [103], DR strategies are able to cope with RES fluctuations based on incentives of real-time pricing. However, limited experiences of real DR schemes can cause extensive assumptions in DR modelling. Linear price/demand relationships and fixed constraints were noticed as typical DR assumptions [103]. In addition, a successful DSM scheme should be primarily evaluated based on utility financial incentive and regulatory support to avoid the overlap between present and new policies [104].

A number of definition and classification of DR programs were reviewed in Ref. [105] to illustrate EV integration into smart grids. DSM strategies were presented in Ref. [106] to smooth electricity demand by shifting EV charging loads away from peak hours, considering weekly and seasonal schemes of demand managements.

### **2.5.3 Decentralized Demand Management Schemes**

The growth of using RES units is predicted to follow a decentralized pattern, which may cause further challenges in distribution networks. These challenges require an effective use of decentralized DR schemes. A strategy of DR program can be managed by network operators or aggregators [107].

In Ref. [108], EV loads were shifted using an algorithm of distributed DR method with other DER units based on a valley-filling method. Nonetheless, this algorithm has not included EV owner preferences. A decentralized algorithm was developed in Ref.

[109] to reschedule EV charging loads using the valley-filling method based on an optimal control problem. However, EV owner preferences were also not considered in Ref. [109], because the algorithm proposed follows a control signal that has been broadcasted by the utility company.

A decentralized DSM scheme was developed in Refs. [110], [111] based on flexible demand participation in electricity markets, modelling the operational characteristics of EVs and HPs. However, distribution network limitations were not considered in Ref. [111] because EV and HP loads were studied at the transmission level. A balanced generic system was used to test the coordination of DER power using a two-level algorithm of another decentralized DSM scheme over a day-ahead time interval [112]. Moreover, non-linear pricing tariffs were developed in Ref. [113] considering a local randomized approach to manage the loads of EVs and other appliances, while excluding the uncertainties of EV owner preferences.

#### **2.5.4 Thesis Contribution to Implement Demand Management Scheme**

In Chapter 6 of this thesis, a decentralized demand management scheme is proposed to adjust EV and HP loads, while considering consumer satisfaction and network constraints. A real, three-phase, and unbalanced network is used to test the performance of the proposed controller.

Consumer satisfaction was included in the decentralized algorithm of Chapter 6, whereas this attribute was not included in the decentralized programs of Refs. [108], [109]. Although operational characteristics of EVs and HPs were considered in the two-part study [110], [111], the level of consumer comfort (e.g. EV final BSoC level) was not evaluated in Ref. [111].

Therefore, EV final BSoC levels and the indoor temperatures of HP house were evaluated in Chapter 6 to indicate consumer satisfaction clearly. In addition, the three-phase structure of the most of real distribution networks was not considered in the decentralized algorithms of Refs. [108]–[113]. Consequently, an appropriate attention has been paid in Chapter 6 to the three-phase structure of real unbalanced networks, while developing the decentralized algorithm of demand management scheme.

## 2.6 Conclusions

Technical challenges that appear due to the connection of DER units into distribution networks were reviewed. The surveyed DER units were EVs, HPs, and PV arrays. The impacts of low carbon technologies on distribution networks were presented using network constraints of voltages, power losses, and operating/planning costs. Real world projects (e.g. the CLNR project in the UK), which consider real electricity networks, were also presented in this literature survey.

Impacts of DER units on distribution networks were highly demonstrated based on network constraints. Studied networks were presented using MV and LV levels, considering temporal (e.g. EV charging durations) and spatial (e.g. EV locational connections) features. Deterministic methods were modelled using non-randomized numbers of DER units (e.g. gradual increase of DER units). Stochastic methods were widely used to address uncertainties of DER units (e.g. EV charging durations) within electricity networks.

Network reinforcement can be used to mitigate the technical challenges of DER integration into networks. Alternatively, DR/DSM schemes were proposed to alleviate these challenges, while connecting DER units into power systems. Network operators and aggregators were highly suggested to be in charge of managing DR/DSM strategies.

It was noticed that, the impact of residential EVs, HPs, and PV arrays on future residential demand was not simultaneously studied. Operational characteristics of individual EVs, HPs, and PV arrays were separately considered using either real or test networks. Although several studies investigated the use of ToU tariffs to coordinate EV charging loads, network constraints can exceed their limits over the time intervals of low electricity prices. In addition, few studies have investigated a simultaneous adjustment of EV and HP loads using decentralized controllers.

Therefore, this thesis studies a simultaneous impact of residential EVs, HPs, and PV arrays on the UK residential demand over the next two decades. It shows the impact of individual EV, HP, and PV integration on real and test networks based on real-world datasets. It proposes a centralized control algorithm to coordinate EV charging loads considering the constraints of MV and LV networks. It investigates a decentralized controller to adjust EV and HP loads considering consumer satisfaction and network constraints.

## CHAPTER 3

### 3. Impacts of Distributed Energy Resources on Future Demand

#### 3.1 Introduction

The impact of electric vehicles (EVs), heat pumps (HPs), and photovoltaic (PV) arrays on the UK residential demand was predicted over the next two decades, highlighting the year of 2035. The UK residential demand was extracted on a yearly basis using the UK historic demand of GridWatch databases in 2014 [114].

Power profiles of distributed energy resources (DER) were synthesized over a year of half-hourly time steps using normal probability distribution and median filter. Mean values of the active power of 133 EVs, 336 HPs, and 151 PV arrays were read from Customer-Led Network Revolution (CLNR) trials on a day of half-hourly time steps for each month of the year between 2012 and 2014 [115].

Thereafter, the UK residential demand was predicted considering the power of residential EVs, HPs, and PV arrays based on Future Energy Scenarios by National Grid [20].

#### 3.2 Methodology

Measurement units are typically installed at the transmission level. Consequently, the power of DER units cannot be observed with their connections to distribution networks. Thus, the total demand will be more challenging to predict, while connecting low carbon technologies to residential feeders. Therefore, this challenging issue can cause a real mismatch between total demand and total generation.

To overcome this problem, the UK residential demand was predicted with the integration of DER units based on Future Energy Scenarios by National Grid over the forthcoming years at half-hourly time steps. The proposed tool was therefore able to predict energy consumption considering different seasons of winter, spring, summer, and autumn.

The UK residential demand was read from GridWatch databases [114] based on the year of 2014 at 5 minute time steps. Then, the UK demand measurements were averaged into half-hourly time steps. Meanwhile, EV, HP, and PV power profiles were

synthesized over a year using normal probability distribution and median filter.

The proposed steps generate annual power values of EVs, HPs, and PV arrays, as follows. Firstly, noisy annual values of power profiles were synthesized using normal probability distribution based on the mean values of the active power of these DER units. Then, a median filter was used to remove the noise. Figure 3.1 represents the workflow of the prediction tool proposed in this research.

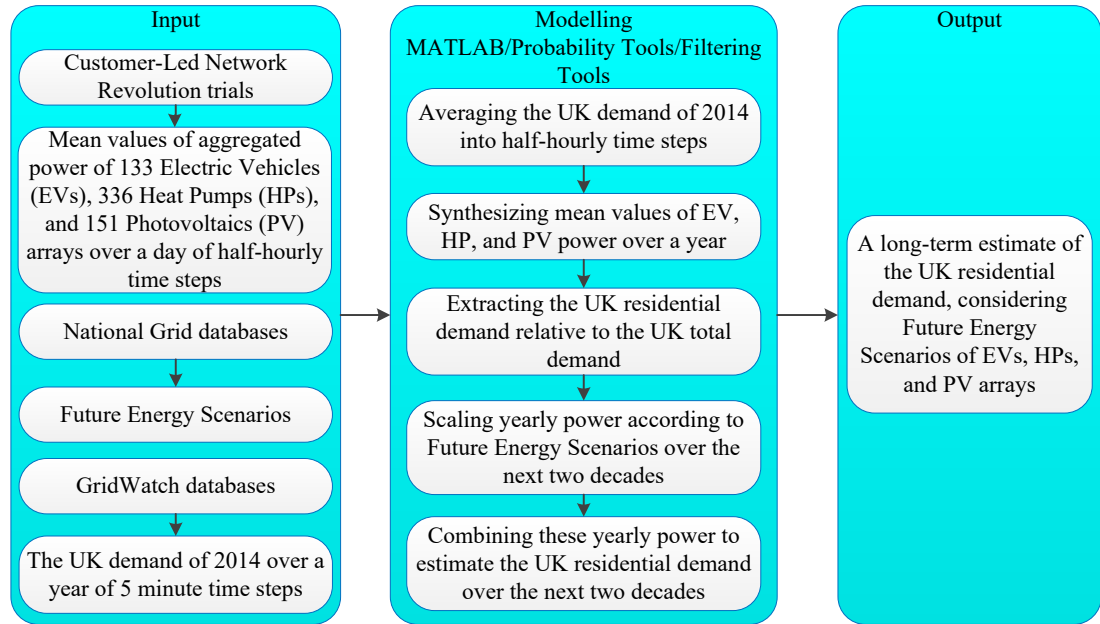


Figure 3.1: The workflow of the proposed long-term prediction tool.

### 3.2.1 Historic Demand Measurements

The UK demand was averaged into half-hourly time steps based on the UK demand of GridWatch databases [114], which was recorded over the year of 2014 at 5 minute time steps. The UK residential demand was calculated using the percentage of the UK residential demand contribution relative to the UK total demand, as reported by National Grid in Ref. [20].

According to National Grid [20], Figure 3.2 shows the percentage of the UK residential demand contribution as compared to the UK total demand at every half-hourly time step. These percentages were used to calculate the UK residential demand over different seasons, as indicated in Figure 3.3 (a) to Figure 3.3 (d). Figure 3.4 presents the UK residential demand and the UK total demand based on these calculations.

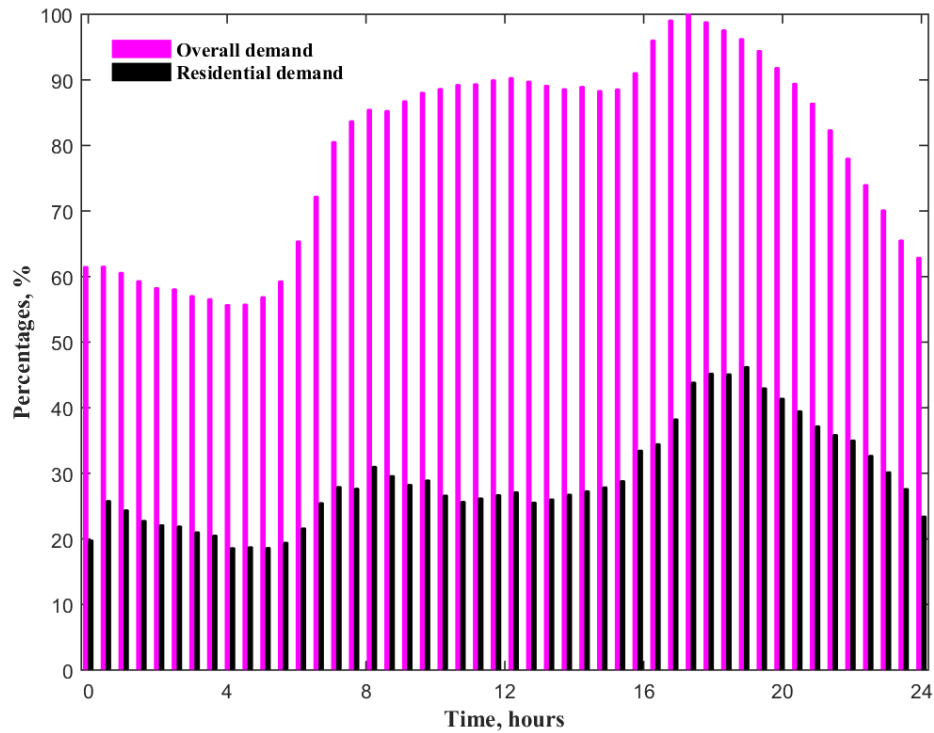


Figure 3.2: The percentages of the UK residential demand contribution relative to the UK demand over a day of half-hourly time steps, as reported by National Grid [20].

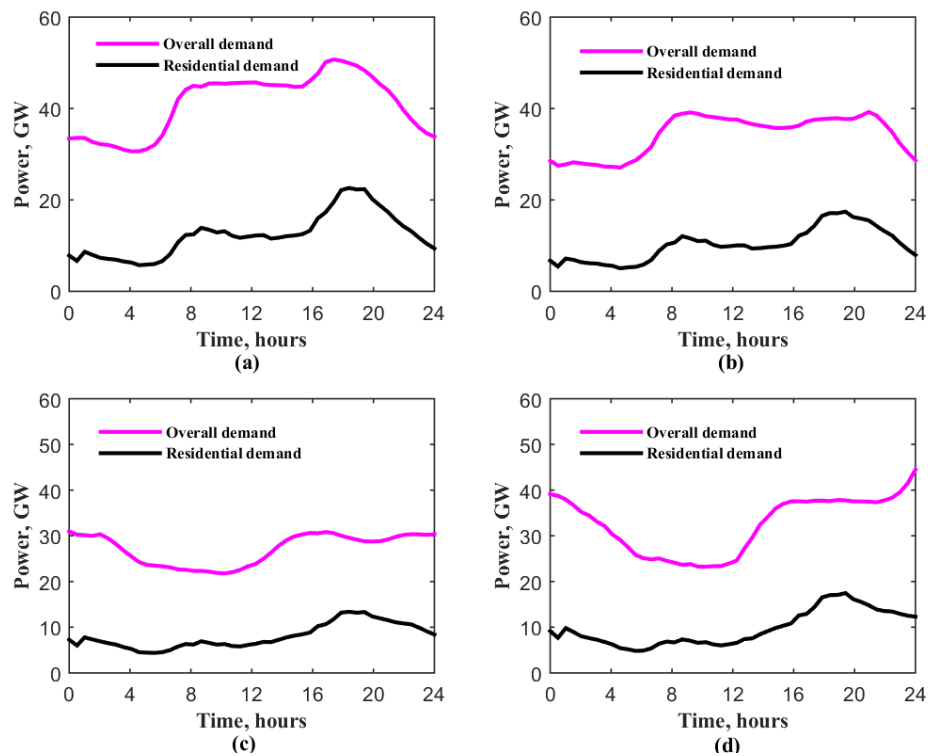


Figure 3.3: The UK total demand and the UK residential demand over a day of half-hourly time steps in 2014 for (a) January, (b) April, (c) July, and (d) October (data from [114]).

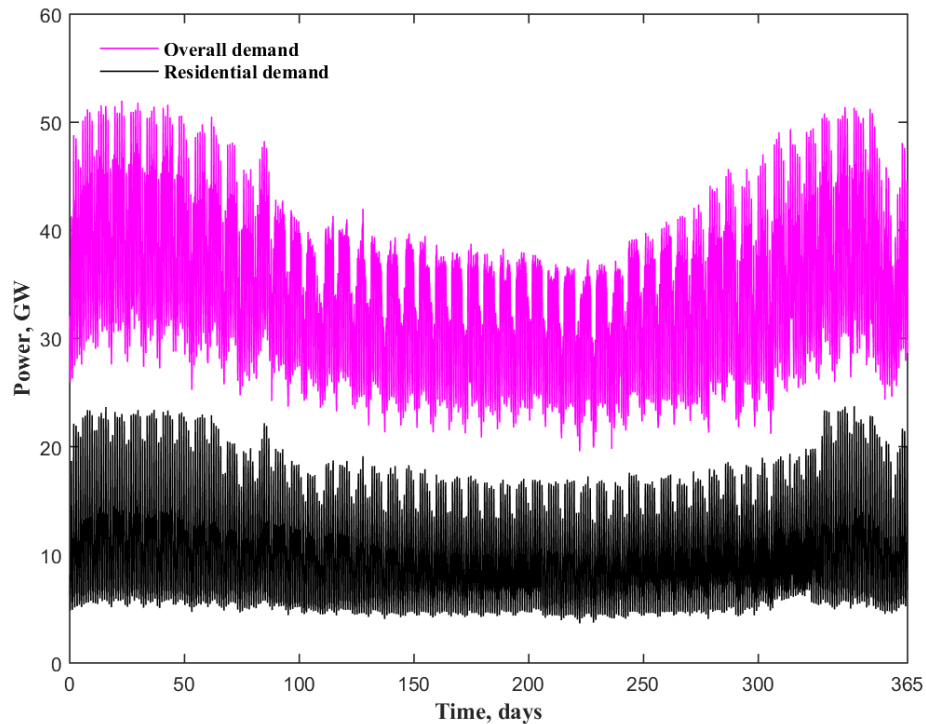


Figure 3.4: The UK total demand and the UK residential demand over the year of 2014 at half-hourly time steps (data from [114]).

### 3.2.2 Synthesized Power of Distributed Energy Resources

Annual EV, HP, and PV power cannot be measured due to the lack of their observability in distribution networks. Therefore, daily mean values of the active power of 133 EVs, 336 HPs, and 151 PVs were used to synthesize the complete annual power of these DER units. Daily mean values of power profiles were provided on a half-hourly basis from CLNR trials [115].

Power profiles of these low carbon technologies were recorded in CLNR trials using smart meters, considering half-hourly time steps for each month of the year between 2012 and 2014. Figure 3.5 and Figure 3.6 show samples of mean values of the active power of 133 EVs and 151 PV arrays in different seasons, as reported by CLNR project [115].

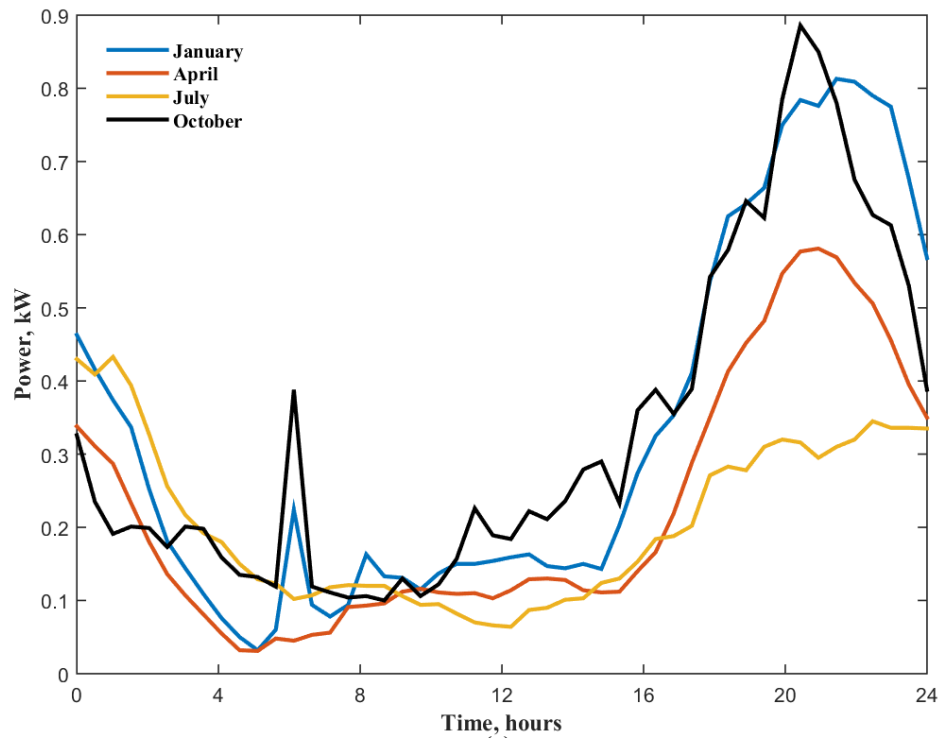


Figure 3.5: Seasonal mean values of EV charging loads (data from [115]).

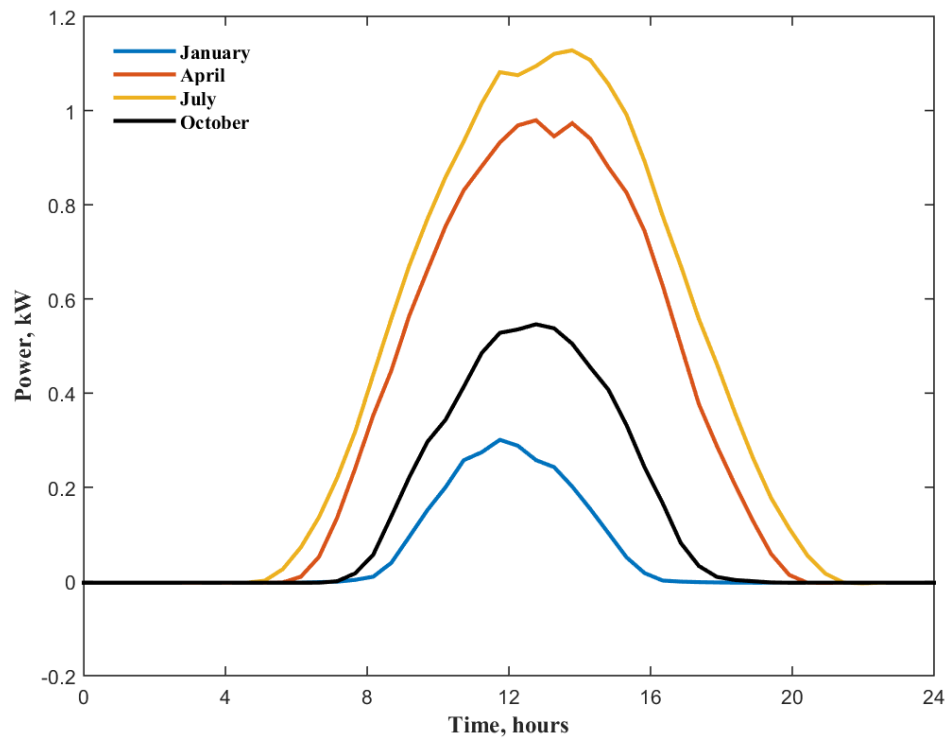


Figure 3.6: Seasonal mean values of PV power generation (data from [115]).

EV charging load profiles were synthesized over each month of the year at half-hourly time steps, as follows.

- The mean values of EV loads for each month (e.g. January) were firstly read from CLNR trials [115], as illustrated in Figure 3.7 (a).
- Then, the mean values of EV loads were disaggregated over a month of half-hourly time steps using normal probability distribution, as shown in Figure 3.7 (b).
- Thereafter, the noisy mean value of EV charging load was smoothed using a median filter, as presented in Figure 3.7 (c). Instead of using a moving average filter, the fifth-order median filter was used to avoid the delay.
- A comparison was made between actual and synthesized values of mean power (i.e. a diagnostic correlation), as demonstrated in Figure 3.7 (d).

Similarly, mean values of EV loads were synthesized for the remaining months of the year (i.e. February to December).

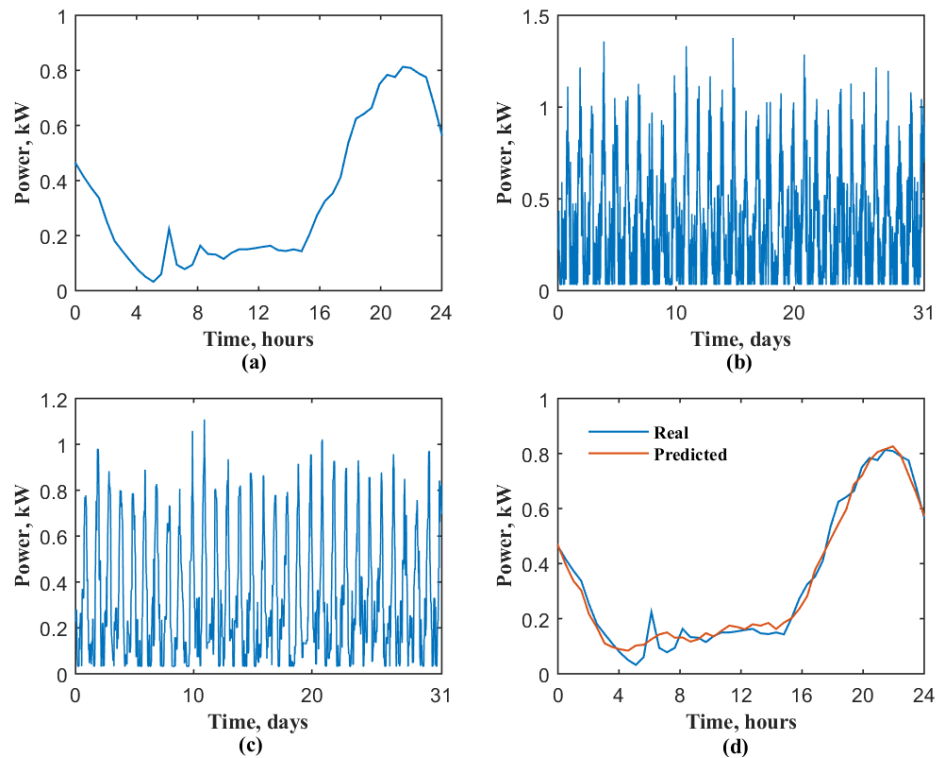


Figure 3.7: (a) Mean values of 133 EV loads (January-2014) based on CLNR trials. (b) Disaggregating. (c) Filtering. (d) Comparing (i.e. a diagnostic correlation).

Figure 3.8 (a) shows the complete mean values of EV charging loads considering a year of half-hourly time steps. Thus, the complete mean values of HP and PV power were similarly synthesized using these steps. Figure 3.8 (b) shows the synthesized power of annual PV generation at half-hourly time steps.

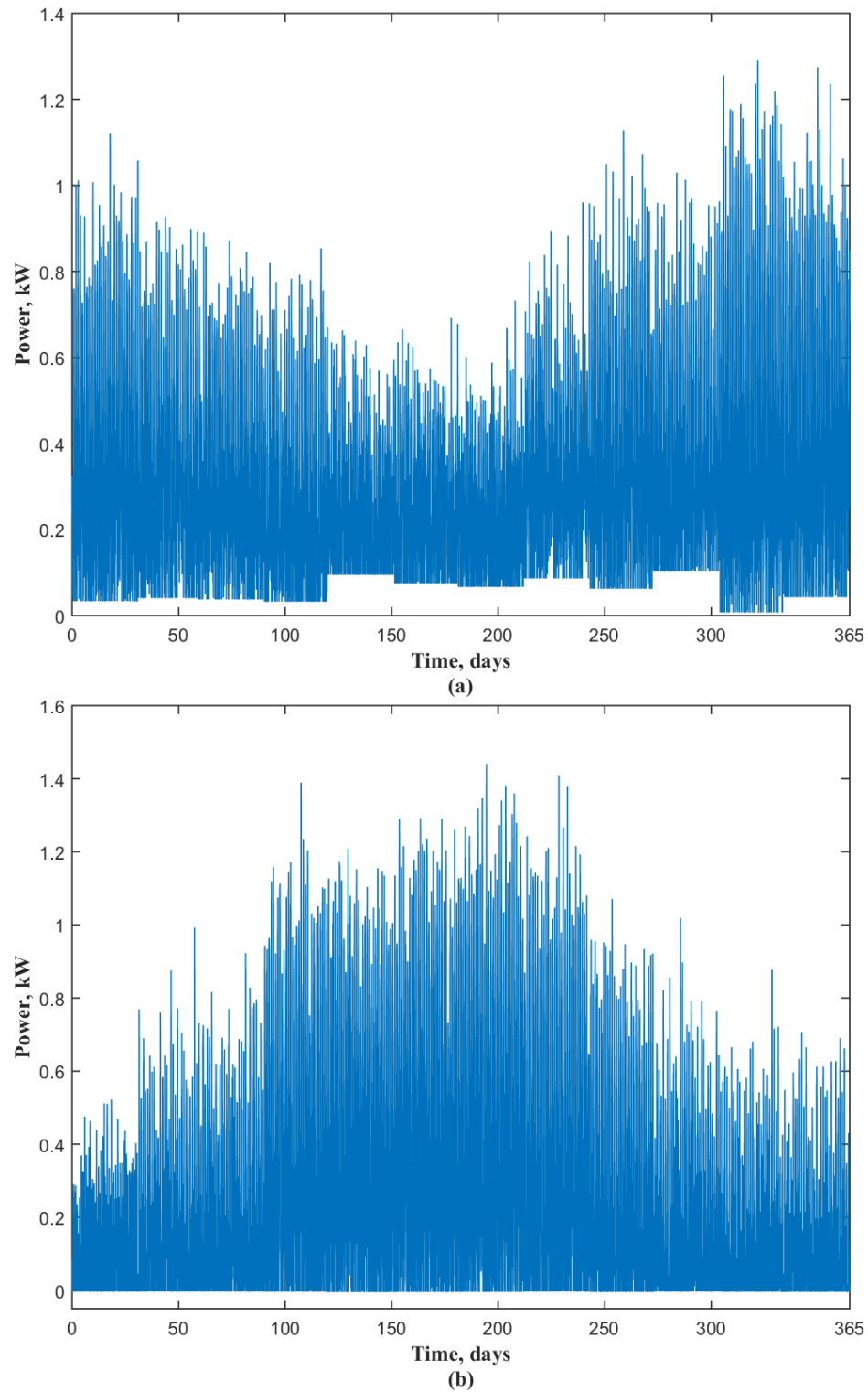


Figure 3.8: The synthesized mean values of power over a half-hourly year of (a) EV charging loads and (b) PV generation.

### 3.3 Demand Predictions with Distributed Energy Resources

According to National Grid ([20], p.6), the four future energy scenarios were defined as follows.

*“Gone Green is a world where green ambition is not restrained by financial limitation... Slow Progression is a world where slower economic growth restricts market conditions... No Progression is a world focused on achieving security of supply at the lowest possible cost... Consumer Power is a world of relative wealth, fast paced research and development and spending”.*

Table 3.1 shows the maximum values of different power profiles over the forthcoming years using “Consumer Power” scenario, as predicted by National Grid in Ref. [20]. These different profiles represent the following quantities:

- The total power of the UK annual demand.
- The total power of EV annual loads.
- The total power of HP annual loads.
- The total power of PV annual generation.

Other three tables were re-arranged for “Gone Green”, “Slow Progression”, and “No Progression” scenarios. For each scenario, these tables were used to scale the following annual profiles: residential demand, EV load, HP load, and PV power. Equation (3.1) is used to predict the UK residential consumption, considering synthesized power profiles of EVs, HPs, and PV arrays.

Table 3.1: The maximum values of the UK total demand and other DER power over the forthcoming years using “Consumer Power” scenario by National Grid [20].

<b>Year</b>	<b>Total demand (GW)</b>	<b>EV load (GW)</b>	<b>HP load (GW)</b>	<b>PV power (GW)</b>
2016	60.5	0.0	0.1	3.9
2020	61.0	0.3	0.6	6.2
2025	62.0	0.9	2.8	9.2
2030	63.0	1.8	5.0	12.1
2035	64.8	3.0	6.6	15.0

$$P_N(t) = A \times x_1 \times P_L(t) + B \times x_2 \times P_{EVs}(t) + C \times x_3 \times P_{HPs}(t) - D \times x_4 \times P_{PVs}(t) \quad (3.1)$$

where  $P_N(t)$  symbolizes the overall predicted residential demand over a year of half-hourly time steps.  $P_L(t)$  symbolizes the UK historic residential demand in 2014.  $P_{EVs}(t)$ ,  $P_{HPs}(t)$ , and  $P_{PVs}(t)$  denote the annual mean values of EV, HP, and PV power, respectively.  $x_1, x_2, x_3$  and  $x_4$  denote the normalizing indices of each power profile, representing the maximum values of power over a year. For example, a 1.29kW is the normalizing index for the synthesized EV charging load profile, as shown in Figure 3.8 (a).  $A, B, C$ , and  $D$  symbolize the scaling factors being evaluated based on the maximum power predicted in Ref. [20] (see Table 3.1) for the ‘‘Consumer Power’’ scenario. Figure 3.9 illustrates the flowchart of the modelling steps to predict the UK residential demand of overall power consumption over the next two decades, considering residential EVs, HPs, and PV arrays.

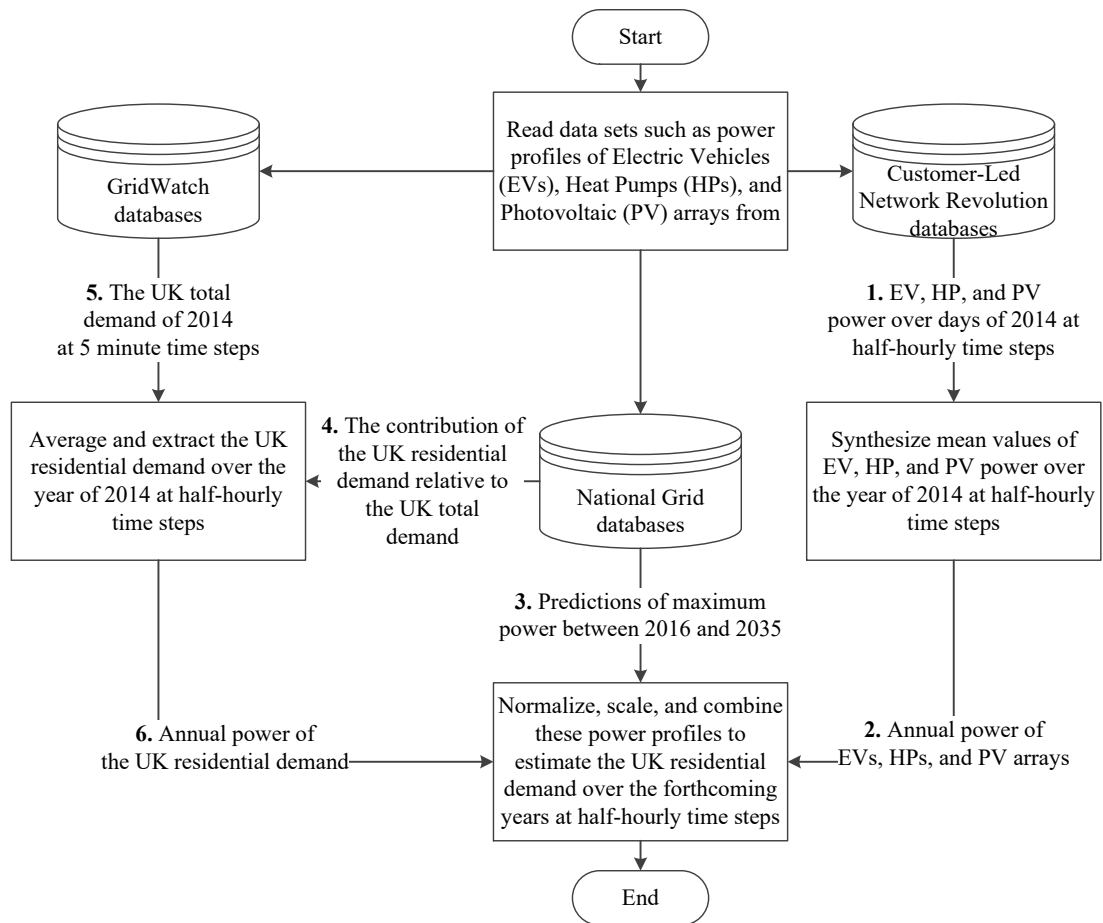


Figure 3.9: The flowchart of the proposed steps to predict the UK residential demand over the next two decades.

### 3.4 Simulation Results

Simulation results were computed using MATLAB R2015a (see Appendix A). Figure 3.10 shows the UK residential demand predicted over the year of 2035 at half-hourly time steps, considering Future Energy Scenarios by National Grid. Figure 3.10 demonstrates the differences of the UK residential demand for each scenario, while considering the aggregated power of residential EVs, HPs, and PV arrays.

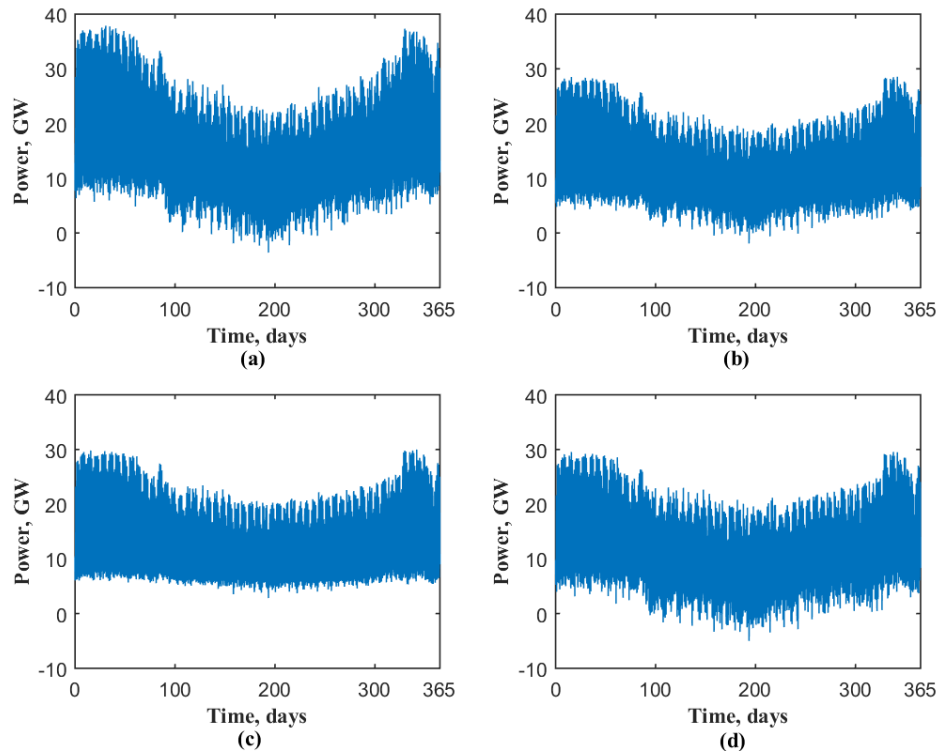


Figure 3.10: A prediction of the UK residential demand with residential EVs, HPs, and PV arrays over a year of half-hourly time steps in 2035 for each scenario. (a) “Gone Green”. (b) “Slow Progression”. (c) “No Progression”. (d) “Consumer Power”.

Figure 3.11 shows the load profiles of the UK residential demand that were predicted for each scenario in 2035, considering four seasonal days. Figure 3.11 (a) presents the UK residential demand on a winter day for these future energy scenarios. Figure 3.11 (b) depicts the UK residential demand on a spring day. Figure 3.11 (c) shows the UK residential demand on a summer day. Residential PV power generation will exceed the UK residential demand by an average power of 2GW during summer mid days in 2035, as shown in Figure 3.11 (c). Figure 3.11 (d) shows the UK residential demand on a day of autumn.

Figure 3.11 illustrates that, a demand increase by an average power of 10GW will occur between 16:00 and 19:00 in 2035 because of the drop in PV generation over that time interval.

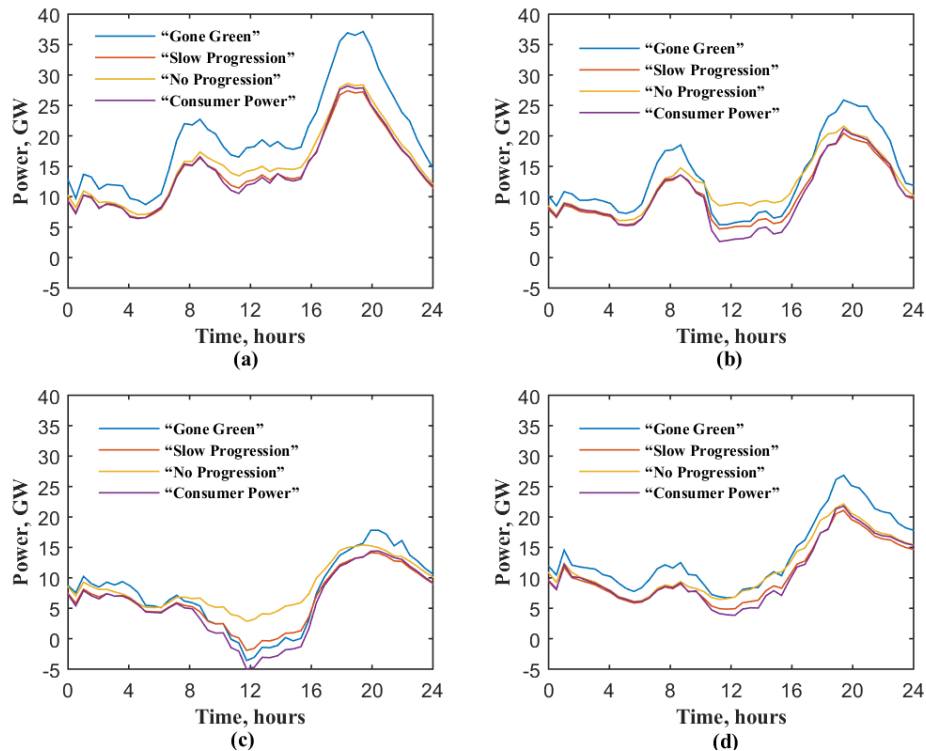


Figure 3.11: The UK seasonal residential demand with residential EVs, HPs, and PV arrays over a day of half-hourly time steps in 2035 of (a) January, (b) April, (c) July, and (d) October.

The UK residential demand was also predicted over the next two decades using “Gone Green” and “No Progression” scenarios, as shown in Figure 3.12 and Figure 3.13, respectively. Boxplots were used to represent the range of the UK residential demand that was predicted for each scenario over the next two decades. The inner edges of these boxplots span between the 25th and 75th percentiles, whereas the outer edges span between the 5th and 95th percentiles.

It can be seen that, the minimum value of the UK residential demand will start to drop below 0GW by 2024 during summer days for “Gone Green” scenario. This drop physically means that, power generation of residential PV arrays will start to meet the minimum value of the UK residential demand by 2024. However, the minimum value of the UK residential demand will continue above 2.78GW during summer mid days for “No Progression” scenario. Therefore, no surplus of PV power generation will be expected with “No Progression” scenario. The 5th, 25th, 75th, and 95th percentiles of

the UK residential demand can be extracted over the next two decades based on Figure 3.12 and Figure 3.13.

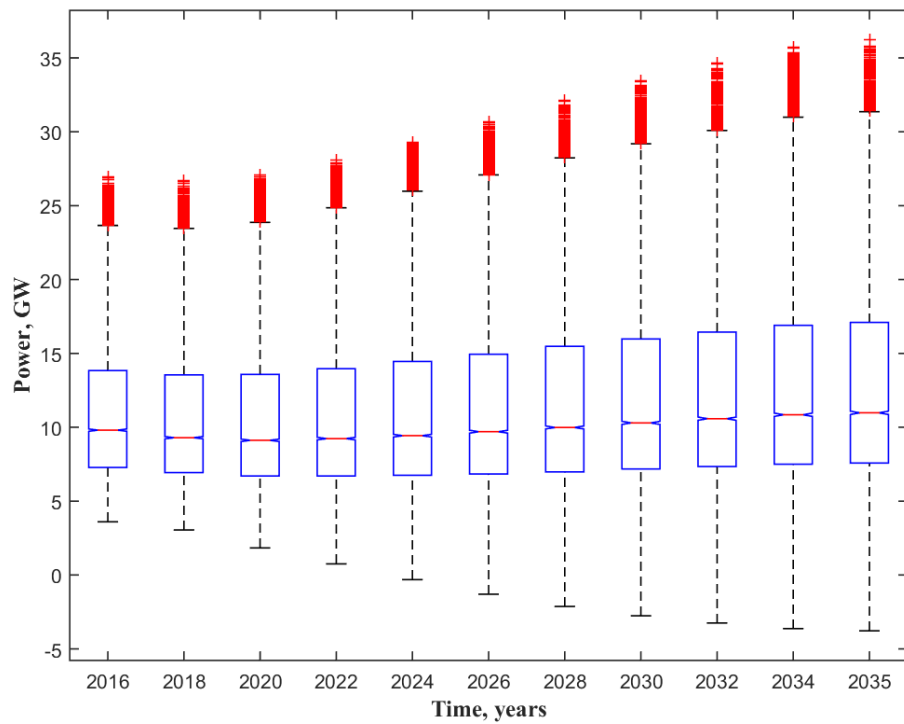


Figure 3.12: A prediction range of the UK residential demand over the next two decades using “Gone Green” scenario.

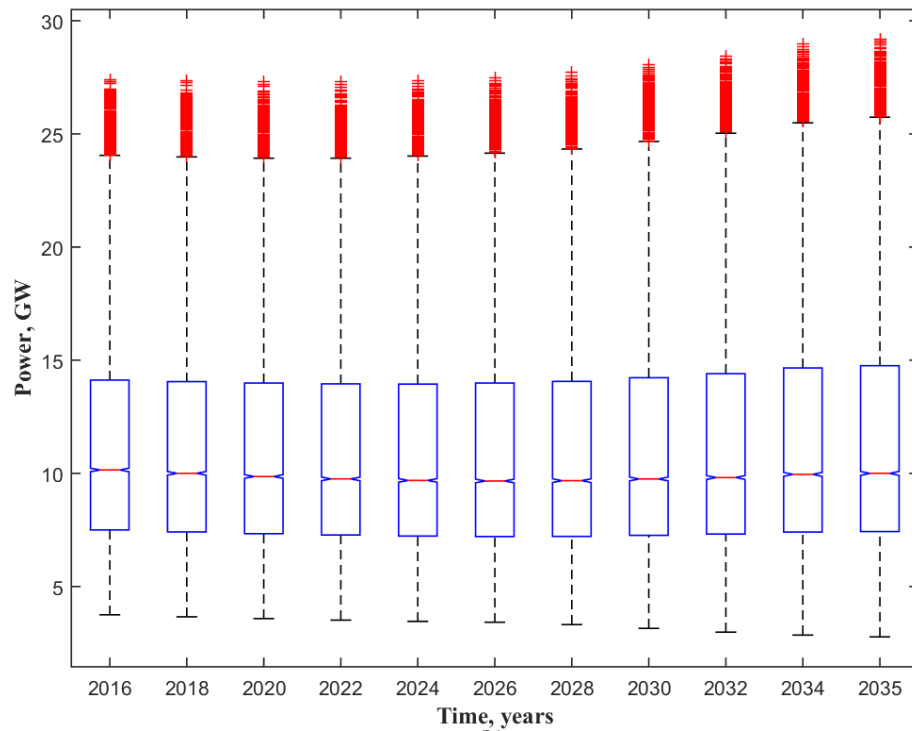


Figure 3.13: A prediction range of the UK residential demand over the next two decades using “No Progression” scenario.

The results of the proposed model are validated, considering a case study presented in Future Energy Scenarios [20]. The minimum value of the UK total demand was predicted to be 16.7GW on a typical summer day by 2020 using “Consumer Power” scenario [20].

Using prediction tool proposed in this project, the minimum value of the UK total demand was calculated to be 16.88GW on 18-July-2020 for “Consumer Power” scenario. The minimum value of the UK total demand was determined using the mid-day percentages of Figure 3.2 (i.e. the UK residential demand contribution relative to the UK total demand). The value of 16.88GW was calculated using Equation (3.2) as follows:

$$P_{total} = (P_{Min} \times C_{non-domestic}) + P_{domestic} \quad (3.2)$$

where  $P_{Min}$  denotes the minimum value of the UK total demand in 2014.  $P_{total}$  and  $P_{domestic}$  denote the minimum values of the UK total demand and residential demand.  $C_{non-domestic}$  denotes the percentage of non-domestic demand contribution. The minimum value of the UK total demand was then calculated in 2020 as follows  $P_{total} = (21 \times 0.72) + 1.76$ . The minimum value of the UK total demand is 16.88GW based on the demand prediction presented in this chapter.

The minimum value of the UK total demand was indicated to be 21GW (see Figure 3.4). Meanwhile, the percentage of non-domestic demand contribution is 72%, as shown in Figure 3.2. Table 3.2 shows that, the minimum value of the UK residential demand is predicted to be 1.76GW in 2020 using “Consumer Power” scenario. Non-domestic PV generations are not considered in Equation (3.2).

Minimum demand was predicted to occur in July-2020 using the proposed model. However, this minimum demand is generally predicted to occur on a typical summer day in 2020 [20]. Table 3.2 shows minimum and maximum values of the UK residential demand over the next two decades for each scenario. This table was generated based on the prediction tool developed in this chapter, using the results of four different boxplots (e.g. Figure 3.12 and Figure 3.13).

Table 3.2: Maximum and minimum values of the UK residential demand over the next two decades based on the proposed prediction calculations.

Scenario	“Gone Green”		“Slow Progression”		“No Progression”		“Consumer Power”	
	Min. demand (GW)	Max. demand (GW)	Min. demand (GW)	Max. demand (GW)	Min. demand (GW)	Max. demand (GW)	Min. demand (GW)	Max. demand (GW)
2016	3.576	27.283	3.688	27.572	3.736	27.704	3.591	27.505
2018	2.970	27.192	3.573	27.616	3.673	27.727	3.115	27.553
2020	1.639	27.736	3.458	27.665	3.629	27.750	1.761	27.738
2022	0.418	29.030	2.849	27.701	3.600	27.823	0.417	28.015
2024	-0.796	30.510	2.116	27.776	3.573	27.936	-0.975	28.109
2026	-1.930	32.028	1.239	27.788	3.454	28.146	-2.278	28.249
2028	-2.879	33.549	0.323	27.807	3.230	28.408	-3.382	28.479
2030	-3.609	35.004	-0.570	27.880	3.043	28.821	-4.289	28.663
2032	-4.184	36.291	-1.355	28.230	2.858	29.242	-5.001	28.893
2034	-4.627	37.464	-2.130	28.495	2.711	29.811	-5.531	29.259
2035	-3.603	37.878	-1.927	28.550	2.835	29.980	-5.002	29.567

### 3.5 Conclusions

The UK overall residential demand was predicted over the next two decades with the integration of residential EVs, HPs, and PV arrays. The proposed prediction tool was implemented over the forthcoming years at half-hourly time steps, considering recorded historic demand measurements and synthesized DER power profiles. Normal probability distribution and median filter were used to synthesize annual power profiles of these low carbon technologies using the mean values of daily power profiles, which were acquired from CLNR trails.

Future energy scenarios, which were presented by National Grid, were re-arranged into tables to store the maximum values of the UK total demand, the EV load, the HP load, and the PV power. Then, these tables were used to scale the normalized values of synthesized power profiles of DER units. Thereafter, these power profiles were combined to predict the UK residential demand over the coming years.

Simulation results indicated that, a surplus of PV power generation will exceed the UK residential demand by an average of 2GW in 2035. The UK residential demand will increase by an average of 10GW between 16:00 and 19:00, because PV power generation will drop over that time interval on a summer day of 2035.

The minimum value of the UK residential demand will be met by residential PV power generation for “Gone Green” and “Consumer Power” scenarios by 2024. However, simulation results of “No Progression” scenario demonstrated that, the minimum value of the UK residential demand would continue above 2.8GW until 2035.

The challenge of a considerable demand reduction followed by a sharp demand increase due to PV power generation, which is predicted over the time interval between 12:00-19:00, can be partially mitigated by incentivizing EV owners to charge their batteries during mid-day time.

## CHAPTER 4

### 4. Impacts of Distributed Energy Resources on Distribution Networks

#### 4.1 Introduction

This chapter studies the impacts of electric vehicles (EVs), heat pumps (HPs), and photovoltaic (PV) arrays on distribution networks based on voltage magnitudes, voltage unbalance factors, and other network constraints. Low voltage sections of test and real networks were studied using deterministic and stochastic methods.

The purpose of the deterministic method is to evaluate the hosting capacity of the network under study with uncoordinated EV charging loads. The purpose of the stochastic method is to determine the uncertainties of different EV, HP, and PV combinations in the network under study.

The low voltage section of the test network was modelled using MATLAB/Simulink. Four deterministic case studies were simulated to record the results of uncoordinated EV charging loads. The low voltage section of the real network was modelled using a MATLAB function of unbalanced load flow that was developed in this research. Results of five stochastic case studies were recorded with different combinations of EVs, HPs, and PV arrays.

#### 4.2 Methodology of Deterministic Studies

The impact of uncoordinated EV charging loads on a low voltage section of the UK generic distribution network (UKGDN) was studied by monitoring voltage magnitudes, voltage unbalance factors, and other network constraints. The specifications of the UKGDN components were acquired from Department of Trade and Industry (DTI) [116]. The low voltage section of this network was modelled using three-phase four-wire system in MATLAB/Simulink/Simscape/SimPowerSystems.

Different case studies were investigated by connecting 96, 192, and 288 EVs to the UKGDN section. Residential loads were modelled over a day of half-hourly time steps based on mean values of the active power of 8,000 customers. Similarly, EV

charging loads were considered on a half-hourly day using mean values of the active power of 133 EVs. The mean values of residential loads and EV loads were read from Customer-Led Network Revolution (CLNR) project [115], compiling data every half hour. Figure 4.1 illustrates the workflow of deterministic case studies.

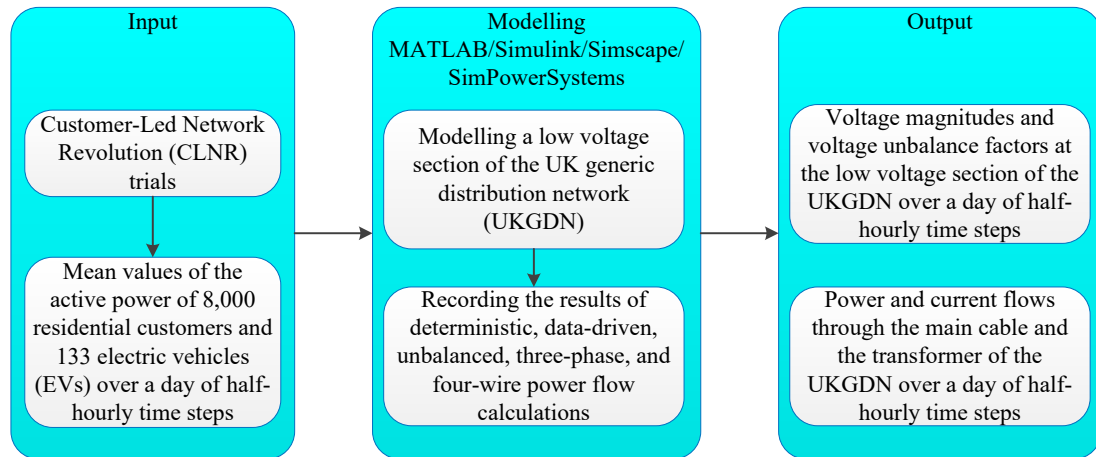


Figure 4.1: The workflow of deterministic case studies.

#### 4.2.1 The Network under Deterministic Studies

Figure 4.2 shows an adapted low voltage section of the UKGDN [116]. Nodes 0, 1, 2, 3, and 4 are allocated to measure voltage magnitudes and voltage unbalance factors along the feeder.

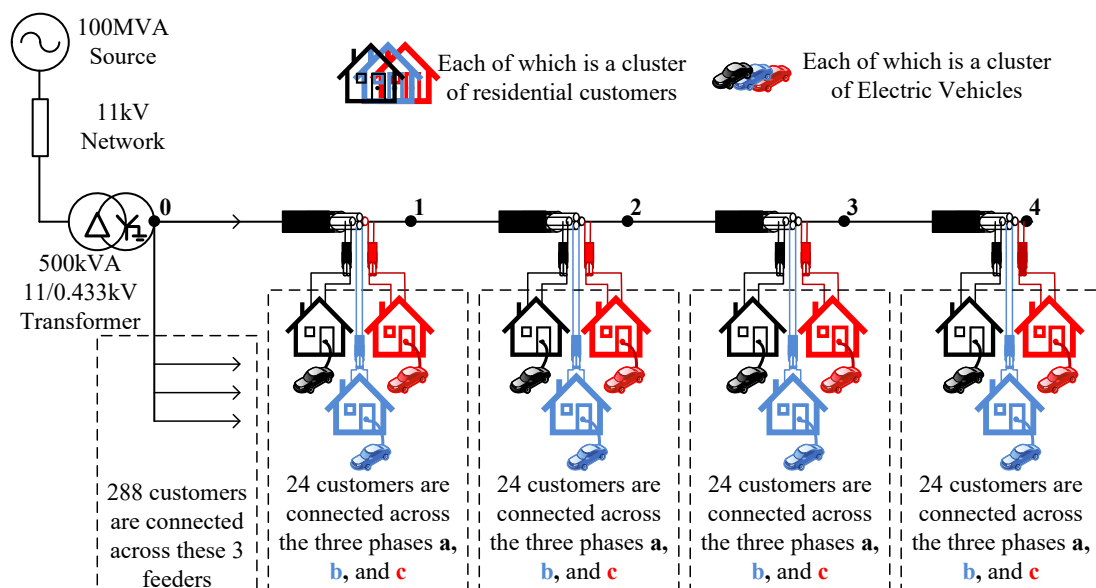


Figure 4.2: The schematic diagram of the network under deterministic studies with EVs.

The modified section of the UKGDN is described as follows. A 500kVA ground-mounted distribution transformer steps down 11kV to 0.433kV, serving 384 customers. These customers are distributed across four feeders with 96 customers for each feeder. The UKGDN feeder is modelled in details with four segments of underground cables, as presented in Figure 4.2.

The characteristics of network cables are [116]:

- A 4-core underground cable (a three-phase line and a neutral line) of 150m long, 185mm<sup>2</sup> spans from node 0 to node 2.
- A 4-core underground cable (a three-phase line and a neutral line) of 150m long, 95mm<sup>2</sup> spans from node 2 to node 4.
- 2-core cables (single-phase lines and neutral lines) of 30m long, 35mm<sup>2</sup> individually serve residential customers.

The other three feeders serve 288 residential customers. Figure 4.2 shows the low voltage section of the UKGDN using three-phase four-wire connections, which were modelled in MATLAB/Simulink/Simscape/SimPowerSystems (see Appendix B).

Figure 4.3 illustrates mean values of the active power of residential loads and EV loads over a day of half-hourly time steps, as recorded by the smart meters of CLNR customers during their trials between 2012 and 2014.

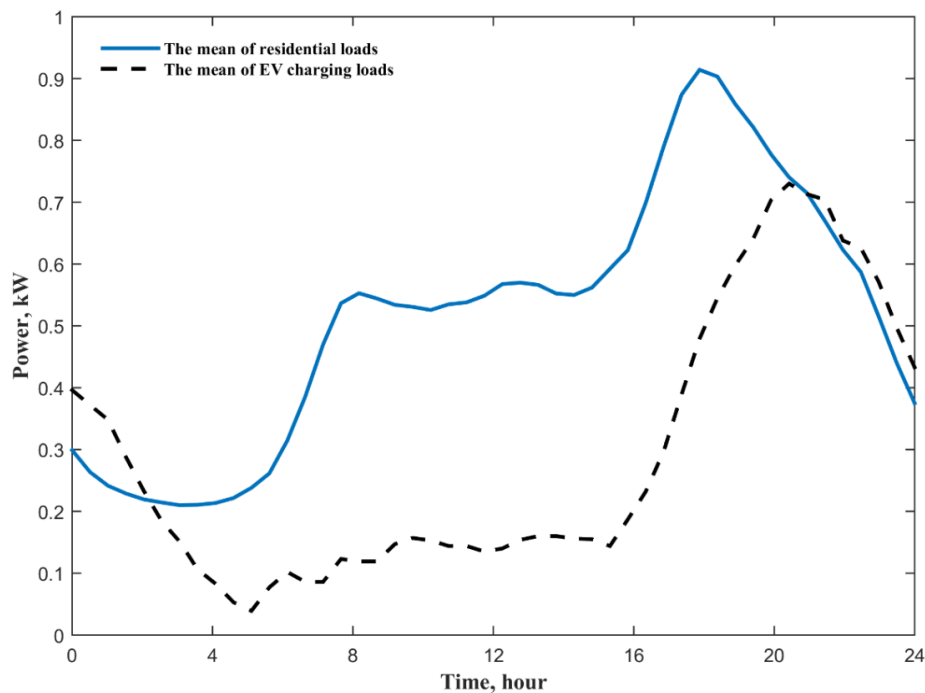


Figure 4.3: Mean values of active power of 8,000 residential customers and 133 EVs (power data from [115]).

Uncoordinated single-phase EV charging loads can violate the limits of voltage magnitudes and voltage unbalance factors. According to Engineering Recommendation P28, the steady-state tolerances of voltage fluctuations were assigned at the low voltage level to be between -6% and +10% of the nominal voltage [117].

The steady-state limit of voltage phase unbalance was indicated to be less than 1.3% according to Engineering Recommendation P29 [118]. Voltage Unbalance Factor ( $VUF\%$ ) in percentage is defined as the ratio of the negative sequence component to the positive sequence component of phase voltages. To avoid dealing with complex numbers,  $VUF\%$  is calculated as follows [119].

$$VUF\% = \frac{\text{Max}(|V_a - V_{av}|, |V_b - V_{av}|, |V_c - V_{av}|)}{V_{av}} \times 100\% \quad (4.1)$$

where  $V_{av} = (V_a + V_b + V_c)/3$ , and  $V_a, V_b, V_c$  denote the voltage magnitude across the three phases “a”, “b”, and “c”.

#### 4.2.2 Deterministic Case Studies

Four case studies were implemented in MATLAB/Simulink to assess the impacts of uncoordinated single-phase EV charging loads on the network under study. The case studies are described as follows.

Case-1 has evaluated the network under study with residential loads only without any EV charging loads. Case-2 has evaluated the network under study with residential loads and uncoordinated 96 EV loads, which were evenly distributed across the three phases. Case-3 has evaluated the network under study with residential loads and uncoordinated 192 EV loads. Case-4 has evaluated the network under study with residential loads and 288 EVs.

Unbalanced phase voltages can particularly occur at the end node of a long radial feeder with a high impedance. Therefore, node 4 was selected to record the results of voltage magnitudes and voltage unbalance factors. Table 4.1 shows the connected numbers of EVs to the low voltage section of the UKGDN for each case study.

Table 4.1: The considered deterministic case studies.

Case studies	The number of EVs	The number of customers
Case-1	0	384
Case-2	96	384
Case-3	192	384
Case-4	288	384

### 4.3 Simulation Results of Deterministic Studies

Figure 4.4 depicts the aggregated loads of residential customers and EVs over a day of half-hourly time steps for each deterministic case study. These loads were aggregated at the distribution transformer. The peak loads of individual residential customers were adjusted to be 1.3kW based on the literature [116]. The individual EV charging load was assumed 3.3kW considering a typical, residential, single-phase, and slow charging mode.

In Case-1, the peak load of distribution transformer was 1pu (i.e. 500kW), as shown in Figure 4.4. The peak load flow of distribution transformer gradually increases with the increase of the number of connected EVs for Case-2, Case-3, and Case-4, as shown in Figure 4.4. The direct increase of transformer overload was recorded because mean values of residential loads and EV loads were nearly coincident over peak-hour intervals, as seen in Figure 4.3.

Figure 4.5 illustrates root mean square (RMS) current flows through the main cable segment (i.e. between node 0 and node 1) for each case study. RMS current values are recorded over a day of half-hourly time steps. There will be different levels of current flows through the three phases even if similar EV charging loads are equally distributed across the three phases. This is a result of different EV charging durations. The current flow of phase “c” was increased by 50% of the rated value in Case-4 over peak-hour time intervals, as indicated in Figure 4.5 (d).

Figure 4.6 presents a separate observation of RMS phase voltage magnitude across the three phase for each case study at the end node of the low voltage feeder (i.e. node 4). It can be seen that, voltage magnitudes did not drop below the limit for all case studies.

The percentages of voltage unbalance factors were recorded to be within the limit (i.e. less than 1.3%) for all deterministic case studies, as demonstrated Figure 4.7.

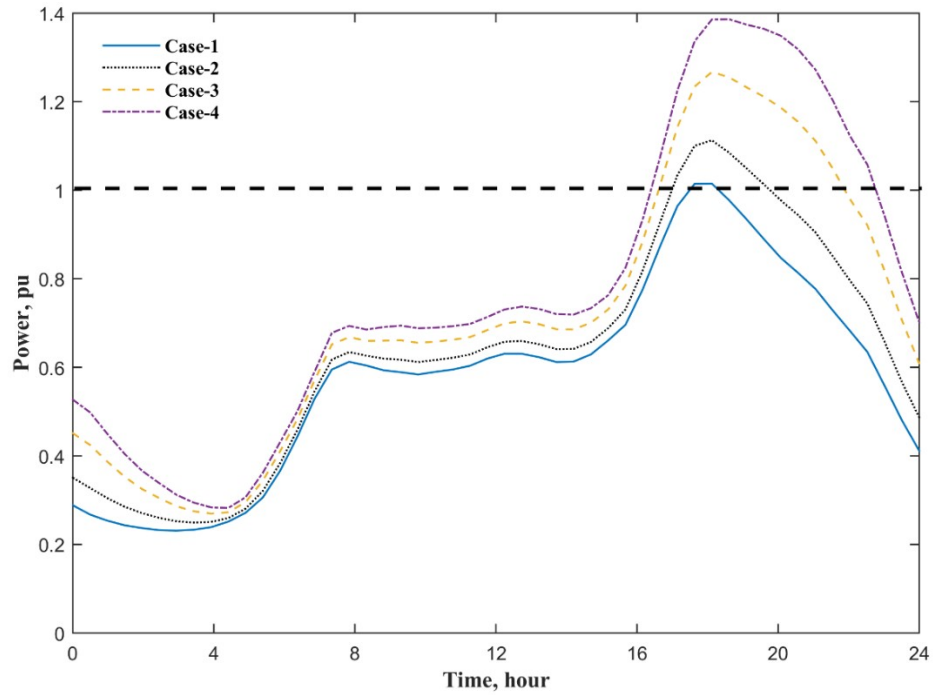


Figure 4.4: The aggregated loads of residential customers and EVs over a day of half-hourly time steps at the distribution transformer of the UKGDN for each case study.

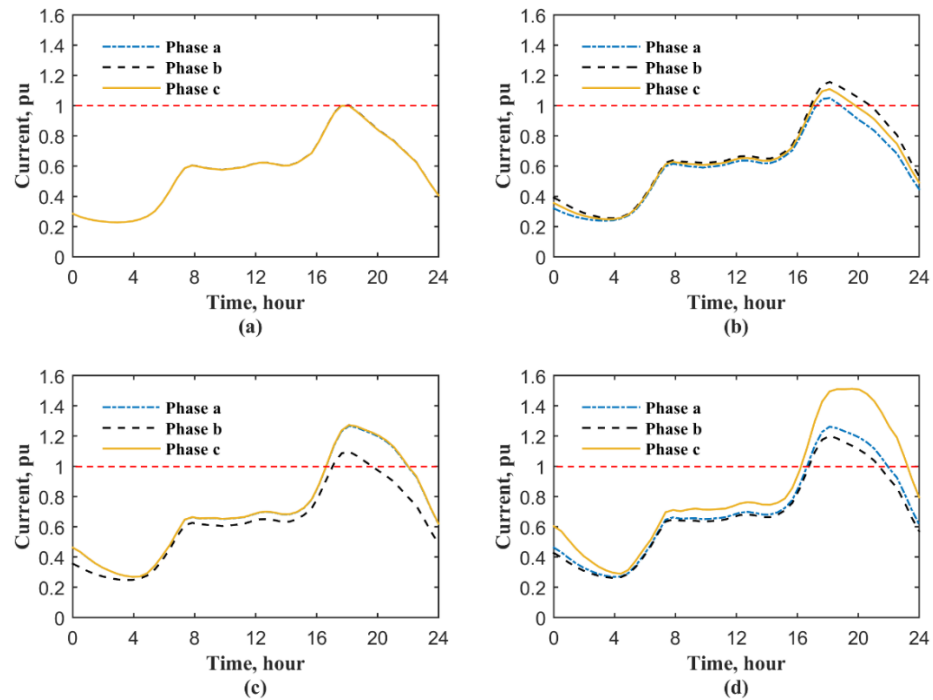


Figure 4.5: RMS phase current flows of the cable segment between node 0 and node 1 for each case study over a day of half-hourly steps (a) Case-1, (b) Case-2, (c) Case-3, and (d) Case-4.

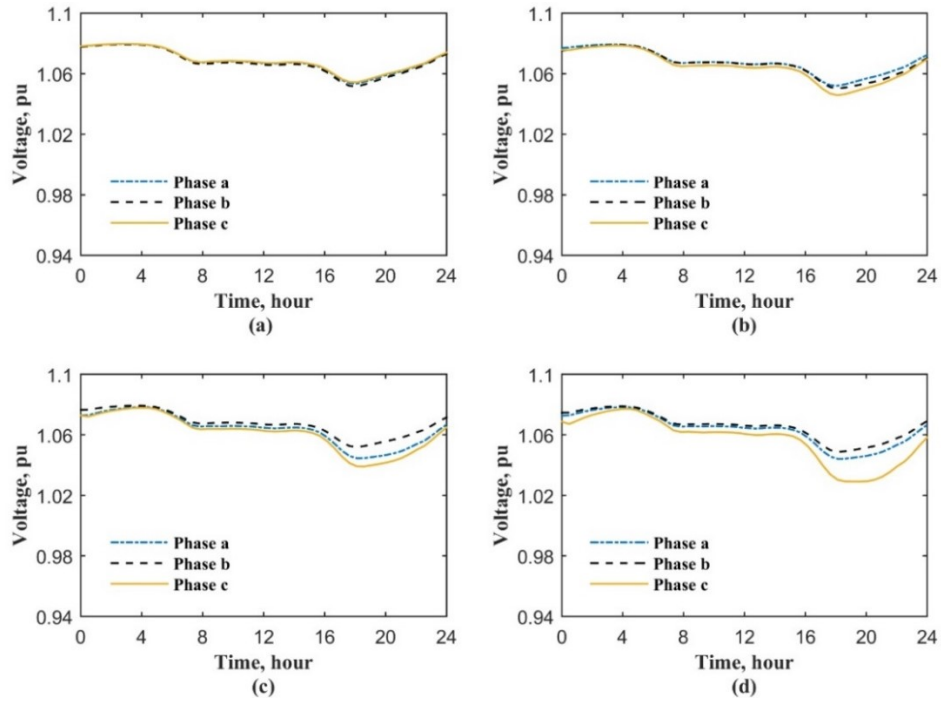


Figure 4.6: RMS voltage magnitudes over a day of half-hourly time steps at node 4 for each case study (a) Case-1, (b) Case-2, (c) Case-3, and (d) Case-4.

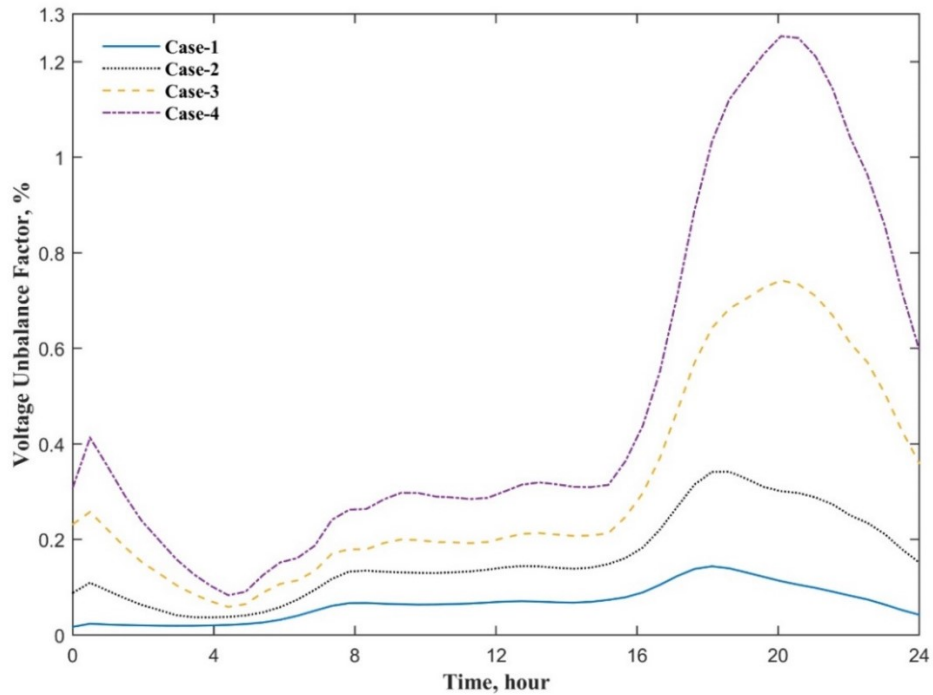


Figure 4.7: The percentages of voltage unbalance factors over a day of half-hourly time steps, as recorded at node 4 for each case study.

#### 4.4 Methodology of Stochastic Studies

Uncertainties of different EV, HP, and PV combinations were determined using stochastic case studies. Stochastic results were recorded using a real low voltage network of Electricity North West, which was adapted from [120].

The loads of residential customers and EVs were individually generated over a day of minute-by-minute time steps using normal and uniform probabilistic distributions based on mean values and standard deviations of 8,000 residential loads and 133 EV loads, as reported by CLNR trials [115].

HP individual loads were mathematically modelled over a day of minute-by-minute time steps based on ambient temperatures [121]. PV individual power was mathematically modelled on a minute-by-minute basis using solar irradiance [121]. A one-minute time step was selected to maintain the use of real-time applications. Simulation results were presented using the following quantities: RMS phase voltage magnitudes, voltage unbalance factors, and load flows through transformer and cables. The results were calculated using a MATAB function of unbalanced load flow that was developed in this project. Figure 4.8 demonstrates the workflow of stochastic case studies.

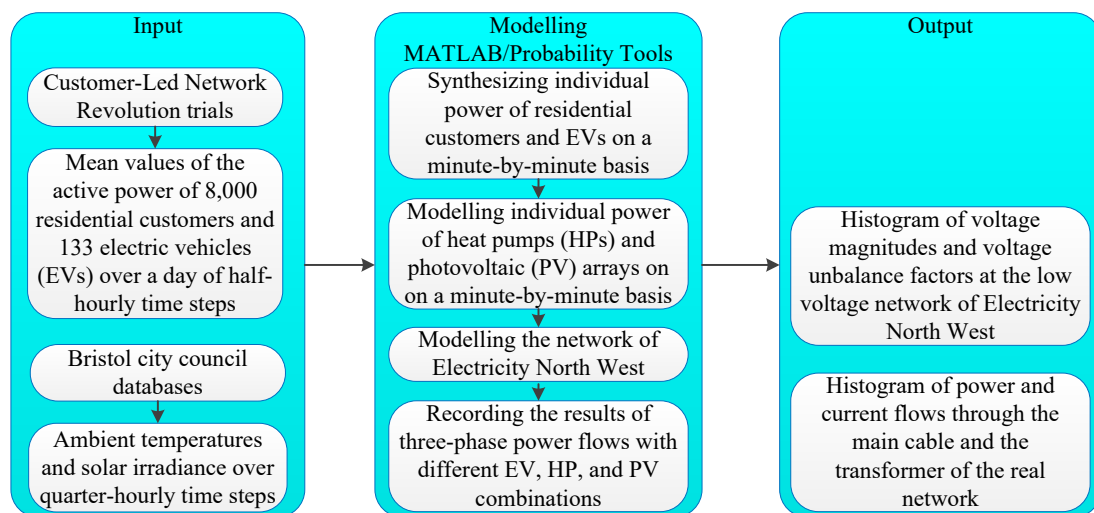


Figure 4.8: The workflow of stochastic case studies.

##### 4.4.1 The Network under Stochastic Studies

An adapted low voltage network of Electricity North West was considered, as presented in Figure 4.9. It consists of a 500kVA ground-mounted distribution transformer as well as two main low voltage feeders serving 135 customers.

Nodes 0, 1 and 2 were allocated to measure RMS phase voltage magnitudes and voltage unbalance factors. Feeder 1 spans from node 0 to node 1, serving 56 customers as illustrated in Figure 4.9. Customers were distributed across the three phases of “a”, “b”, and “c” as reported in [120], as follows. Twenty-one customers were connected to the phase “a”, while connecting 20 and 15 customers to the phase “b”, and to the phase “c”, respectively. Feeder 2 spans from node 0 to node 2, serving 76 customers. Twenty-two customers were connected to the phase “a”, whereas 37 and 20 customers were connected to the phase “b” and the phase “c”, respectively.

It was assumed that, the distribution transformer serves a lumped load as twice as the load of these two feeders, as shown in Figure 4.9. This assumption was made because low voltage transformers were typically allocated to serve an average of 400 residential customers in the UK, as reported in [116]. The sizes of main underground cables were  $185\text{mm}^2$  and  $95\text{mm}^2$ . Meanwhile, the sizes of individual service cables are  $35\text{mm}^2$  and  $25\text{mm}^2$ .

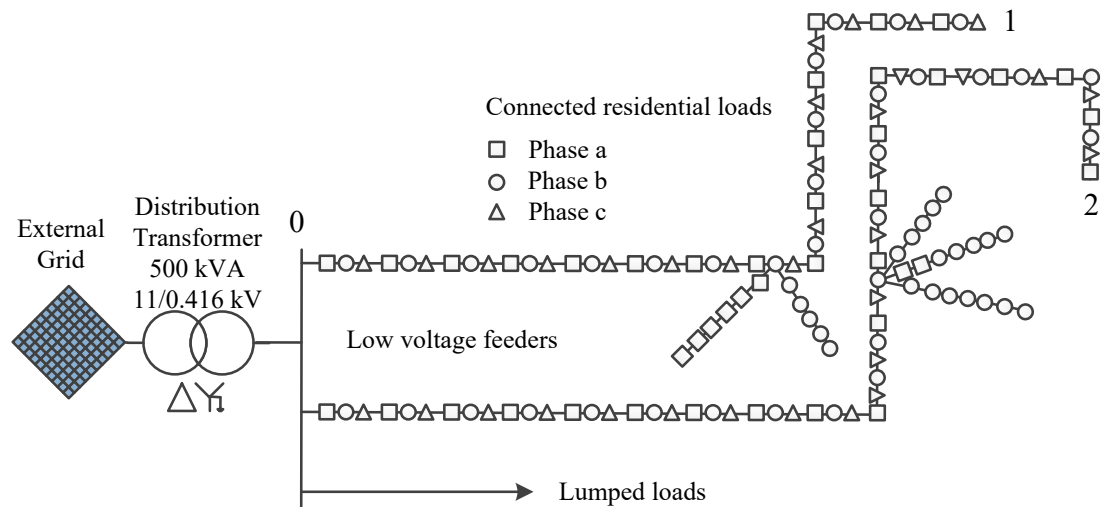


Figure 4.9: The network under stochastic studies (adapted from [120]).

#### 4.4.2 Individual Loads of Residential Customers

A normal probability distribution was used to synthesize the individual loads of residential customers over a day of minute-by-minute time steps. Figure 4.10 illustrates the steps of synthesizing individual daily profiles of residential customers using MATLAB R2015a, considering mean values (Figure 4.11) and standard deviations of 8,000 residential of CLNR project [115]. The numbers of generated individual residential loads can be adjusted in the third step of the proposed algorithm, as shown

Figure 4.10. In this study, only 135 individual residential loads were generated over a day of minute-by-minute time steps to maintain a near real-time observation.

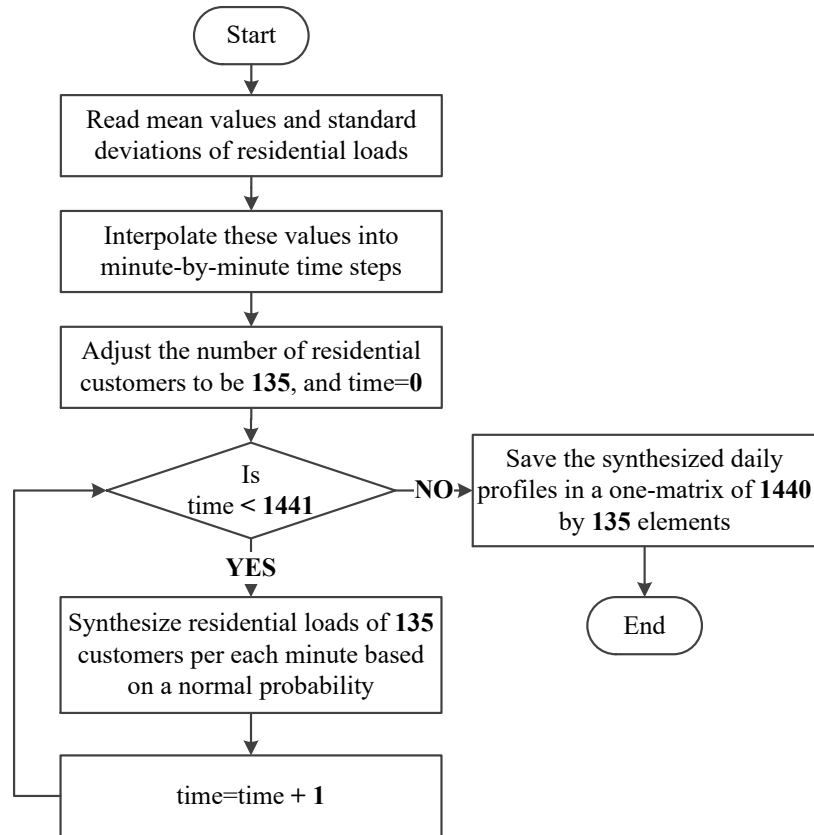


Figure 4.10: The flowchart of stochastically generating residential load profiles.

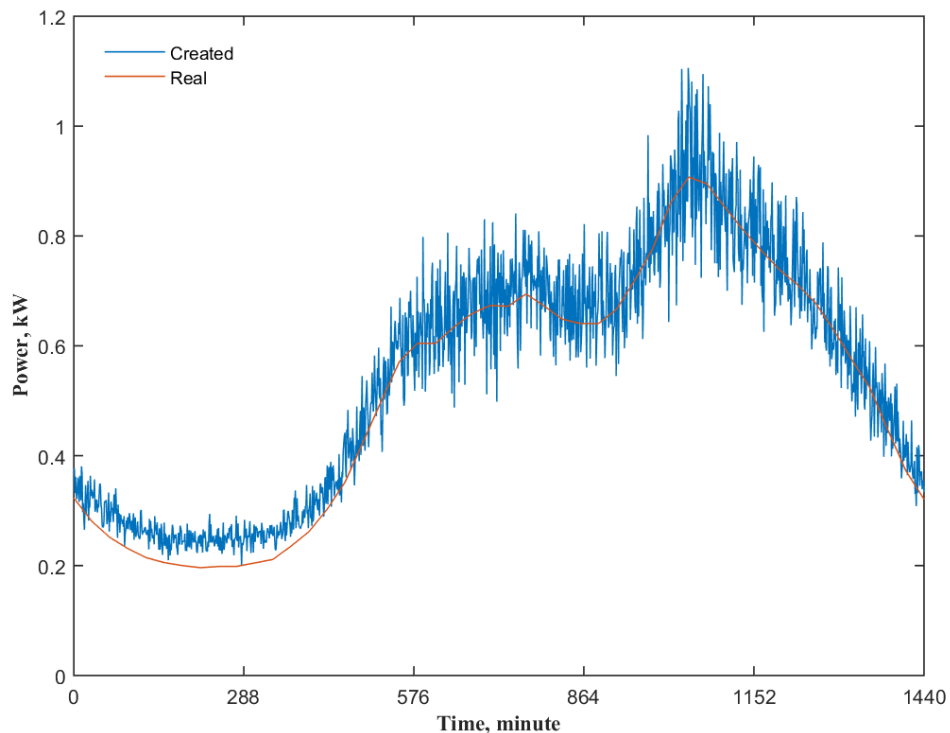


Figure 4.11: Daily demand means of stochastically generated residential loads relative to the actual residential demand mean (real).

Figure 4.11 shows the mean value of 135 generated residential customers, as compared to the real mean value of residential loads. Mean values of generated and actual residential loads are relatively similar on a day, as shown in Figure 4.11. The mean values of the active power of 8,000 residential customers over a day of half-hourly time steps were acquired from CLNR project [115]. Mean values of individual loads have illustrated that, an acceptable correlation was achieved between synthesized and real loads of residential customers.

#### 4.4.3 Individual Loads of Electric Vehicles

EVs were assumed to be recharged using uncoordinated charging patterns. A flat, residential, single-phase, and slow charging mode was considered with 3.3kW to recharge EVs. Different capacities of EV batteries were considered with less than or equal to 24kWh. EV charging efficiencies were assumed to be 90.9%. Hence, 8 hours are required to recharge a 24kWh EV battery from 0% to 100% BSoC level.

Figure 4.12 represents the mean values of synthesized EV charging loads using a uniform integer probability distribution. Mean values of 133 EV charging loads were read from CLNR trails over a day of half-hourly time steps to guide a MATLAB function of uniform probability distribution. Then, EV charging loads were individually generated over a day of minute-by-minute time steps.

The synthesized mean values of EV charging loads were verified based on daily trips of UK commuters, as reported in [122]. An 80% of EVs was assumed to be charged between 17:00 and midnight, whereas a 20% of EVs has been assumed to be recharged between midnight and 17:00 on the next day. This assumption was made because the majority of the daily trips of private vehicles occur between 06:00 and 17:00 according to the literature [122].

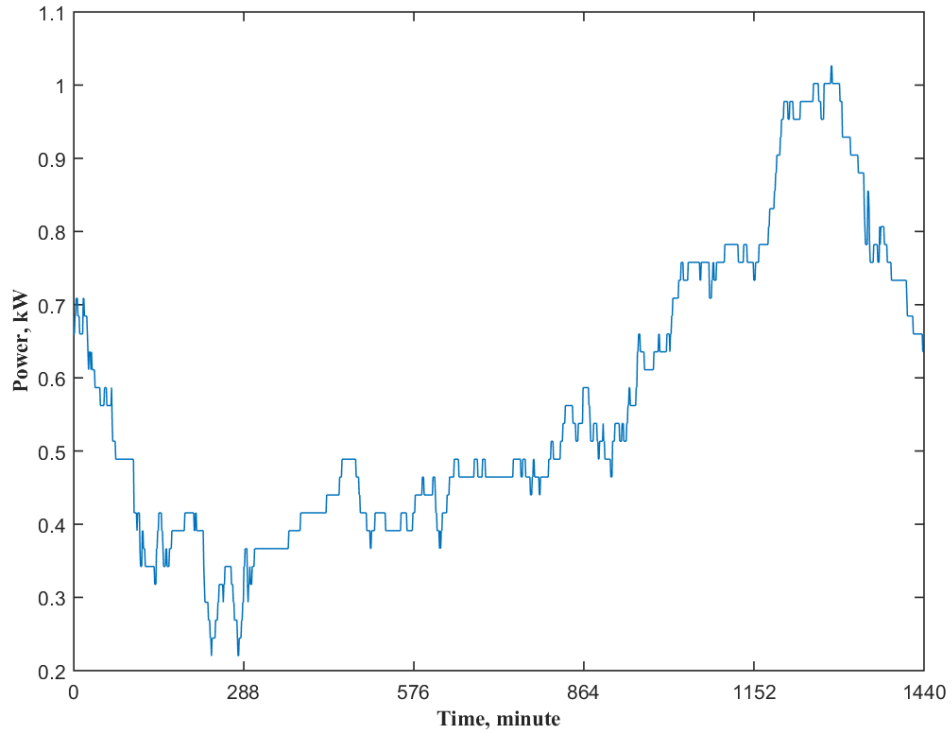


Figure 4.12: The mean values of synthesized EV charging loads of 135 EVs.

#### 4.4.4 Modelled Loads of Heat Pumps

Electrical power drawn by the indoor/outdoor units of an air source HP unit is mainly driven by HP coefficient of performance ( $CoP$ ). The maximum value of ( $CoP$ ) is evaluated as follows [123].

$$CoP_{Max} = \frac{T_2}{T_2 - T_1} \quad (4.2)$$

where  $CoP_{Max}$  denotes the maximum coefficient of performance.  $T_1$  and  $T_2$  denote the outdoor and indoor temperatures of HPs in Kelvin. Equation (4.3) is used to calculate HP demands, including demand by fan and compressor units [124].

$$p_{HP} = \frac{\rho \times (T_2 - T_1)}{3160 \times CoP} \quad (4.3)$$

where  $p_{HP}$  denotes the total HP demand in W.  $\rho$  denotes the HP compressed air density by both indoor and outdoor units in cubic feet per minute. Meantime,  $T_2, T_1$  are measured in Fahrenheit ( $^{\circ}F$ ). Equation (4.4) is acquired by substituting (4.2) in (4.3) for the maximum coefficient of performance with temperatures in centigrade ( $^{\circ}C$ ).

$$p_{HP} = \frac{\rho \times [1.8 \times (T_2 - T_1)^2 + 32 \times (T_2 - T_1)]}{3160 \times \alpha \times (T_2 + 273.15)} \quad (4.4)$$

where  $T_1$  and  $T_2$  denote HP supply and HP return temperatures in °C. HPs were assumed to operate based on a parameter ( $\alpha$ ) of less than “1” to reduce the substituted value of  $CoP_{Max}$ , as indicated in Equation (4.4).

Figure 4.13 depicts daily profiles of HP demand over 135 days. A total capacity of 1000 cubic feet per minute was assumed for the compressed air by indoor and outdoor fans. Ambient temperatures are used to generate daily HP profiles, as recorded by Bristol city council over winter days in 2014 [121]. HP thermostatic load control devices were stochastically modelled using a uniform distribution probability by multiplying Equation (4.4) with generated values of “0” and “1”.

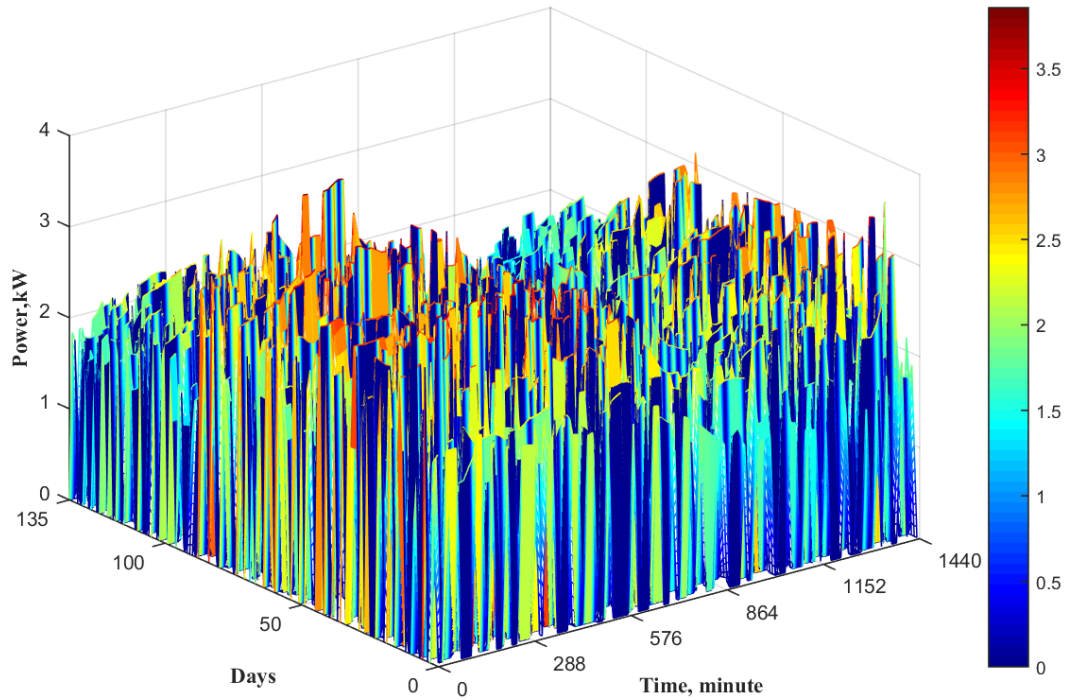


Figure 4.13: HP loads over 135 days of minute-by-minute time steps.

#### 4.4.5 Modelled Power of Photovoltaic Arrays

Power generations from solar panels are calculated by considering solar irradiance as indicated in the following equation [120].

$$p_{PV} = \beta \times PV_{cap.} \times PV_{area} \times PV_{efficiency} \times INV_{efficiency} \quad (4.5)$$

where  $p_{PV}$  denotes the output power of PV array in W.  $\beta$  denotes the solar irradiance in  $W/m^2$ .  $PV_{cap.}$  denotes the installed capacity of PV panel in W (i.e. 2000 W).  $PV_{area}$  denotes the area of each 1000 W of installed PV in  $m^2$  (i.e.  $2 m^2$ ).  $PV_{efficiency}$  denotes the efficiency of the solar panel (i.e. randomly generated between 10% and 19%).  $INV_{efficiency}$  denotes the efficiency of the inverter (i.e. randomly generated between 88% and 96%). Solar irradiance in Bristol is used to create daily PV power generation profiles over 135 days over April, May, June, July, and August 2014 [121]. These readings have been interpolated into datasets of a one-minute time resolution. Figure 4.14 shows diurnal profiles of the installed PV array during 135 days.

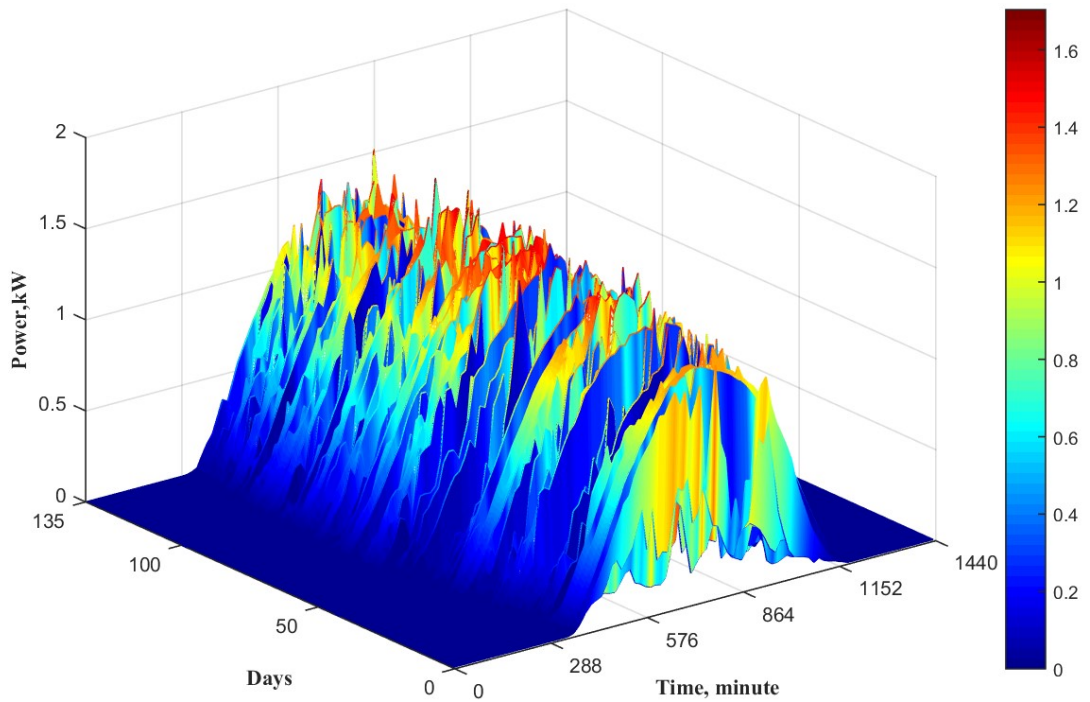


Figure 4.14: PV generations over 135 days of minute-by-minute time steps.

#### 4.4.6 Stochastic Case Studies

The case studies were structured as follows:

- Case 1 evaluated the network using the unbalanced power flow without EV, HP, and PV connections. Therefore, only stochastic residential loads were considered.
- Case 2 evaluated the network using the unbalanced power flow with PV connections only. Hence, residential customers and PV arrays were considered.

- Case 3 evaluated the network using the unbalanced power flow with EV connections only. Therefore, residential loads and EV loads were considered.
- Case 4 evaluated the network using the unbalanced power flow by considering residential loads and HP loads.
- Case 5 evaluated the network using the unbalanced power flow by considering residential loads with EVs, HPs, and PV arrays together.

#### 4.5 Simulation Results of Stochastic Studies

Simulation results were computed using MATLAB R2015a (see Appendix C), considering the individual power of residential customers, EVs, HPs, and PV arrays, as follows.

Figure 4.15 represents the histograms of Case 1 with the real network of Electricity North West. Figure 4.15 (a) illustrates the histogram of RMS voltage magnitudes at node 1 and node 2 for Case 1. Recorded voltage magnitudes are within the limits in Case 1 (i.e. 1pu =230V). Figure 4.15 (b) demonstrates voltage unbalance factors of these nodes, which are within their limits. The power flow through the transformer did not exceed 0.7pu, as shown in Figure 4.15 (c). RMS current flow through the underground cables of the feeder did not exceed 0.5pu, as presented in Figure 4.15 (d).

Figure 4.16 shows the histograms of Case 2. Figure 4.16 (a) shows an increase of RMS voltage magnitudes due to the reversed power flow of PV power, but this increase is still within the accepted limit. Figure 4.16 (b) shows an increase of voltage unbalance factors. The power flow through the distribution transformer is decreased due to the injected power of PV arrays over the mid-day interval, as presented in Figure 4.16 (c). The reversed power flow of PV generation has also led to a decrease in RMS current flow through underground cables of residential feeders, as depicted in Figure 4.16 (d).

In Case 3, Figure 4.17 (a) shows a decrease of RMS voltage magnitude due to the additional charging demand of EVs. Voltage unbalance factors are significantly increased with EV charging loads, as seen in Figure 4.17 (b). The power flow through the distribution transformer is recorded to be 140% of the rated value, as shown in Figure 4.17 (c). RMS current flow through feeders is recorded to reach the rated value, as presented in Figure 4.17 (d).

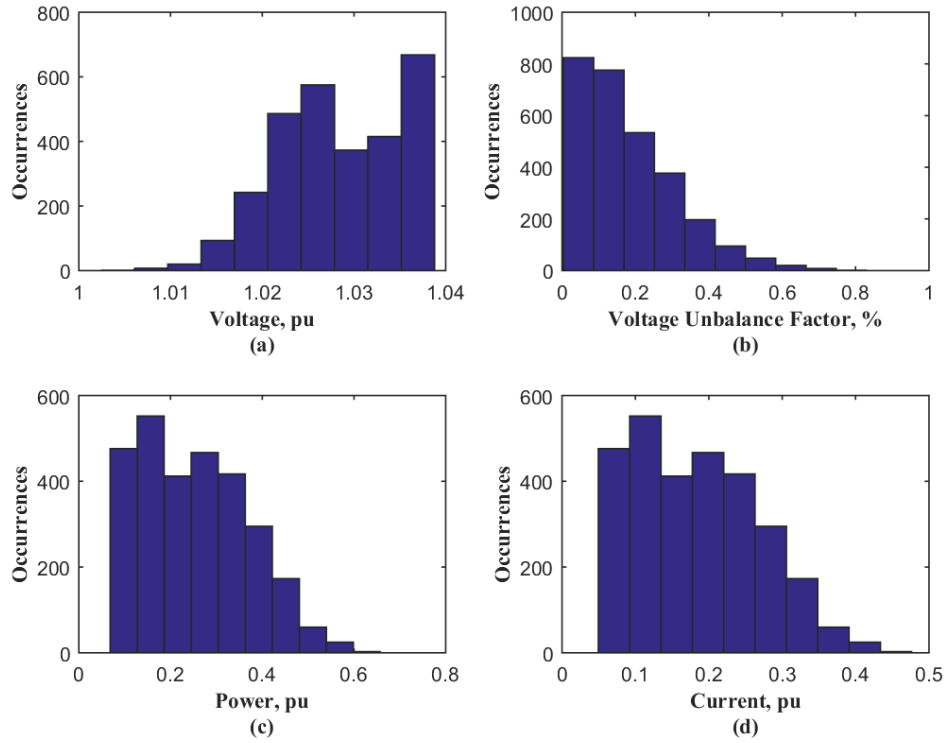


Figure 4.15: In Case 1, histograms of the network under study. (a) Voltage magnitudes. (b) Voltage unbalance factors. (c) Transformer's loading. (d) Current flow through cables.

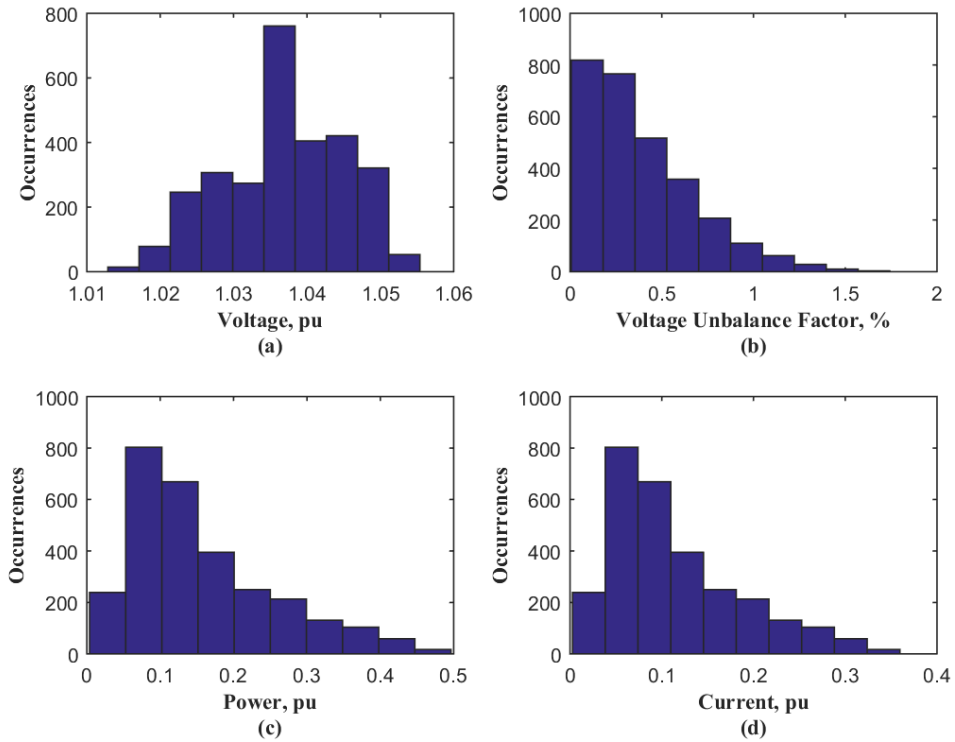


Figure 4.16: In Case 2, histograms of the network under study. (a) Voltage magnitudes. (b) Voltage unbalance factors. (c) Transformer's loading. (d) Current flow through cables.

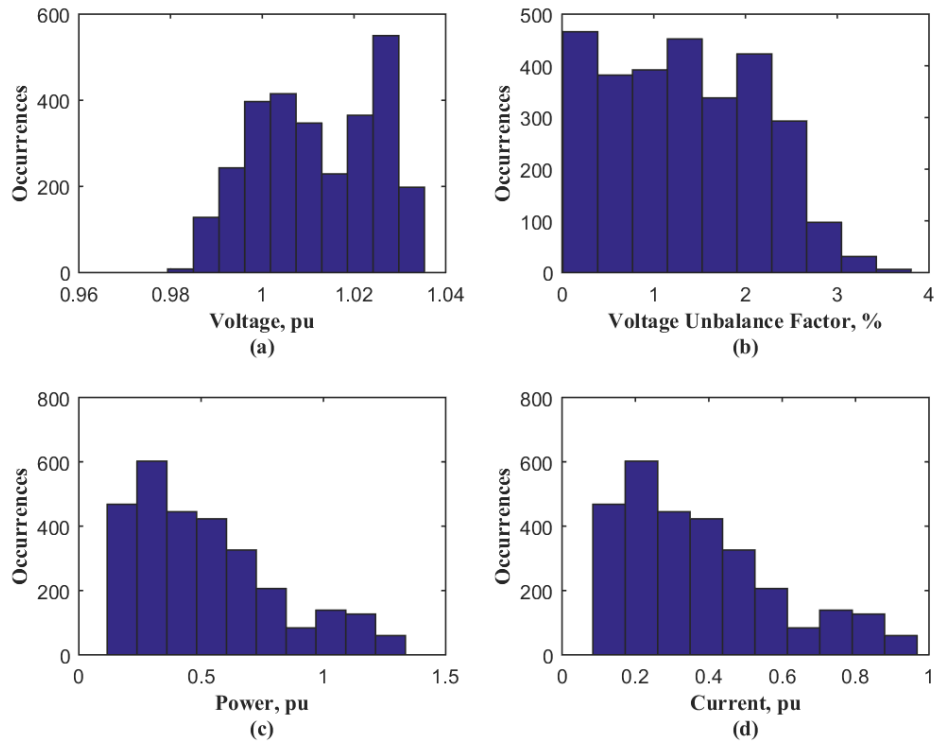


Figure 4.17: In Case 3, histograms of the network under study. (a) Voltage magnitudes. (b) Voltage unbalance factors. (c) Transformer's loading. (d) Current flow through cables.

In Case 4, Figure 4.18 (a) demonstrates the reduction of RMS voltage magnitudes when HPs were connected to the real network of Electricity North West. Voltage unbalance factors exceeded the limit due to high numbers of HP connections, as shown in Figure 4.18 (b). The power flow through the distribution transformer exceeded 110% with HP connections, as depicted in Figure 4.18 (c). RMS current flow through feeders reach a 75% with HP loads, as shown in Figure 4.18 (d).

In Case 5, Figure 4.19 (a) shows a further decrease of voltage magnitudes. Figure 4.19 (b) illustrates a remarkable increase of voltage unbalance factors. Figure 4.19 (c) presents that, the power flow through the distribution transformer has increased to less than a 200% of the rated power of the transformer. RMS current flow through residential feeder reach a 150% of the rated current of underground cables.

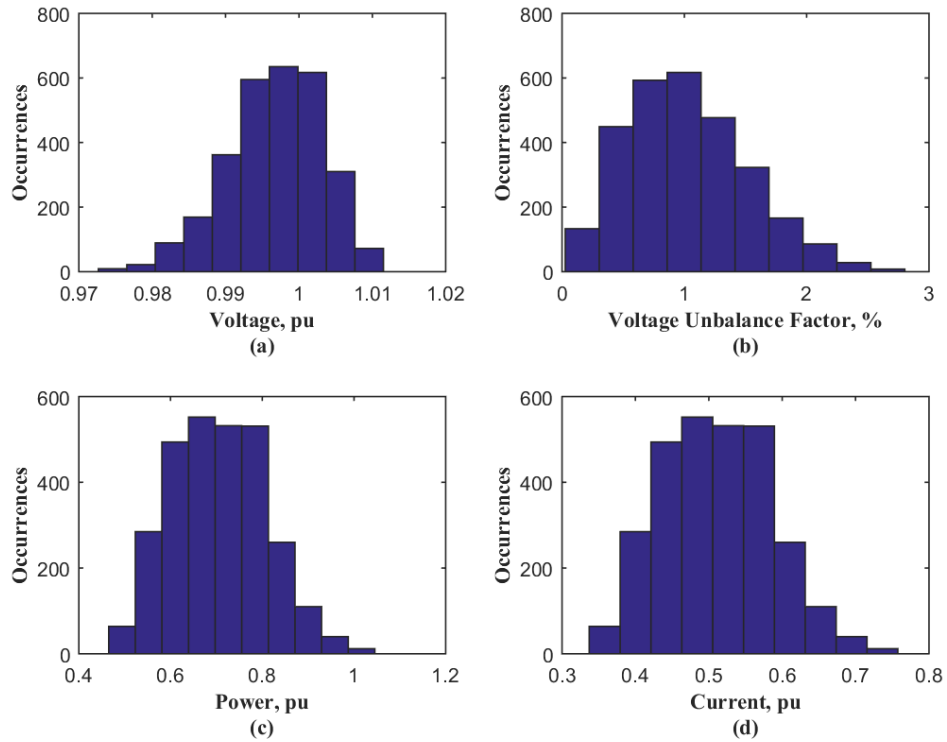


Figure 4.18: In Case 4, histograms of the network under study. (a) Voltage magnitudes. (b) Voltage unbalance factors. (c) Transformer’s loading. (d) Current flow through cables.

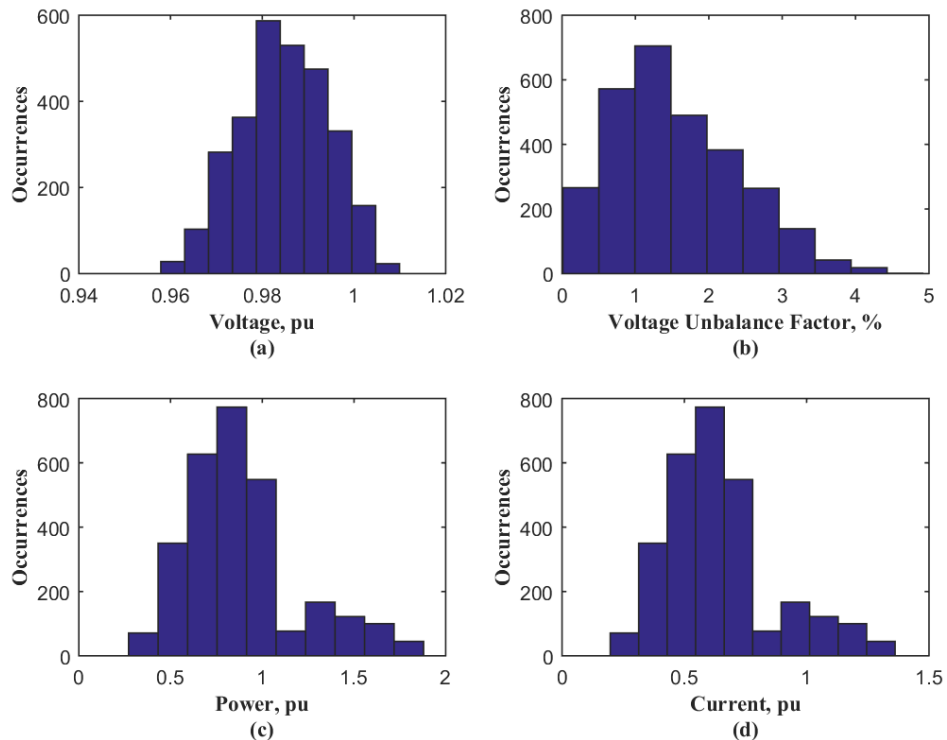


Figure 4.19: In Case 5, histograms of the network under study. (a) Voltage magnitudes. (b) Voltage unbalance factors. (c) Transformer’s loading. (d) Current flow through cables.

## 4.6 Conclusions

The impact of uncoordinated EV charging loads on a low voltage section of the UKGDN was studied using MATLAB/Simulink/Simscape/SimPowerSystems with three-phase four-wire connections. Different deterministic case studies were evaluated based on 96, 192, and 288 EVs, respectively. Residential loads and EV loads were dynamically modelled considering half-hourly time steps. Mean values of the active power of 8,000 residential customers and 133 EVs were acquired from real trials.

Four case studies illustrated that, power flows through network components have increased due to uncoordinated EV charging loads. Single-phase EV charging loads caused unbalanced phase voltages. Simulation results showed that, high numbers of EVs could increase voltage unbalance factors during peak-hour intervals. Different charging durations of EVs can cause unbalanced demand even if EVs are equally distributed across the three phases. Voltage magnitudes did not exceed their tolerances with charging 288 EVs.

The impacts of different EV, HP, and PV combinations on the real low voltage network was evaluated using the MATLAB function of unbalanced power flow.

Individual residential loads were synthesized using a normal probability distribution, whereas individual EV loads were synthesized using a uniform probability distribution. The individual loads were generated over a day of minute-by-minute time steps based on mean values of their active power, which were acquired at half-hourly time steps from a real-world project.

Individual PV power generation was modelled considering minute-by-minute time steps using the solar irradiance of a typical summer season in the UK. HP loads were modelled using readings of ambient temperatures over UK winter days.

Five case studies showed that, the considered network could tolerate high separate numbers of PV, EV, or HP connections in term of voltage magnitudes. However, voltage unbalance factors will increase with the connection of additional DER units. Unbalanced single-phase HP loads have less impact on the network under study, as compared to EV loads. This is because HPs are switched on and off over a day using thermostatic load control devices.

Therefore, EV/PV or HP/PV combinations have less impact on distribution networks, because EV and HP loads can be partially compensated using the generation of PV arrays.

## CHAPTER 5

### 5. Centralized Load Allocation of Electric Vehicles in Distribution Networks

#### 5.1 Introduction

In Chapter 4, it was shown that network constraints exceeded their limits with uncontrolled charging loads of electric vehicles (EVs). Therefore, this chapter presents a centralized control algorithm to re-allocate EV charging loads over a day-ahead of minute-by-minute time steps. Voltage magnitudes, voltage unbalance factors, and power flows were considered, while coordinating EV charging loads.

The UK generic distribution network (UKGDN) [116] was extended to include its medium voltage section. The centralized control algorithm was implemented based on non-iterative unbalanced power flow equations, which were developed in this chapter for monitoring network constraints.

The centralized control algorithm re-allocates EV charging loads in advance based on a short-term load forecasting. It is assumed that the proposed control algorithm receives the short-term load forecasting from distribution network operators (DNOs). However, the performance of the proposed control algorithm is tested based on real mean values of EV charging loads, which were acquired from the smart meters of Customer-Led Network Revolution (CLNR) trials [115].

Minute-by-minute time steps were used to synthesize individual loads, because this time resolution provides a near real-time observation using the proposed algorithm, as reported in Ref. [125]. Two-way communications in smart grids are important to coordinate EV charging loads using the proposed centralized controller. Distribution networks will evolve into smart grids with two-way communication technologies using smart meters and measuring sensors [126], [127].

#### 5.2 Methodology

Mean values of residential and EV loads at half-hourly time steps were acquired from the CLNR trials [115]. Individual residential loads were synthesized using normal probability distribution over a day of minute-by-minute time steps, as presented in Chapter 4. Meanwhile, EV charging durations were individually

synthesized in Subsection 5.4.3 at minute-by-minute time steps, considering unbalanced allocation of EV charging loads across the three phases.

The central controller is capable to coordinate high EV charging loads without upgrading the network components. Figure 5.1 shows the workflow of the proposed centralized algorithm for re-allocating EV charging loads.

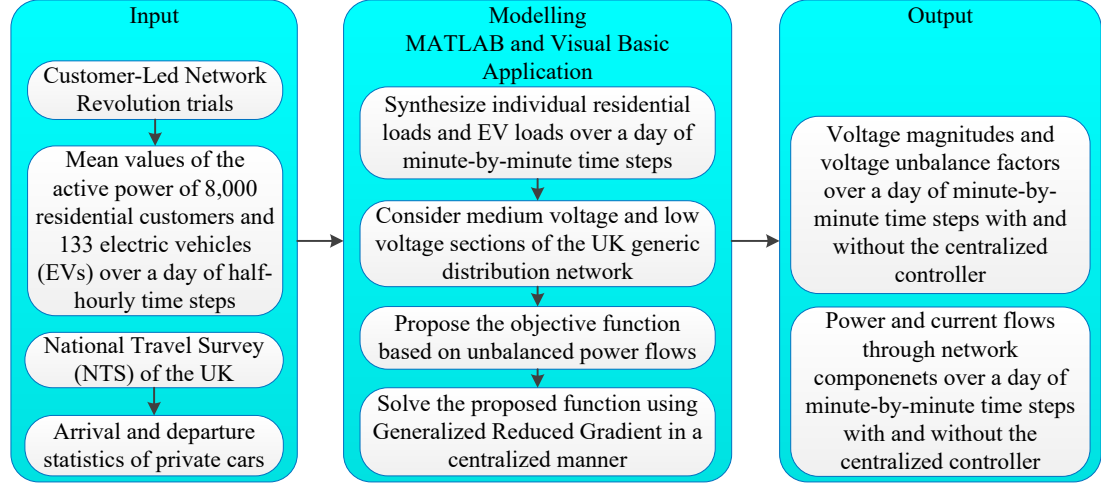


Figure 5.1: The workflow of re-allocating EV charging loads.

### 5.2.1 The Proposed Objective Function

One contribution of this work is related to the re-allocation of EV charging durations to avoid violating network limits using non-linear programming algorithms. The aggregated EV charging power was maximized across the three phases using Equation (5.1), considering the dynamic model of aggregated residential loads in every minute.

$$\text{Max } F = \sum_{t=0}^{1440} \left( \sum [F(t)_{a,b,c}] + \sum_{l=1}^N p(t)_{a,b,c\text{Cust.}n_l} \right) \forall N \in \mathbb{Z}^+, F = F_0 \quad (5.1)$$

where

$$\begin{aligned} \sum [F(t)_{a,b,c}] = & \left( \sum_{k_a=1}^{M_a} P(t)_{aEV_{k_a}} + \sum_{k_b=1}^{M_b} P(t)_{bEV_{k_b}} \right. \\ & \left. + \sum_{k_c=1}^{M_c} P(t)_{cEV_{k_c}} \right) \forall M_{a,b,c} \in \mathbb{Z}^+ \end{aligned} \quad (5.2)$$

where  $F$  is the objective function representing the aggregated charging power of EV loads in kW during a day (i.e. 1440 min),  $F_0$  is the initial value of  $F$ ,  $t$  is the current time step, and  $a, b, c$  are the three phases of the considered system.  $[F(t)_{a,b,c}]$  represents the requested aggregated EV charging loads across the three phases (i.e.  $3 \times 1$  decision variables).  $P(t)_{aEV}, P(t)_{bEV}$  and  $P(t)_{cEV}$  represent the charging power of each EV per minute per phase in kW.  $p(t)_{a,b,cCust.n}$  is the dynamic residential load for each customer per minute across the three phases in kW.  $N$  is the total number of customers, while  $M_a, M_b, M_c$  representing the numbers of EVs across the three phases.  $\mathbb{Z}^+$  is the real integer positive number.

The hosting capacity of the network components is calculated with the objective function  $F$  in every minute across the three phases. Further, high time-step resolution means a fast-queuing process of re-allocating EV charging loads. Therefore, the convenience of deferred EV can be maintained using these minute-by-minute time steps.

The main advantage of the proposed centralized control algorithm is that EV charging loads are regularly shifted toward new charging time intervals, maintaining the distribution network within its limits. If EV charging loads violate the network constraints, the centralized control algorithm will evaluate the number of EVs that should be deferred.

The total loading power was determined using Equation (5.3) for each low voltage (LV) distribution transformer.

$$S(t)_{Tr.loading} = \sum_{j=1}^{N_f} S(t)_L \quad \forall N_f \in \mathbb{Z}^+ \quad (5.3)$$

where  $S(t)_{Tr.loading}$  is the apparent power of the distribution transformer in kVA at the time step  $t$ ,  $N_f$  is the total number of radial feeders that are served by the distribution transformer, and  $S(t)_L$  is the aggregated apparent power per LV feeder in kVA at the time step  $t$ . The predefined constraints are assigned as follows:

$$V_{min} \leq V(t)_{a,b,cn} \leq V_{max} \quad (5.4)$$

$$VUF(t)_n \% \leq VUF\%_{max} \quad (5.5)$$

$$I(t)_{a,b,cL} \leq I_{a,b,cLrating} \quad (5.6)$$

$$S(t)_{Tr.loading} \leq S_{Tr.rating} \quad (5.7)$$

where  $V_{min}, V_{max}$  are the lower and the upper limits of steady-state voltages ( $V(t)_{a,b,cn}$ ) per phase in V,  $VUF\%_{max}$  is the maximum percentage of the voltage unbalance factor ( $VUF(t)_n$ ) that can be allowed,  $I_{a,b,cL,rating}$  is the rated current of steady-state currents ( $I(t)_{a,b,cL}$ ) per phase at the main distribution lines in Amps, and  $S_{Tr.rating}$  is the rated power of the distribution transformer in kVA.

### 5.2.2 The Centralized Control Algorithm

Aggregated EV charging loads are considered to be the decision variables. These aggregated EV charging loads are optimally re-allocated across the three phases to maintain the network constraints within their limits. The flowchart of the proposed control algorithm (see Figure 5.2) is systematically described as follows.

Decision variables are evaluated using the generalized reduced gradient “GRG Nonlinear” solver with Microsoft Excel. However, this solver is limited in terms of assigning the number of decision variables and constraints. Therefore, these decision variables are evaluated with hourly time resolution (i.e.  $3 \times 24$  values) across the three phases during a day. Accordingly, the evaluated decision variables are interpolated into a lookup table of ( $3 \times 1440$  elements) using MATLAB R2015a, as shown in the next step.

This lookup table represents the hosting capacity of the network components (i.e.  $[F(t)_{a,b,c}]_{3 \times 1440}$ ) during a day of minute-by-minute time steps across the three phases. The fluctuations of unbalanced residential loads and unbalanced EV charging loads are considered based on real daily load profiles from CLNR trials. The hosting capacity for each minute (i.e. *Optimized*  $[F(t)_{a,b,c}]_{3 \times 1}$ ) is then compared to the *Requested*  $[F(t)_{a,b,c}]_{3 \times 1}$ , as shown in Figure 5.2. The *Requested*  $[F(t)_{a,b,c}]_{3 \times 1}$  is directly calculated in this step using Equation (5.2) based on the charging power of each EV per minute per phase ( $P(t)_{aEV}, P(t)_{bEV}, P(t)_{cEV}$ ).

If *Optimized*  $[F(t)_{a,b,c}]_{3 \times 1} \geq$  *Requested*  $[F(t)_{a,b,c}]_{3 \times 1}$  is true, all requested EV charging loads can occur at this minute considering randomized delays (i.e. less than 60 s) among them. Otherwise, a number of EVs with the amount of power of (*Requested*  $[F(t)_{a,b,c}]_{3 \times 1} -$  *Optimized*  $[F(t)_{a,b,c}]_{3 \times 1}$ ) will be re-allocated to

charge at other time steps, whenever the pre-defined constraints can be maintained. Then, EV users can accordingly reschedule their charging loads.

If the aggregated EV charging power is not achieved during that day, the controller allows the remaining EVs to complete their charging demand on the next day depending on Boolean signals from “AND” gate (see Figure 5.2).

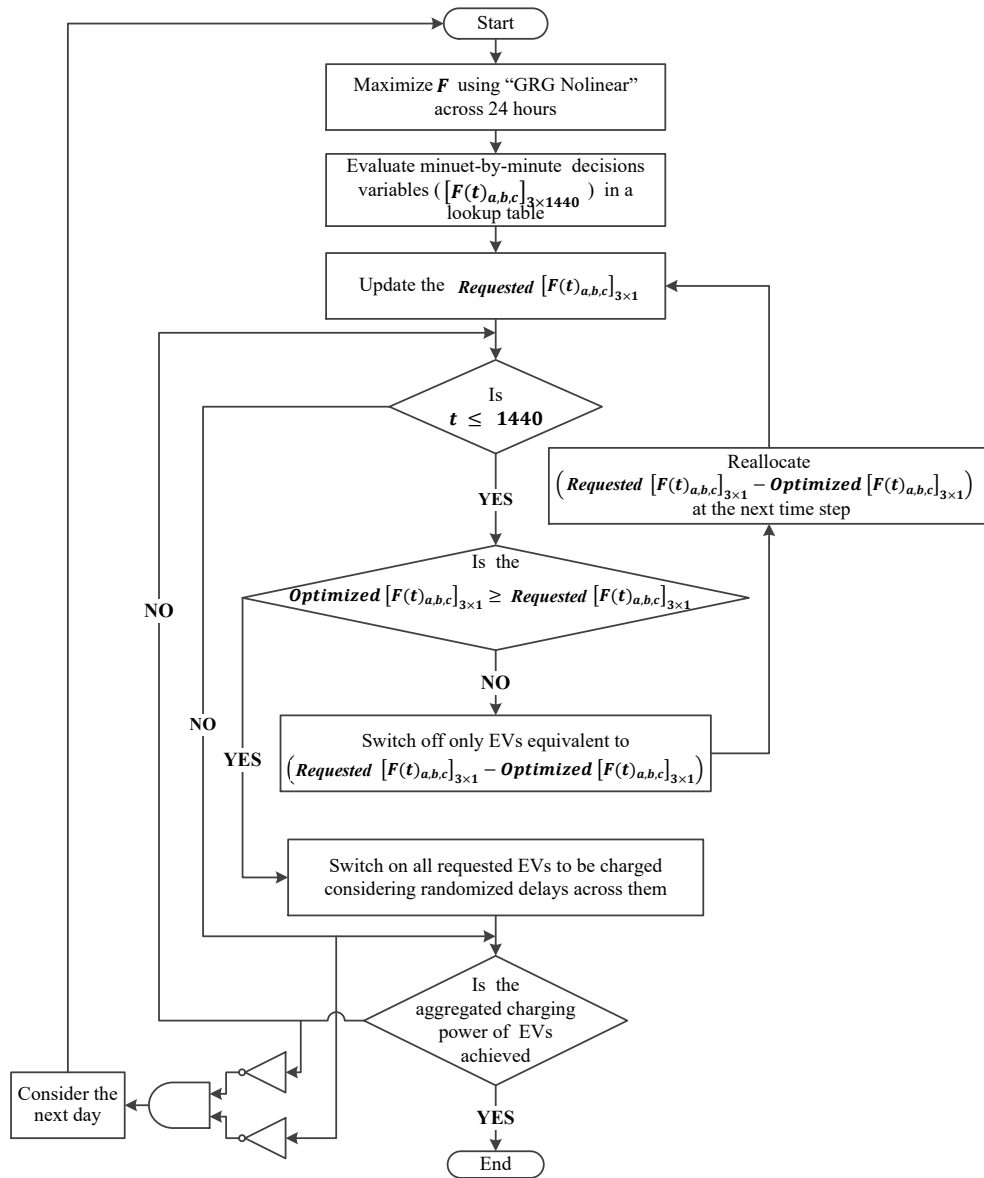


Figure 5.2: The flowchart of the centralized control algorithm.

### 5.3 Non-iterative Unbalanced Power Flow Calculations

A non-iterative unbalanced power flow solver is developed to calculate voltage magnitudes, voltage unbalance factors, and power flows of network components. The

developed solver was implemented based on the forward and backward sweep method [128].

The main advantage of the developed solver is the non-iterative method compared to the forward and backward sweep method, which is iterative. Unbalanced power flow results were compared using these two methods. Very close results were observed using both methods, while significantly reducing the number of calculation steps.

Phase voltage matrices were represented with complex quantities using Euler's method. The unbalanced power flow requires phase impedance matrices between any two adjacent nodes along radial feeders. Equation (5.8) represents the phase impedance matrix between adjacent nodes, including impedances due to self and mutual inductances [128].

$$[Z_{a,b,c}]_{3 \times 3} = \begin{bmatrix} Z_{aa} & Z_{ab} & Z_{ac} \\ Z_{ba} & Z_{bb} & Z_{bc} \\ Z_{ca} & Z_{cb} & Z_{cc} \end{bmatrix} \quad (5.8)$$

where  $[Z_{a,b,c}]_{3 \times 3}$  is the phase impedance matrix of the feeder in  $\Omega$ . The diagonal elements of this matrix are the impedances due to the self-inductance (e.g.  $Z_{aa}$ ). The off diagonal elements are the impedances due to the mutual-inductance (e.g.  $Z_{ab}$ ). If only positive ( $Z_1$ ) and zero ( $Z_0$ ) sequence impedances are available, the impedance matrix is approximated as follows [128]:

$$[Z_{a,b,c}]_{3 \times 3} = \frac{1}{3} \begin{bmatrix} (2Z_1 + Z_0) & (Z_0 - Z_1) & (Z_0 - Z_1) \\ (Z_0 - Z_1) & (2Z_1 + Z_0) & (Z_0 - Z_1) \\ (Z_0 - Z_1) & (Z_0 - Z_1) & (2Z_1 + Z_0) \end{bmatrix} \quad (5.9)$$

Then, the phase voltage matrix is calculated using Equation (5.10).

$$\begin{aligned} & [V(t)_{a,b,cn} \exp(i\phi(t)_{a,b,cn})]_{3 \times 1} \\ & = [V(t)_{a,b,c1} \exp(i\phi(t)_{a,b,c1})]_{3 \times 1} \\ & - [Z_{a,b,c}]_{3 \times 3} [I(t)_{a,b,cLn} \exp(i\theta(t)_{a,b,cn})]_{3 \times 1} \end{aligned} \quad (5.10)$$

where  $[V(t)_{a,b,c1} \exp(i\phi(t)_{a,b,c1})]_{3 \times 1}$  is the phase voltage matrix at the swing bus in V,  $[V(t)_{a,b,cn} \exp(i\phi(t)_{a,b,cn})]_{3 \times 1}$  is the phase voltage matrix at the adjacent node  $n$  in V,  $[I(t)_{a,b,cLn} \exp(i\theta(t)_{a,b,cn})]_{3 \times 1}$  is the phase current matrix consumed by all groups of customers at node  $n$  in Amps,  $\phi(t)_{a,b,cn}$  is the angle between phase voltage and reference axis at the end node  $n$  in degree,  $\theta(t)_{a,b,cn}$  is the angle between phase

current and reference axis at the specified node  $n$  in degree, and  $i = \sqrt{-1}$ . The phase current matrix at node  $n$  is calculated using the following equation:

$$[I(t)_{a,b,cLn} \exp(i\theta(t)_{a,b,cn})]_{3 \times 1} = \begin{bmatrix} \frac{S(t)_{aLn}^*}{V(t)_{an} \exp(i\phi(t)_{an})} \\ \frac{S(t)_{bLn}^*}{V(t)_{bn} \exp(i\phi(t)_{bn})} \\ \frac{S(t)_{cLn}^*}{V(t)_{cn} \exp(i\phi(t)_{cn})} \end{bmatrix} \quad (5.11)$$

where  $S(t)_{a,b,cLn}$  is the apparent power of aggregated customers at node  $n$  in kVA per phase at the time step  $t$ . \* is the conjugated value. Equation (5.10) is modified into Equation (5.12) by substituting Equation (5.11) in Equation (5.10) for a unity power factor.

$$\begin{aligned} & [V(t)_{a,b,cn} \exp(i\phi(t)_{a,b,cn})]_{3 \times 1} \\ = & [V(t)_{a,b,c1} \exp(i\phi(t)_{a,b,c1})] - [Z_{a,b,c}]_{3 \times 3} \left[ \frac{P(t)_{a,b,cLn}}{V(t)_{a,b,cn} \exp(i\phi(t)_{a,b,cn})} \right] \end{aligned} \quad (5.12)$$

where  $P(t)_{a,b,cLn}$  is the aggregated power consumed by all groups of customers at the specified node  $n$  in kW per phase at the time step  $t$ . The power term (i.e.  $P(t)_{a,b,cLn}$ ) in Equation (5.12) is determined by the following equations:

$$P(t)_{a,b,cLn} = P(t)_{a,b,cIn} + P(t)_{a,b,cEVsn} \quad (5.13)$$

where

$$\begin{aligned} P(t)_{a,b,cIn} &= \sum_{l=1}^N p(t)_{a,b,cCust.n_l} \\ P(t)_{a,b,cEVsn} &= \sum_{k_{a,b,c}=1}^{M_{a,b,c}} y_{a,b,c,k_{a,b,c}} \times p(t)_{a,b,cEVn_{k_{a,b,c}}} \end{aligned} \quad \forall M_{a,b,c}, N \in \mathbb{Z}^+ \quad (5.14)$$

where  $p(t)_{a,b,cCust.n}$  and  $P(t)_{a,b,cIn}$  are the power consumed by individual and aggregated customers, respectively, at node  $n$  in kW without EVs per phase at the time step  $t$ , and  $p(t)_{a,b,cEVn}$  and  $P(t)_{a,b,cEVsnt}$  are the power consumed by individual and aggregated EV chargers, respectively, at node  $n$  in kW per phase at the time step  $t$ .

$$y_{a,b,ck} = \begin{cases} 1, & \text{for EV charging states} \\ 0, & \text{for EV idle states} \end{cases} \quad (5.15)$$

Equation (5.12) is rewritten considering EV fleet aggregated power and customers from Equation (5.13) as shown below:

$$\begin{aligned} & [V(t)_{a,b,cn} \exp(i\phi(t)_{a,b,cn})]_{3 \times 1} \\ & = [V(t)_{a,b,c1} \exp(i\phi(t)_{a,b,c1})]_{3 \times 1} - [B(t)_{a,b,cn}]_{3 \times 1} \end{aligned} \quad (5.16)$$

where

$$\begin{aligned} [B(t)_{a,b,cn}]_{3 \times 1} & = [Z_{a,b,c}]_{3 \times 3} \\ & \times \left[ \left( \frac{\exp(-i\phi(t)_{a,b,cn})}{V(t)_{a,b,cn}} \right) \left( \sum_{l=1}^N p(t)_{a,b,cCust.n_l} \right) \right. \\ & \quad \left. + P(t)_{a,b,cEVsn} \right]_{3 \times 1} \quad \forall N \quad (5.17) \\ & \in \mathbb{Z}^+ \end{aligned}$$

where  $[B(t)_{a,b,cn}]$  is the matrix resulted from multiplying  $(3 \times 3)$  impedance matrix by  $(3 \times 1)$  phase current matrix at the time step  $t$ . Across all phases, the objective function is derived from Equations (5.16) and (5.17) by discriminating the aggregated charging power of EVs ( $P(t)_{a,b,cEVsn}$ ) as follows:

$$\begin{aligned} [F(t)_{a,b,c}] & = \{ [Z_{a,b,c}]_{3 \times 3}^{-1} \times [B(t)_{a,b,cn}]_{3 \times 1} \times V(t)_{a,b,cn} \times \exp(-i\phi(t)_{a,b,cn}) \} \\ & \quad - \sum_{l=1}^N p(t)_{a,b,cCust.n_l} \quad \forall N \in \mathbb{Z}^+ \end{aligned} \quad (5.18)$$

where  $[F(t)_{a,b,c}]$  is the aggregated charging power of EVs to be maximized per phase, excluding all residential loads. By adding residential loads to the both sides of Equation (5.18), the objective function  $F$  across the three phases during a day of minute-by-minute time steps was rewritten as follows:

$$F = \sum_{t=0}^{1440} \left( \sum [F(t)_{a,b,c}] + \sum_{l=1}^N p(t)_{a,b,cCust.n_l} \right) \quad \forall N \in \mathbb{Z}^+ \quad (5.19)$$

It can be observed that Equations (5.1) and (5.19) are identical. The  $VUF(t)_n\%$  is calculated in percentage using Equation (5.20) for each time step  $t$ .

$$\begin{aligned}
& VUF(t)_n \\
&= \frac{\text{MAX}(|V(t)_A - V(t)_{an}|, |V(t)_A - V(t)_{bn}|, |V(t)_A - V(t)_{cn}|)}{V(t)_A} \quad (5.20) \\
&\times 100\%
\end{aligned}$$

where  $V(t)_A = \frac{(V(t)_{an} + V(t)_{bn} + V(t)_{cn})}{3}$  at each time step  $t$ .

## 5.4 Configurations of the System under Study

The performance of the centralized controller was tested using the UKGDN that includes medium voltage (MV) and LV feeders. Residential loads and EV loads were individually synthesized.

### 5.4.1 The Network under Study

Figure 5.3 illustrates the proposed architecture of the centralized controller. An adapted UKGDN [116] was used to test the performance of the centralized control algorithm for the smart charging of EVs.

Six radial feeders are emanating from the MV side of the two parallel on-load tap changing transformers. The capacity of each transformer is 15 MVA 33/11 kV. The MV feeders serve 18,432 customers in total with 3,072 customers for each feeder. Each MV feeder is divided into 8 segments, serving 8 ground-mounted distribution transformer. Each one (i.e. 500 kVA 11 kV/0.4 kV ground-mounted distribution transformer) serves 384 customers distributed across four LV feeders. Ninety-six customers were distributed along each LV feeder (see Figure 5.3). More details about the original UKGDN can be found in the literature [116].

Meter points were allocated at the emanating point of each LV feeder. These meters are used to upload readings of measured phase currents using two-way communication systems (see Figure 5.3). When these readings are received by the centralized control algorithm, unbalanced power flow calculations are performed to re-allocate EV charging loads. The unbalanced power flow updates voltage magnitudes, voltage unbalance factors and power flows of network components. If EV users upload their unscheduled EV charging loads via these two-way communication systems, EV users can accordingly reschedule their charging loads based on the charging duration received from the control algorithm. EV charging loads will be

accordingly re-allocated using the centralized control algorithm as illustrated in Section 5.2.2.

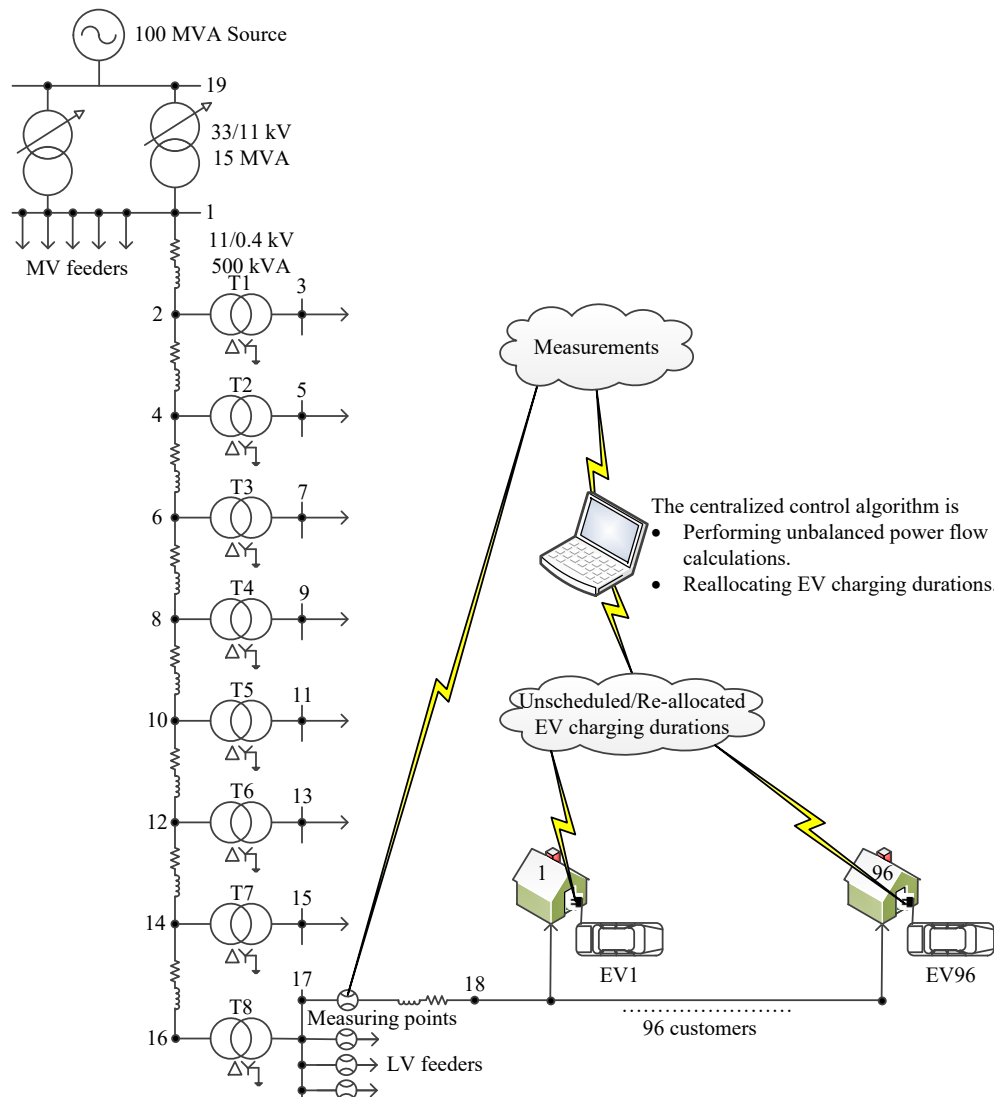


Figure 5.3: The proposed architecture of the centralized controller.

To solve the power flow for the UKGDN (Figure 5.3) using the solver developed, the following steps are followed:

- Calculation of the total power at node 1 using Equations (5.13) and (5.14).
- Calculation of the total current at node 1 using Equation (5.11).
- Calculation of the phase voltages at node 2 using Equation (5.12).
- Sequentially repeat the above calculations to determine the phase voltages at nodes 2, 4, 6, 8, 10, 12, 14, and 16.

### 5.4.2 Synthesizing loads of Residential Customers

Figure 5.4 (a) shows aggregated daily load profiles of 384 customers for each distribution transformer over a day of minute-by-minute time steps. Loads can be modelled as a constant active/reactive power (PQ), a constant current (I), a constant impedance (Z) or a combination of PQ, I and Z [128].

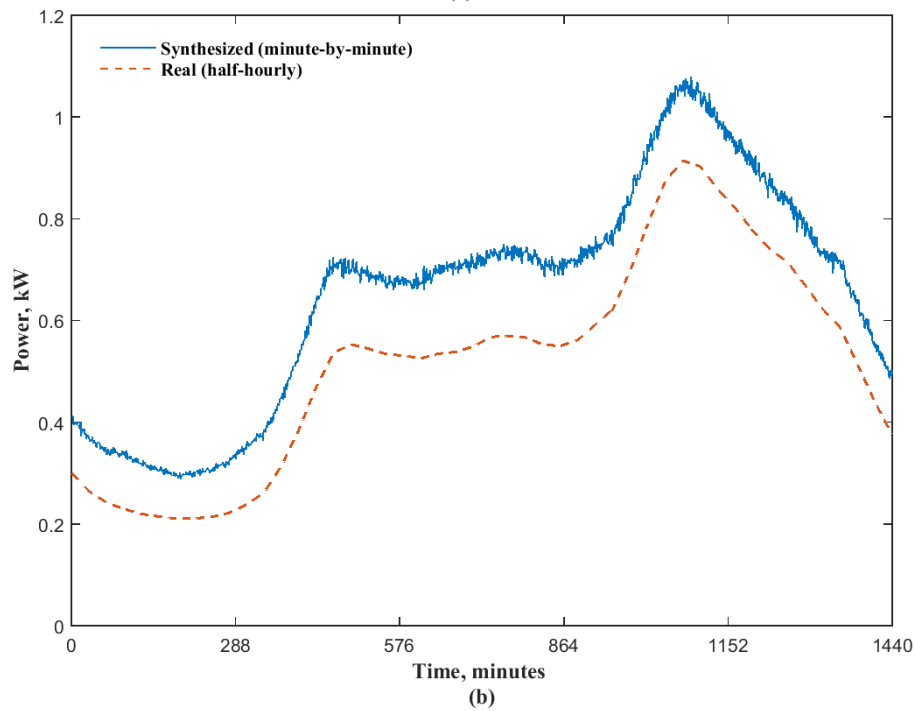
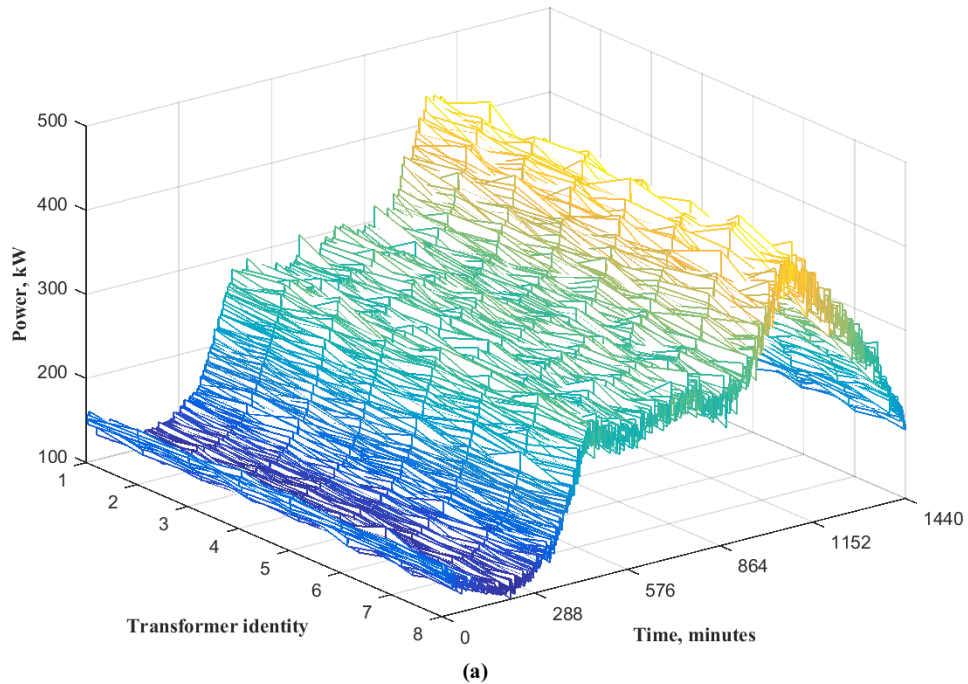


Figure 5.4: Profiles of, (a) the aggregated load of 384 customers for each low voltage (LV) transformer, (b) the daily mean of real and generated loads.

In this work, residential loads were modelled as a dynamic PQ changing their values in every minute. Daily load profiles were synthesized using means and standard deviations recorded in CLNR project during real trials [115]. Daily profiles of the standard deviations and means were obtained from CLNR trials [115]. Figure 5.4 (b) shows the minute-by-minute mean profile (i.e. stochastically synthesized with 3072 customers), as compared to the half-hourly mean profile (i.e. recorded in CLNR project).

### 5.4.3 Synthesizing Loads of Electric Vehicles

EV charging loads were modelled as a dynamic PQ capturing their aggregated demand in every minute. Daily profiles of EV charging loads were synthesized based on real datasets. A real diurnal mean profile was selected as a reference from the CLNR project (i.e. the daily mean profile of charging power for 133 EVs) [115].

EV charging profiles were individually generated in MATLAB using the “*randi*” function to produce the diversity across EV charging profiles. This function generates integer random numbers. Matrices of “0” and “1” were generated using the “*randi*” function (“1” for charging state and “0” for idle state). Departure and arrival times were assigned per EV based on the National Travel Survey (NTS) of the UK from the Department for Transport [122] during working days.

At transformer T8 (see Figure 5.3), all residential customers were assumed to have a single phase charger of 3.3 kW per hour at slow charging mode. Therefore, 384 EV connections were considered across residential customers at transformer T8, as shown in Figure 5.3. EV load profiles were synthesized as follows:

- Generate the requested minutes for charging each EV (less than or equal 480 minutes a day) using the “*randi*” function.
- Synthesize the daily load profile of each EV by assigning “0” for idle state and “1” for charging state.
- Concatenate the minute-by-minute charging profiles of 384 EVs in one matrix ( $384 \times 1440$ ).
- Shift the charging loads of the produced matrix according to arrival and departure times of the daily trips to match the daily mean profile of the CLNR project [115].

Figure 5.5 represents the comparison between the daily mean of the synthesized EV charging loads and the daily mean of the real EV charging loads. It can be seen

that the synthesized daily mean of 384 EVs is greater than the daily mean of 133 EVs obtained from CLNR datasets. However, their daily patterns are approximately similar. Figure 5.6 illustrates the charging durations of 384 EVs over a day of minute-by-minute time steps.

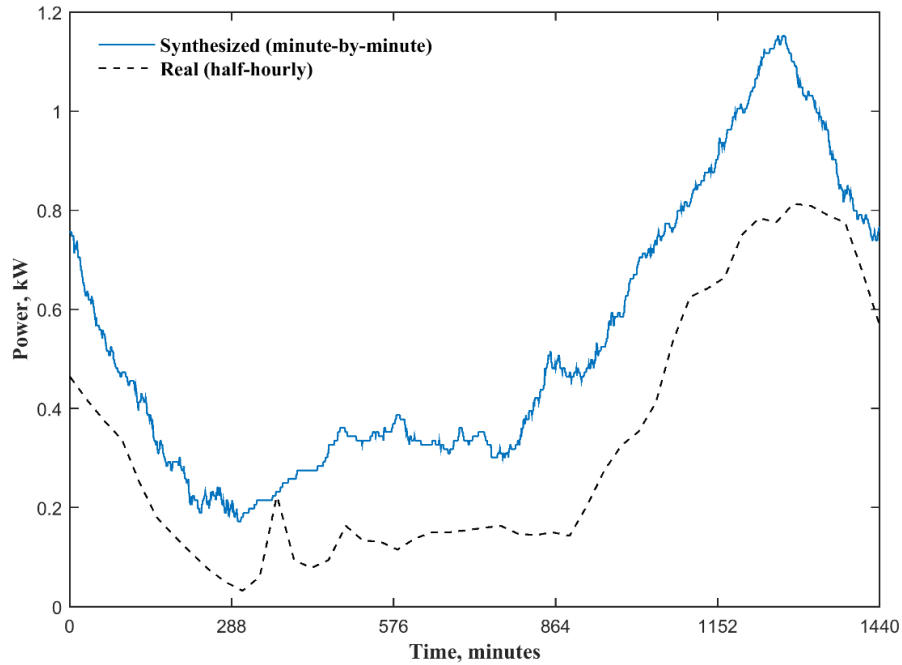


Figure 5.5: The daily mean profiles of the real/synthesized electric vehicle (EV) charging loads.

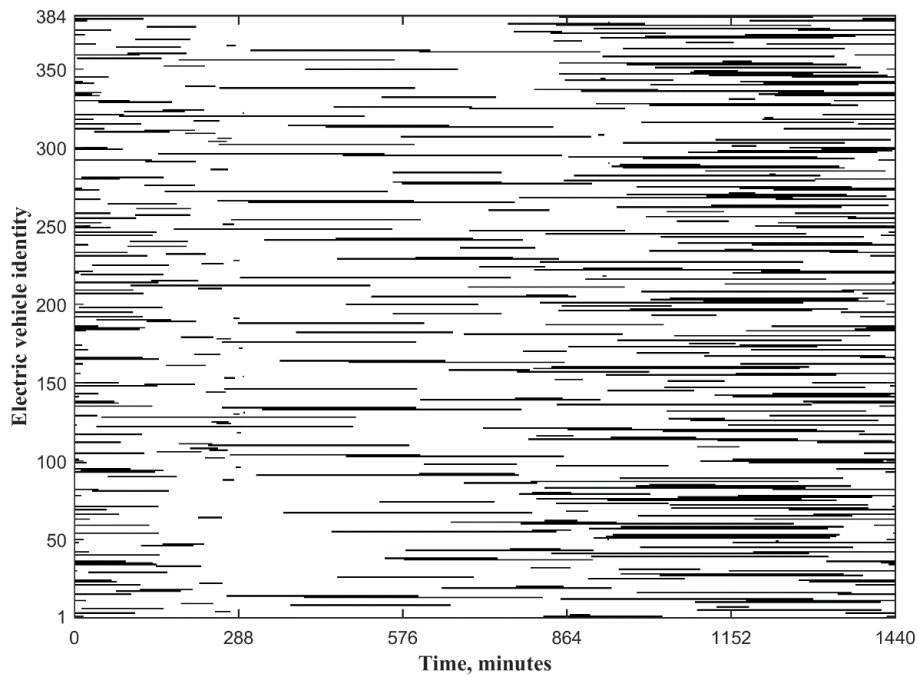


Figure 5.6: The pattern of the synthesized 384 EV charging loads during a day.

## 5.5 Simulation Results

To monitor the performance of the centralized control algorithm, steady-state profiles of the UKGDN were calculated over a day of minute-by-minute time steps for two scenarios:

- Scenario I (without smart allocation): 384 EVs at the distribution transformer T8 were charged, as modelled in Section 5.4.3.
- Scenario II (with smart allocation): 384 EVs at T8 were charged with the centralized control algorithm.

Equations (5.1)–(5.3), (5.12), (5.16)–(5.18), and (5.20) were used to model the considered network in a spreadsheet using Microsoft Excel. Equations (5.4)–(5.7) were used to assign the constraints of the solver used in Excel. Then, the objective function was solved using “GRG Nonlinear” in a matter of seconds. Simulation results were performed using an Intel® Core™ i7-4500U CPU, 1.80 GHz, 8.00 GB installed RAM laptop, operating with Microsoft Windows 10 Pro. of 64-bit operating system (see Appendix D). MATLAB R2015a was used to write the code for solving unbalanced power flow equations, as shown in Appendix D. Results were computed and visualized with a single MATLAB-script file in less than one minute. The constraints of the studied system were assigned according to the policy regulation for UK distribution networks as presented in the following subsections.

### 5.5.1 Voltage Magnitudes and Voltage Unbalances

Steady-state phase voltages and voltage unbalances were normally maintained within the limits. The upper and the lower limits of the voltage magnitudes were assigned between 1.06 pu and 0.94 pu, respectively, for the MV level. Meanwhile, these limits were allocated between 1.1 pu and 0.94 pu, respectively, for the LV level [116], [117]. The base voltage was assumed the nominal voltage (230 V). The  $VUF(t)_n\%$  did not to exceed 1.3% according to the Engineering Recommendations P29 [116]. Uncontrolled charging loads of EVs were clustered at the transformer T8 (see Figure 5.3), in which 384 EVs are connected to node 16. However, daily profiles of RMS voltages did not drop below the limit at the MV level, as shown in Figure 5.7 (a) for Scenario I. In addition, voltage unbalances did not exceed the limit, as presented in Figure 5.7 (b). On the other hand, voltage magnitudes and voltage unbalances did exceed the limits at the LV side, as shown in Figures 4.7 (a) and Figure 5.8 (b),

respectively. These undesired impacts of EV charging loads were minimized using the centralized control algorithm as demonstrated in Figures 4.8 (a) and Figure 5.9 (b), respectively.

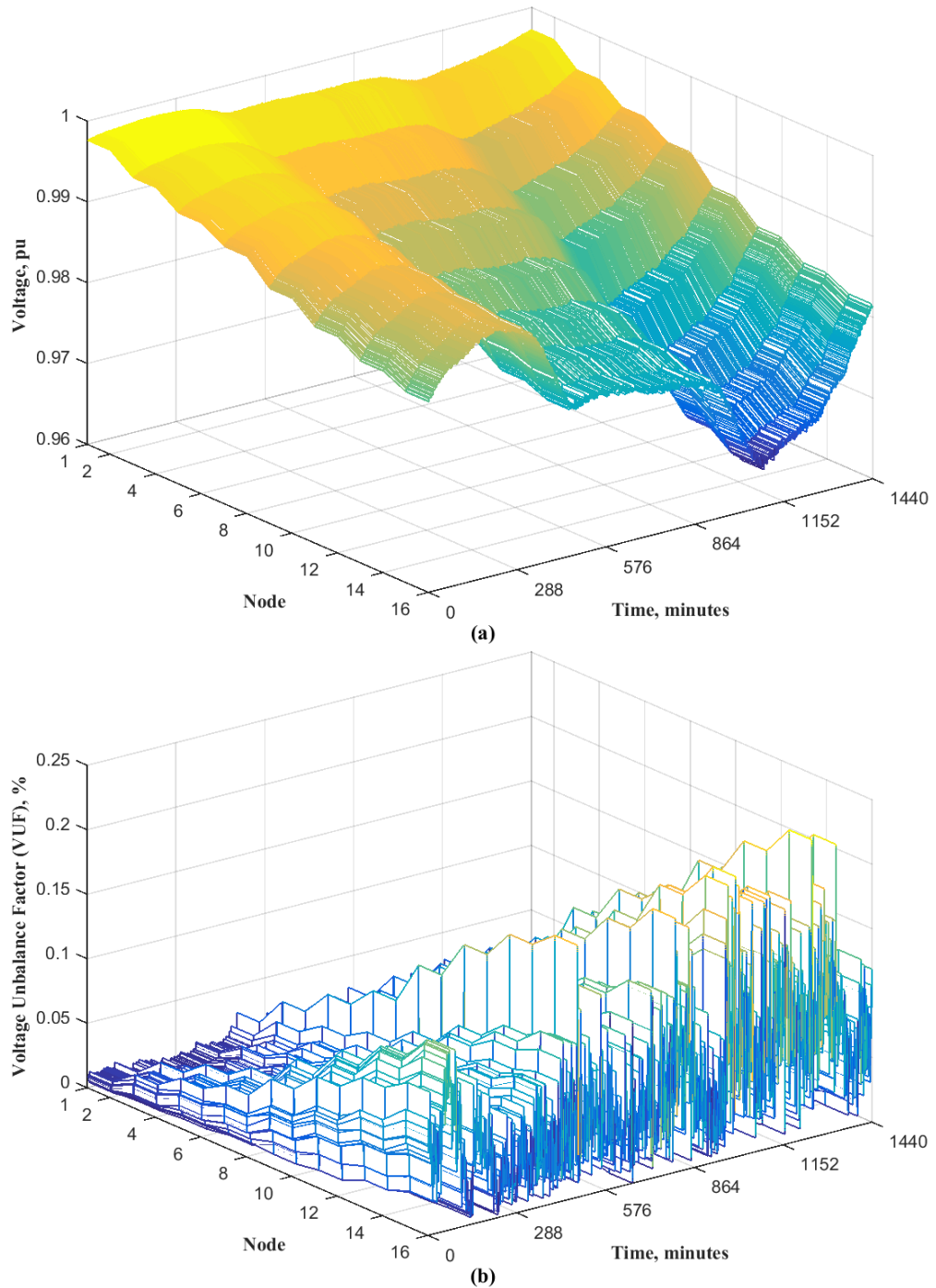


Figure 5.7: UKGDN daily profiles of Scenario I with (a) RMS voltages at each node of the MV feeder; (b) voltage unbalance at each node of the MV feeder.

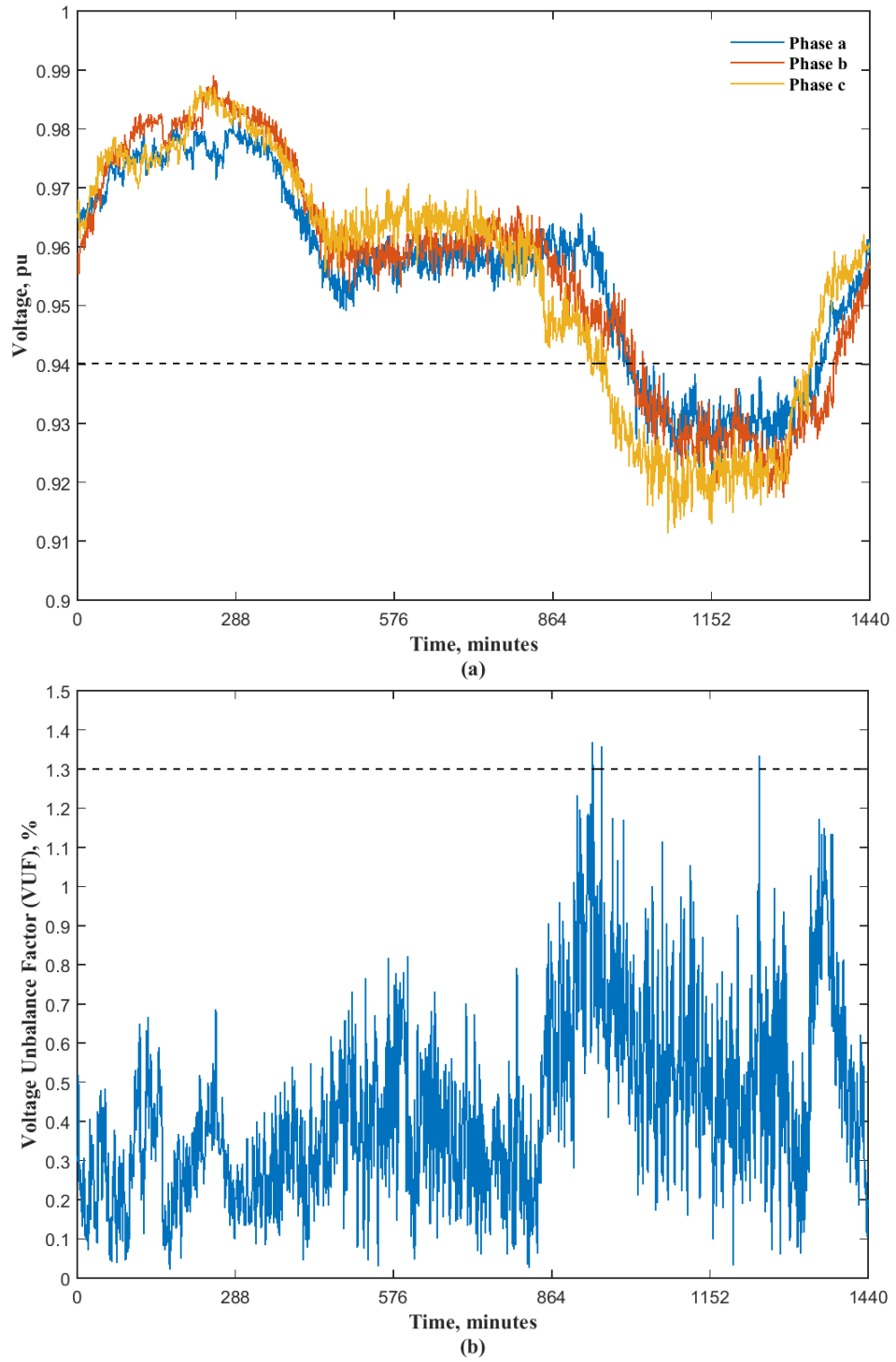


Figure 5.8: UKGDN daily profiles of Scenario I with (a) phase voltages at node 18; (b) voltage unbalance at node 18.

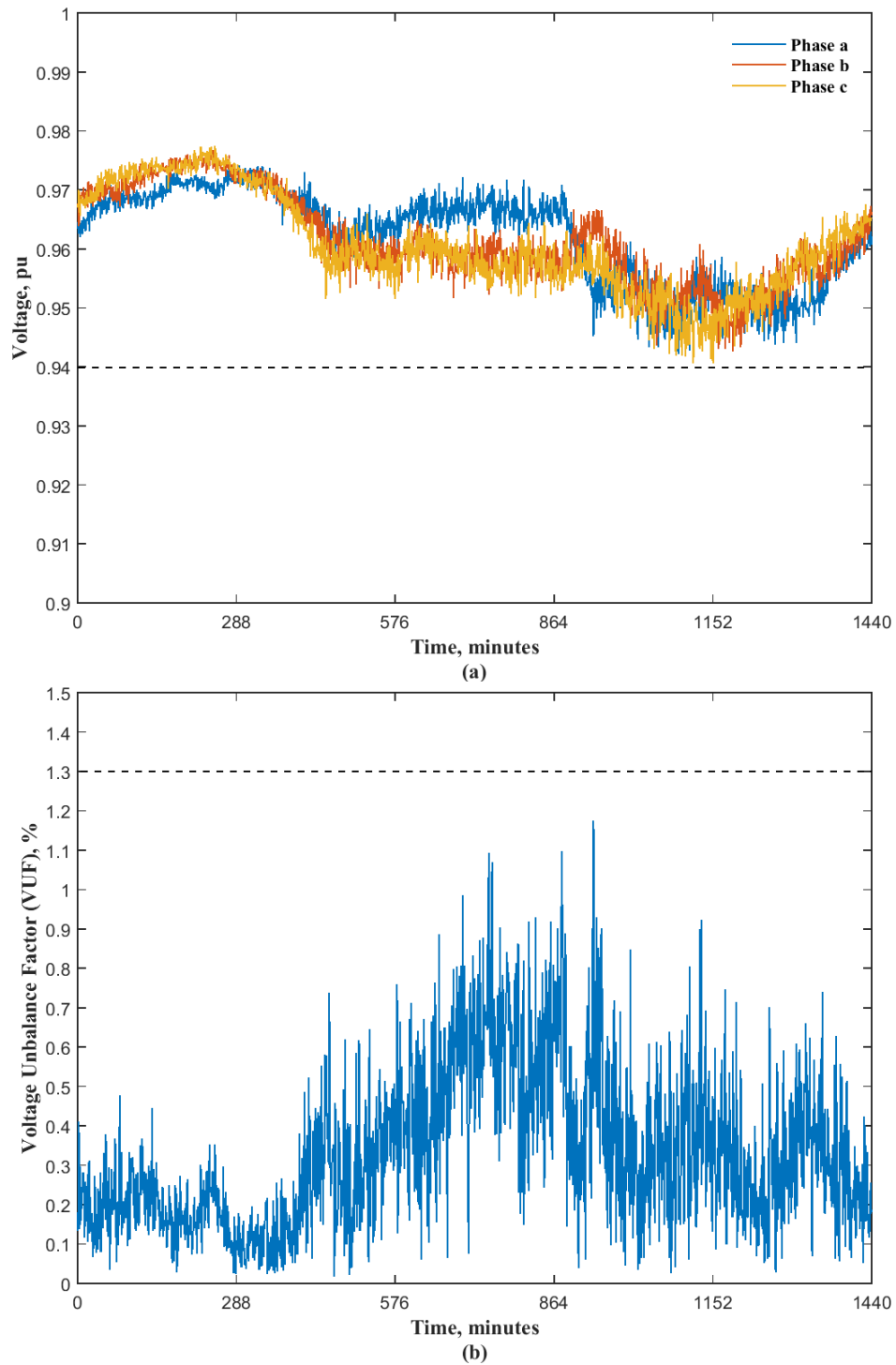


Figure 5.9: UKGDN daily profiles of Scenario II with (a) phase voltage at node 18; (b) voltage unbalance at node 18.

### 5.5.2 Limitations of Network Components

Using the centralized controller, the daily profiles of phase currents have not exceeded the rated current of the distribution lines. Additionally, the distribution transformer was not overloaded beyond the rated apparent power.

Base values of power and current were assigned using the rated power and the rated current of LV network components. These components were: 500 kVA distribution transformer and 185 mm<sup>2</sup> underground cable [129]. Therefore, the limits of network components are  $I(t)_{a,b,cL} \leq 1$  pu and  $S(t)_{Tr.loading} \leq 1$  pu for the underground cable and distribution transformer, respectively.

Figure 5.10 presents the daily profiles of the loading power at the main substations (i.e. the 15 MVA transformers) for Scenario I and Scenario II. The considered EV charging loads had a small effect on the capacity of the MV transformers. However, these EV charging loads at the peak intervals were re-allocated at suitable intervals (Scenario II), as shown in Figure 5.10. In addition, Figure 5.10 shows how the fast-queuing time process can lead to the consistent re-allocation of EV charging loads. Distribution transformer T8 and distribution line were significantly overloaded with uncontrolled EV charging loads (Scenario I), as depicted in Figure 5.11 (a) and Figure 5.11 (b).

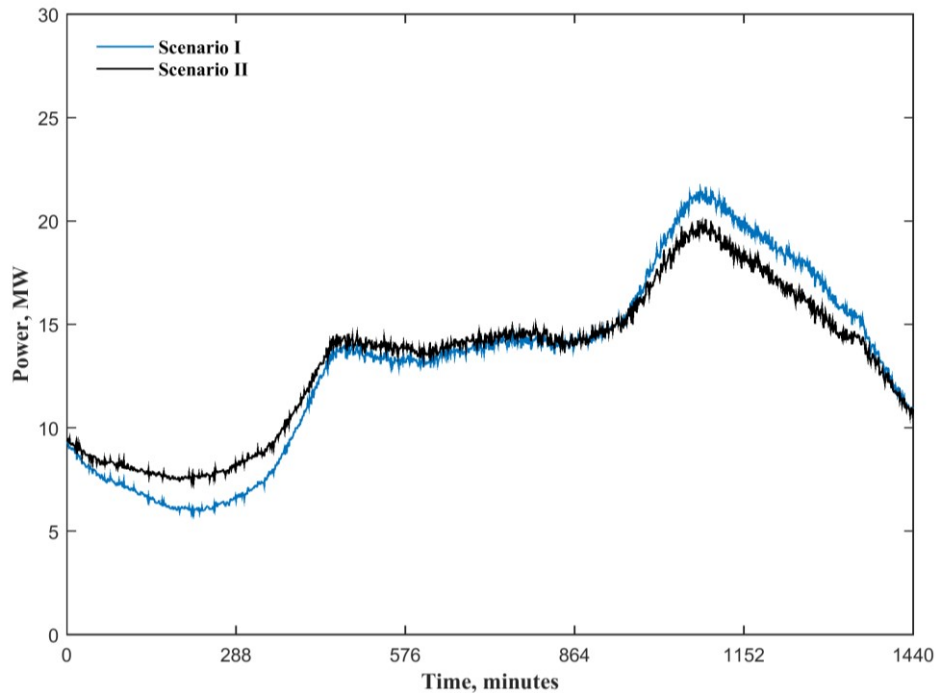


Figure 5.10: UKGDN daily load profiles at the main substations (the MV transformers) for Scenario I and II, respectively.

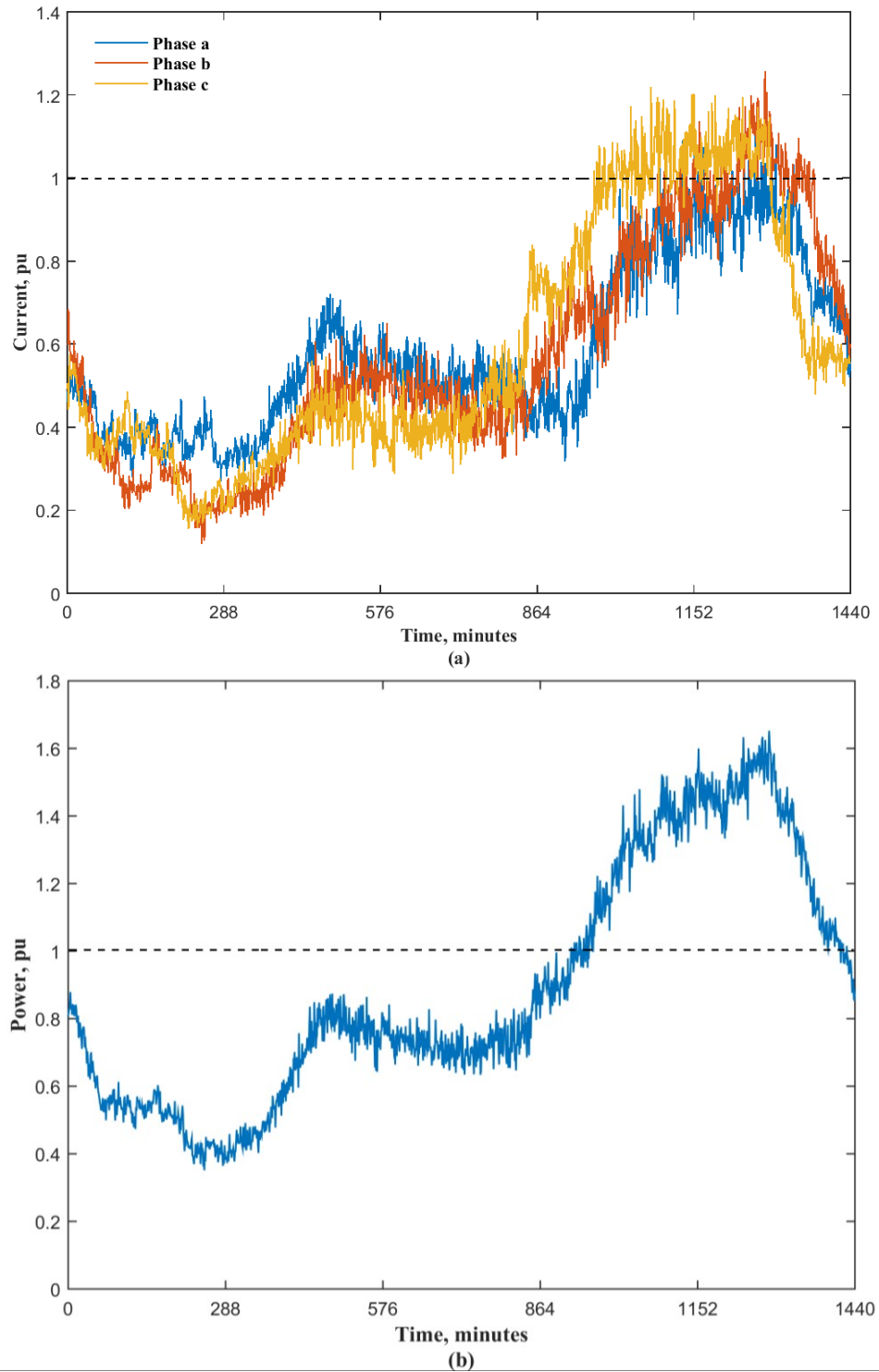


Figure 5.11: Scenario I UKGDN daily profiles (a) phase currents of the underground cable between nodes 17 and 18; (b) loading power of the transformer T8.

By the use of the centralized control algorithm, loading power of the underground cable and distribution transformer was maintained within the desired limits as shown in Figure 5.12 (a) and Figure 5.12 (b), respectively.

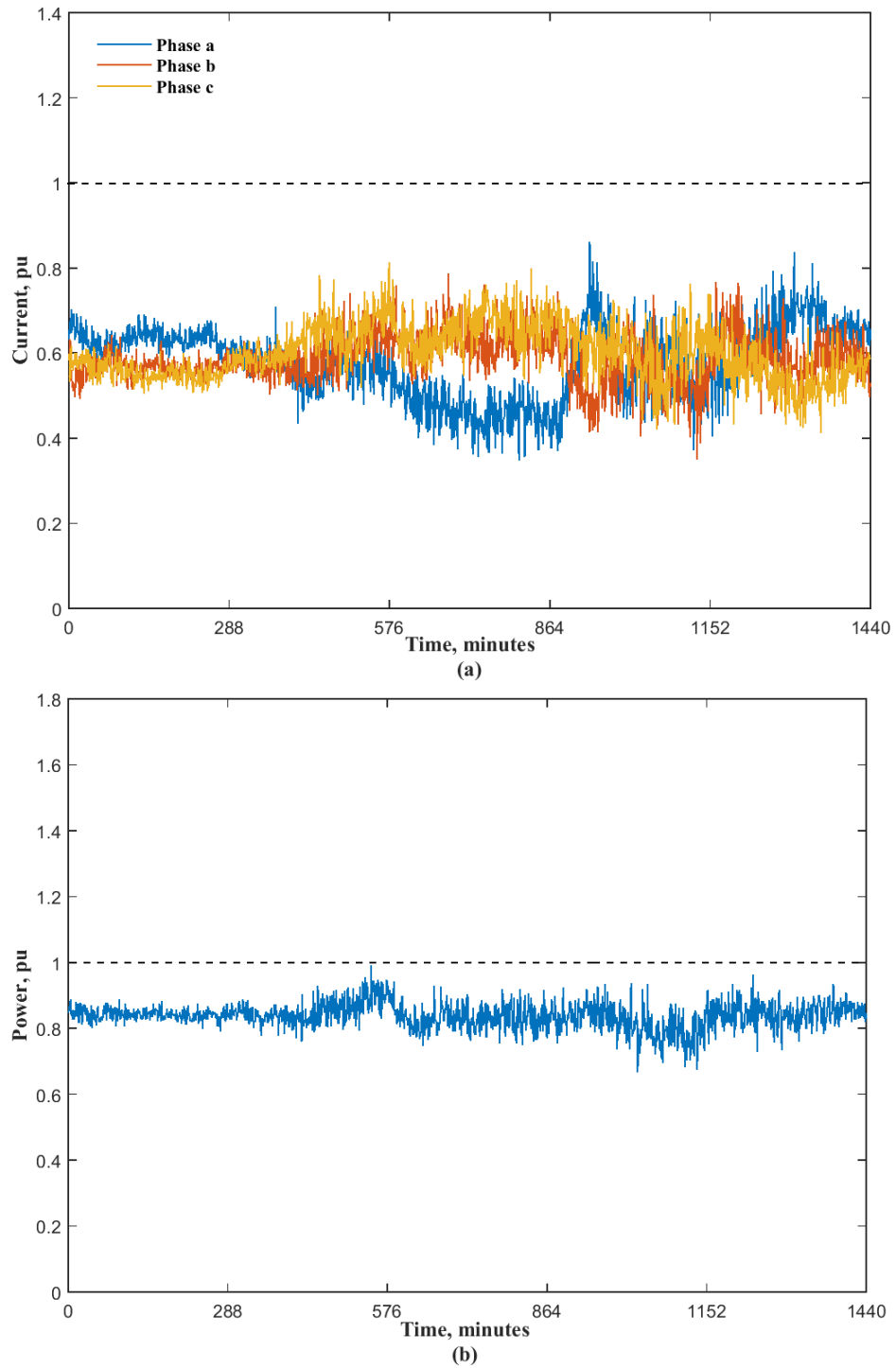


Figure 5.12: Scenario II UKGDN daily profiles (a) phase currents of the underground cable between node 17 and node 18; (b) loading power of the transformer T8.

## 5.6 Conclusions

EV charging loads were coordinated via the proposed centralized control algorithm using unbalanced power flow calculations. The non-iterative unbalanced power flow calculations were implemented to formulate the proposed objective function. EV charging loads were re-allocated according to the hosting capacity of the electricity network, while maintaining voltage magnitudes, voltage unbalance factors, and power flows within their limits.

Daily profiles of EV charging loads were modelled based on real datasets acquired from trials of the real project. Two scenarios were investigated to monitor the performance of the centralized control algorithm with uncontrolled and controlled EV charging loads. The results showed that network components at the MV level can cope with uncontrolled EV charging loads. However, high uncontrolled EV charging loads can lead to the following issues at the LV level:

- Deviating from the normal value of the voltage magnitude and voltage unbalance.
- Overloading the main distribution line and the distribution transformer.

These issues were mitigated by re-allocating EV charging loads via the centralized control algorithm (see Scenario II).

The centralized control algorithm can be adopted by network operators to defer upgrading needs for network infrastructure (underground cables and distribution transformers) as can be easily integrated into existing power system control paradigms.

## CHAPTER 6

### 6. Decentralized Load Adjustment of Electric Vehicles and Heat Pumps

#### 6.1 Introduction

In Chapter 5, the centralized controller is proposed to re-allocate charging loads of electric vehicles, overcoming their impacts on distribution networks. However, the centralized controller requires two-way communication systems to be implemented. To overcome the need for extensive communication technologies, Chapter 6 proposes a decentralized controller to adjust EV and HP loads, considering consumer satisfaction and network constraints. The levels of satisfaction of EV and HP users were evaluated using mathematical models of EV battery state-of-charge (BSoC) levels and the indoor temperatures of HP houses.

The decentralized control algorithm was proposed for minimizing electricity bills of EV and HP users based on mixed integer linear programming. Time-varying tariffs were modelled over a day of quarter-hourly time steps considering a real flat-rate tariff. This consideration ensures equivalent revenues of electricity suppliers using time-varying and flat-rate tariffs to protect consumers from being overcharged.

RMS voltage magnitudes, voltage unbalance factors, and RMS current flows were determined in this study using unbalanced power flow, while adjusting EV and HP loads. Current flows through network components can be monitored using smart meters to implement the proposed decentralized controller in real-world applications.

#### 6.2 Methodology

A real, three-phase, and unbalanced distribution network of Electricity North West, which is different from the one modelled in Chapter 4, was used in this chapter to test the performance of the controller. This different network serves a high number of residential customers, as compared to the network of Chapter 4. The network under study of this chapter supports the scalability of the control algorithm into the real world, because it emulates the complexity of high numbers of customers in real networks. The decentralized control algorithm was modelled based on the following considerations.

- The numbers of EVs and HPs, which were connected to the network under study, were evaluated using the prediction model of Chapter 3.
- Typical residential loads were modelled using the method that was developed in Chapter 4.
- Unbalanced power flow, which was presented in Chapter 5, was used to monitor RMS voltage magnitudes, voltage unbalance factors, and RMS current flows of the network under study.
- The final BSoC level of EVs and the indoor temperature of HP houses were used to monitor consumer satisfaction over a day.
- Residential EV charging loads were only considered based on arrival and departures statistics of the daily trips of UK commuters.
- Discharging EV batteries were excluded in the decentralized controller, because an increase in the number of charging and discharging cycles degrades the life span of EV batteries.
- Residential HP heating loads were modelled using the operational characteristics of air source heat pumps.

Figure 6.1 represents the workflow of the decentralized control algorithm.

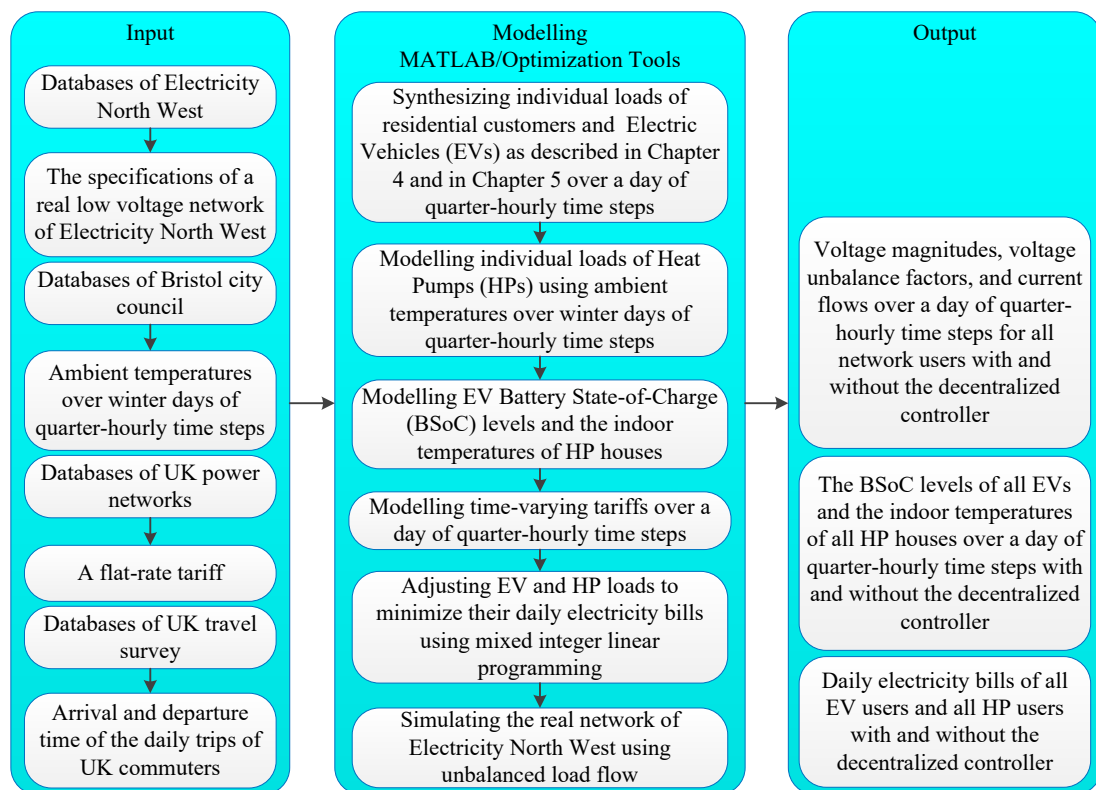


Figure 6.1: The workflow of the decentralized control algorithm of EVs and HPs.

### 6.2.1 Mathematical Model of Electric Vehicles

EV charging loads were modelled as a discrete rectangular demand of slow charging mode of 3.3kW charging capacity [130]. EV charging durations were synthesized based on the arrival/departure times of the UK commuters, as presented in Ref. [122]. According to these statistics, nearly a quarter of daily trips occurred between 17:00 and midnight. Other trips appeared between midnight and 17:00 on the next day. EV charging loads were accordingly modelled over a day of quarter-hourly time steps, as illustrated in detail in Chapter 5. Thus, EV daily BSoC level is calculated as follows.

$$\mathcal{S}(t) = \mathcal{S}_0 + \Delta t \sum_{i=1}^{\mathbb{N}} \mathcal{P}_i \quad (6.1)$$

where  $\mathcal{S}(t)$  symbolizes EV final BSoC level in kWh at time step  $t$  relative to EV initial BSoC level ( $\mathcal{S}_0$ ) in kWh.  $\Delta t$  symbolizes the width of each time step in a fraction of an hour ( $h$ ).  $\mathbb{N}$  symbolizes the total number of EV charging time intervals to increase BSoC level from  $\mathcal{S}_0$  to  $\mathcal{S}(t)$ .  $\mathcal{P}$  symbolizes the rated power of EV charger in kW (i.e. 3.3kW).

### 6.2.2 Mathematical Model of Heat Pumps

Air source HPs were only considered for space heating (i.e. without water heating). The coefficient of performance (CoP) measures HP efficiency, as follows.

$$CoP = \frac{Q_{out}}{Q_{in}} \quad (6.2)$$

where  $CoP$  symbolizes the CoP value of HP.  $Q_{out}$ ,  $Q_{in}$  symbolize the output and input HP power in kW. Equation (6.3) calculates HP electrical power consumption [124].

$$Q_{in} = \frac{\rho \times c_{sp} \times \Phi \times (T_s - T_r)}{CoP} \quad (6.3)$$

where  $\rho$  symbolizes the air density in  $\text{kg/m}^3$ .  $c_{sp}$  symbolizes the specific heat of air in  $\text{kJ/kg}^\circ\text{C}$ .  $\Phi$  symbolizes the volume of air that is compressed by the HP unit into space in  $\text{m}^3/\text{s}$ .  $T_s$  and  $T_r$  symbolize the supply and return temperatures of the HP unit in  $^\circ\text{C}$ . According to Carnot's cycle, the difference of temperatures across a heating engine is

used to calculate the efficiency of that engine. Carnot's equation is modified into (6.4), because HPs can achieve a 10% of the calculated value using Carnot's cycle [131], [132].

$$CoP = \frac{0.1}{1 - \left[ \frac{(273 + T_{out})}{(273 + T_s)} \right]} \quad (6.4)$$

where  $T_{out}$  symbolizes variable outdoor temperatures in °C. Therefore, HP power consumption is calculated using Equation (6.5), as follows.

$$Q_{in}(t) = \frac{1}{0.1} \times \rho \times c_{sp} \times \Phi \times (T_s - T_r) \times \left( 1 - \left[ \frac{(273 + T_{out})}{(273 + T_s)} \right] \right) \quad (6.5)$$

where  $Q_{in}(t)$  symbolizes the rate of HP power consumption in kW at time step  $t$  relative to variable outdoor temperatures ( $T_{out}$ ). Equation (6.6) determines the rate of heat losses from indoor environments toward outdoor environments through walls and windows [133].

$$Q_{loss}(t) = \frac{T_o - T_{out}}{\mathfrak{R}_{eq}} \quad (6.6)$$

where  $Q_{loss}(t)$  symbolizes the rate of heat losses in kW at the time step  $t$  relative to variable outdoor temperatures.  $T_o$  symbolizes the off-state temperature of thermostatic control devices in °C.  $\mathfrak{R}_{eq}$  symbolizes the equivalent thermal resistivity of wall ( $\mathfrak{R}_{wall}$ ) and windows ( $\mathfrak{R}_{windows}$ ) in °C/kW. The indoor temperatures of HP houses are updated as shown below.

$$T_{in}(t) = T_o + \Delta \left( \frac{CoP \times Q_{in}(t) - Q_{loss}(t)}{M_a \times c_{sp}} \right) \quad (6.7)$$

where  $T_{in}(t)$  symbolizes the updated indoor temperature of HP houses in °C at the time step  $t$ .  $M_a$  symbolizes the mass of air compressed in kg/s. In this study, the value of  $\mathfrak{R}_{eq}$  is considered to be 1.56 °C/kW, whereas the value of  $M_a$  is 1 kg/s [133].

HPs are inherently equipped with thermostatic load control devices. The off-state temperature of thermostatic control equipment is adjusted to be 20°C. Therefore, the model of HP demand is completed by considering HP thermostatic operational cycles, as follows.

$$\mathbb{Q}_{HP}(t) = \begin{cases} 0 & \text{if } T_{in}(t) \geq T_o \\ \mathbb{Q}_{in}(t) & \text{if } T_{in}(t) < T_o \end{cases} \quad (6.8)$$

where  $\mathbb{Q}_{HP}(t)$  symbolizes HP demand in kW at time step  $t$  considering thermostat operations. Table 6.1 shows the numerical values of considered HP parameters. These parameters are evaluated based on the HP presented in Ref. [124], considering a residential heating performance.

Table 6.1: The numerical values of considered HP parameters.

Parameters	Values	Units
$\rho$	1.275	kg/m <sup>3</sup>
$c_{sp}$	1.005	kJ/kg°C
$\Phi$	0.613	m <sup>3</sup> /s
$T_s$	28	°C
$T_r$	20	°C
Rated $CoP$	3.5	-

### 6.2.3 Synthesized Time-varying Tariffs

In this study, time-varying tariffs were synthesized based on the predicted demand over a one-day-ahead time interval. Electricity suppliers can use smart meters to design more tariffs, incentivizing customers to use less energy over peak-hour time intervals [134]. Two-level time-varying tariffs were used to charge consumers with expensive and cheap tariffs considering fixed time intervals. For example, ‘‘Economy 7’’ tariff has been used in the UK since 1970s to charge customers with a cheap tariff overnight [134]. Dynamic time-varying tariffs charge variable tariffs over time intervals depending on specific factors (e.g. the availability of predicted wind energy) [134]. In another study [135], a model was developed to compare annual bills using flat-rate and time-varying tariffs.

In Ref. [136], time-varying tariffs were adjusted to ensure that, the average of electricity bills is equivalent with time-varying and flat-rate tariffs for unchanged energy consumption. These tariffs were £0.672/kWh, £0.118/kWh, and £0.04/kWh for high, mid, and low electricity prices, respectively. Meanwhile, the value of £0.142/kWh was the standard flat-rate tariff in 2014, as presented in Ref. [136].

In this work, Equations (6.9) and (6.10) are used to synthesize time-varying tariffs considering the stability of supplying revenues and consuming bills. A good pricing model should consider this stability, as demonstrated in Ref. [137]. Time-varying tariffs are synthesized over a day of quarter-hourly time steps based on the demand predicted, as shown in Equation (6.9).

$$C_{FRT} \sum_{t=0}^{t=24h} P(t) = \sum_{t=0}^{t=24h} C_{DTou}(t)P(t) \quad (6.9)$$

subject to the following constraints

$$C_{DTou}(t) = \begin{cases} y & \text{if } P(t) \geq P_{Mx} \\ z & \text{if } P(t) \leq P_{Mn} \\ z < x < y & \text{if } P_{Mn} < P(t) < P_{Mx} \end{cases} \quad (6.10)$$

where  $C_{FRT}$  denotes the standard flat-rate tariff.  $C_{DTou}(t)$  is the synthesized time-varying tariff in £/kWh.  $y$  and  $z$  denote high and low tariffs.  $x$  denotes a changeable tariff between  $y$  and  $z$  values.  $P(t)$  denotes the predicted overall network demand at each time step.  $P_{Mx}$  and  $P_{Mn}$  denote maximum and minimum values of network demand over a day-ahead time interval. Residential network demands are dynamically modelled as presented in detail in Chapter 4. The values of  $C_{DTou}(t)$  are synthesized over a day of quarter-hourly time steps by solving Equation (6.9) using the generalized reduced gradient solver [138].

Equation (6.9) includes the real flat-rate tariff to ensure that, the total revenues of electricity suppliers are equivalent with time-varying and flat-rate tariffs over a 24 hour time interval ( $24h$ ). The model of time-varying tariff is constrained by Equations (6.9) and (6.10) to protect customers from being overcharged, while keeping the interest of electricity suppliers.

#### 6.2.4 Objective Functions

Both of EV and HP loads are considered to be the decision variables during the optimization process. The flexibility of EV/HP demand is restricted depending on consumer satisfaction and network constraints.

Equation (6.11) is the first objective function, which is used to minimize the electricity bill of each EV user over a day of quarter-hourly time steps.

$$\min_{\forall \ell \in \mathbb{L}} \Delta t \sum_{t=0}^{t=24h} C_{DTou}(t) \mathcal{P}_\ell(t) \quad (6.11)$$

$$\text{subject to } \left[ \sum_{t=0}^{t=24h} \mathcal{P}_\ell(t) \right] \geq \mathcal{F}_{ev\ell} \times \mathcal{S}_\ell \quad \forall \mathcal{F}_{ev\ell} \in \mathcal{F}: \mathcal{F}_{Mn} \leq \mathcal{F} < 1$$

where  $\mathbb{L}$  denotes the number of EVs that is considered while adjusting their charging loads.  $\mathcal{S}_\ell$  denotes the complete BSoC level of an EV.  $\mathcal{F}_{ev\ell}$  denotes a numerical parameter that is determined based on the driving pattern of each EV.  $\mathcal{F}_{Mn}$  denotes the minimum value of all numerical parameters of  $\mathcal{F}_{ev\ell}$  that can satisfy the expectation of EV users. The value of  $\mathcal{F}_{Mn}$  is calculated using initial EV charging loads.

Equation (6.12) is the second objective function, which minimizes the electricity bill of each HP user over a day of quarter-hourly time steps.

$$\min_{\forall j \in \mathbb{J}} \Delta t \sum_{t=0}^{t=24h} C_{DTou}(t) \mathcal{Q}_{HPj}(t) \quad (6.12)$$

$$\text{subject to } \left[ \sum_{t=0}^{t=24h} \mathcal{Q}_{HPj}(t) \right] \geq F_{hpj} \times \mathcal{E}_j \quad \forall F_{hpj} \in F: F_{Mn} \leq F < 1$$

where  $\mathbb{J}$  denotes the number of HPs that is counted while adjusting their heating loads.  $\mathcal{E}_j$  denotes the non-optimized heating energy of each HP over a day in kWh.  $F_{hpj}$  denotes an empirical parameter that is evaluated based on the comfortable temperatures of each HP premise.  $F_{Mn}$  denotes the minimum value of all empirical parameters of  $F_{hpj}$ . The value of  $F_{Mn}$  is iteratively calculated by solving Equation (6.12), while monitoring the indoor temperatures of HP houses using Equation (6.7). In other words, the empirical threshold of  $F_{Mn}$  is determined using Equations (6.12) and (6.7) to maintain the indoor temperatures of HP houses between 18-21.5°C.

Non-iterative unbalanced power flow evaluates network constraints, as illustrated in Chapter 4. The network constraints are monitored during the optimization process by recording RMS voltages, RMS current flows, and voltage unbalance factors, as follows.

$$\left\{ \begin{array}{l} I_i(t) \leq I_{max} \\ V_{min} \leq |V_i(t)| \leq V_{max} \\ VUF_i(t) \leq VUF_{max} \end{array} \right\} \quad \forall i \in \mathbb{K} \quad (6.13)$$

where  $I_i(t)$  denotes RMS current flows through the cables of feeder segments across adjacent connection points at time step  $t$ .  $V_i(t)$  denotes RMS voltages at each connection point at time step  $t$ .  $VUF_i(t)$  denotes the voltage unbalance factor ( $VUF$ ) at each connection point in percentage at time step  $t$ .  $I_{max}$  denotes the cut-out value of fuse current for each main feeder.  $V_{min}$  and  $V_{max}$  denote the lower and upper tolerances of voltage magnitudes.  $VUF_{max}$  denotes the maximum value of allowed  $VUF$  in percentage.  $\mathbb{K}$  denotes the number of EV/HP connection points.

The constraints of Equations (6.11) and (6.12) are re-arranged into the following linear form to solve them using MATLAB.

$$\begin{aligned} -1 \times A \times X &\geq -1 \times b \\ LB &\leq X \leq UB \end{aligned} \quad (6.14)$$

where  $A$  denotes a  $(1 \times n)$  matrix.  $n$  denotes the total number of daily time steps, which is 96 by considering  $\Delta t = (1/4)h$ . Therefore,  $A$  is a  $(1 \times 96)$  matrix of “1”.  $X$  denotes the matrix of decision variables with  $(96 \times 1)$  elements per each EV/HP user. Each element of  $X$  represents an integer value of operational state variables (i.e.  $1 \vee 0$ ) multiplied by another value of power consumption.  $b$  denotes either the minimal BSoC level of each EV (i.e.  $\mathcal{F}_{evl} \times \mathcal{S}_\ell$ ), or  $b$  denotes the empirical HP threshold (i.e.  $F_{hpj} \times \mathcal{E}_j$ ).  $LB$  denotes the lower limit of decision variables, which is a  $(1 \times 96)$  matrix of “0”.  $UB$  denotes the upper limits of decision variables.  $UB$  is a  $(1 \times 96)$  matrix of initial EV charging loads, whereas  $UB$  is calculated using Equation (6.8) for HPs.

Equations (6.11) and (6.12) are then locally solved for EVs and HPs using mixed integer linear programming. MATLAB R2015a is used to solve Equations (6.11) and (6.12) with “*intlinprog*” function.

Figure 6.2 shows the proposed steps to solve these objective functions. The three-phase unbalanced network constraints of Equation (6.13) are considered using a recursive approach, as shown in Figure 6.2. This recursion calls “*intlinprog*” function with updated values of the  $UB$  matrix until network constraints are maintained within

their limits. The  $UB$  matrix is updated by substituting the last feasible solutions of Equations (6.11) and (6.12) in the pre-assigned  $UB$  matrix (i.e. the upper limits of decision variables). Equation (6.9) is used to synthesize time-varying tariffs over a one-day-ahead time interval based on the pre-loaded overall demand of the network under study. Afterwards, EV/HP objective functions are solved over a day of quarter-hourly time steps (see Figure 6.2).

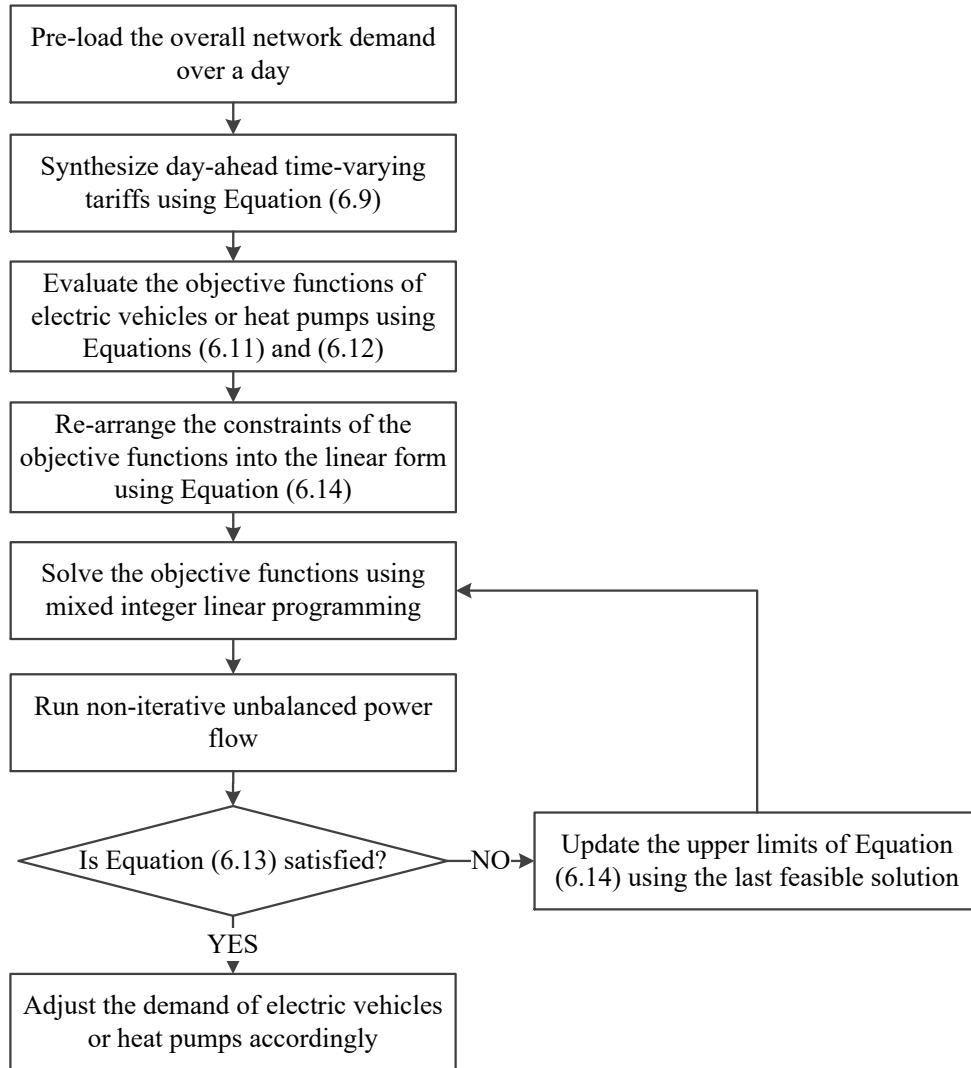


Figure 6.2: The proposed steps of the decentralized control algorithm.

Although mixed integer algorithms have a non-deterministic polynomial (NP) hardness, the proposed “*intlinprog*” function uses heuristic techniques to cope with NP hardness. This function tightens the feasible area using cutting planes. Further, the “*intlinprog*” function solves a series of linear programming relaxation problems to transform integer programming into linear programming. Therefore, this transformation is later used to ensure a near optimality of the results achieved [139].

### 6.3 The Network under Study

A real low voltage (LV) network (see Figure 6.3) is adapted from [120], [140] to test the performance of the decentralized control algorithm. This real network consists of a 500kVA distribution transformer, which steps down the voltage from 11kV to 0.416kV. This transformer serves 330 consumers as shown in Figure 6.3. Feeders are constructed using underground cables of the following sizes: 300mm<sup>2</sup>, 185mm<sup>2</sup>, and 95mm<sup>2</sup>. Meantime, consumers are served using 35mm<sup>2</sup> and 25mm<sup>2</sup> cables.

In Refs. [120], [140], network users are distributed across feeders considering 90 users along one feeder, while distributing other 157 and 83 users across the remaining feeders. Meanwhile, 108 users are connected to one phase, while connecting other 109 and 113 users to the remaining phases.

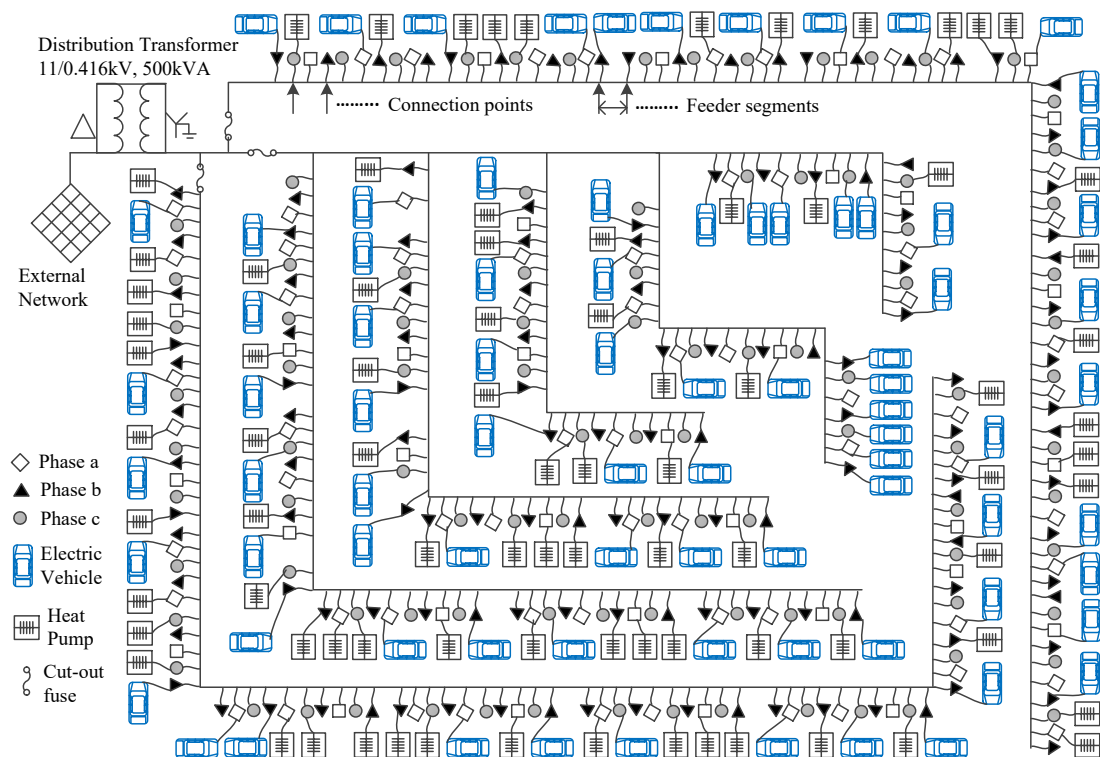


Figure 6.3: The real LV distribution network under study (adapted from [120], [140]). The thicknesses of network feeders and service cables are not to scale.

According to the prediction model of Chapter 3, EV and HP connections to UK electricity networks will not exceed a 32.47% (10.15% for EVs, and 22.32% for HPs) by 2035. These percentages are calculated using EV and HP demands in Table 3.1 relative to the maximum value of residential demand in Table 3.2. Consequently, the deployments of EVs and HPs are considered a 25% of EVs and another 25% of HPs. These percentages are evaluated by dividing the number of EV and HP users to the

number of all network users. Therefore, 82 EVs and 82 HPs are deployed across the network under study, as shown in Figure 6.3.

Figure 6.4 (a) shows the individual loads of 82 HPs alongside their average heating demand over a day. Figure 6.4 (b) illustrates the individual CoP values of these 82 HPs, as calculated using Equation (6.4).

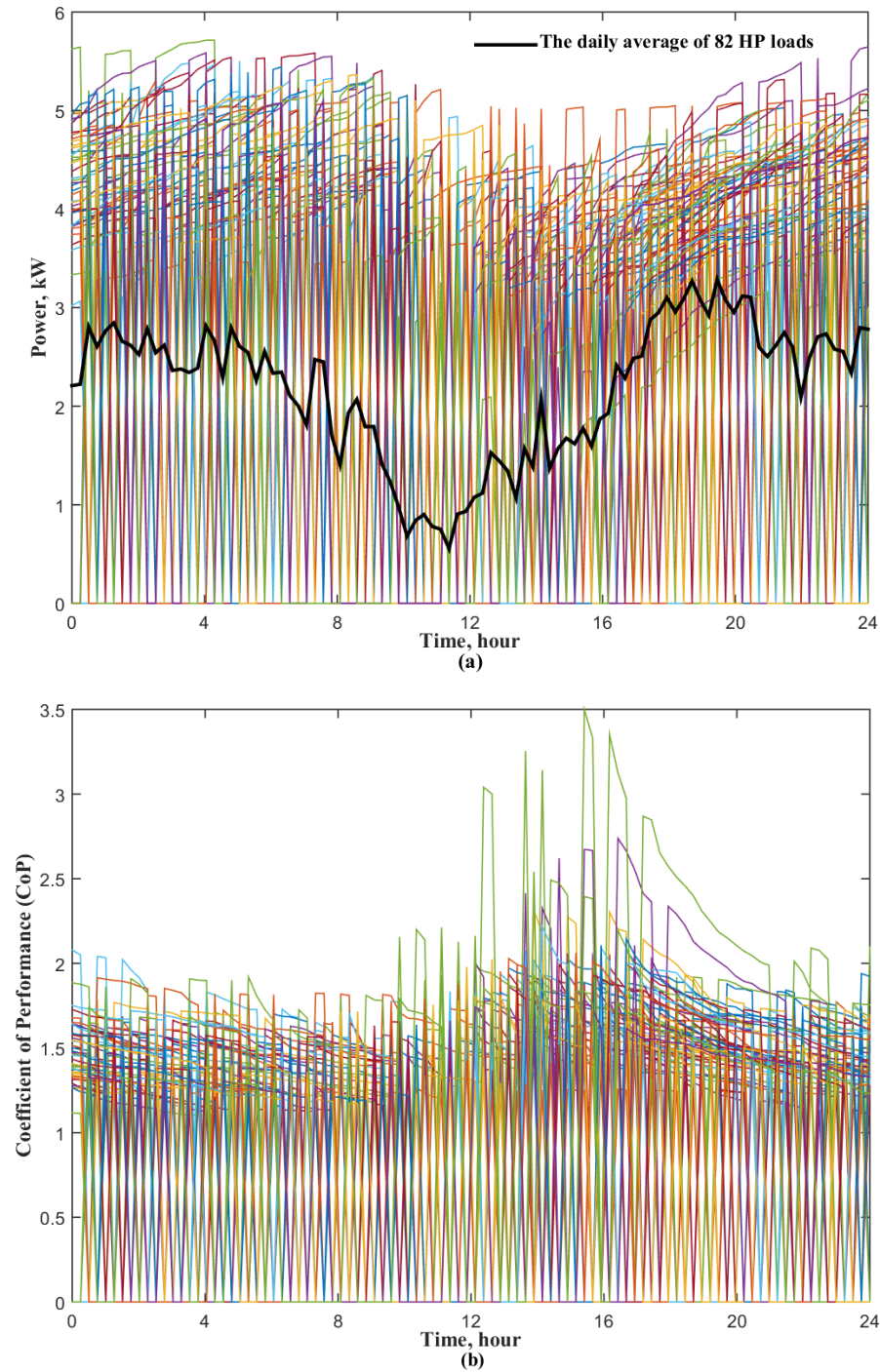


Figure 6.4: (a) Daily 82 HP heating demands. (b) Daily CoP values of these 82 HPs.

HP heating loads were diversified by considering different initial conditions per each HP user. These HPs were modelled based on UK ambient temperatures over winter days in 2014 [121]. Quarter-hourly time steps were considered while modelling individual loads of 82 HPs. Figure 6.5 (a) indicates the indoor temperatures of the 82 HP houses over a day of quarter-hourly time steps along with their histogram.

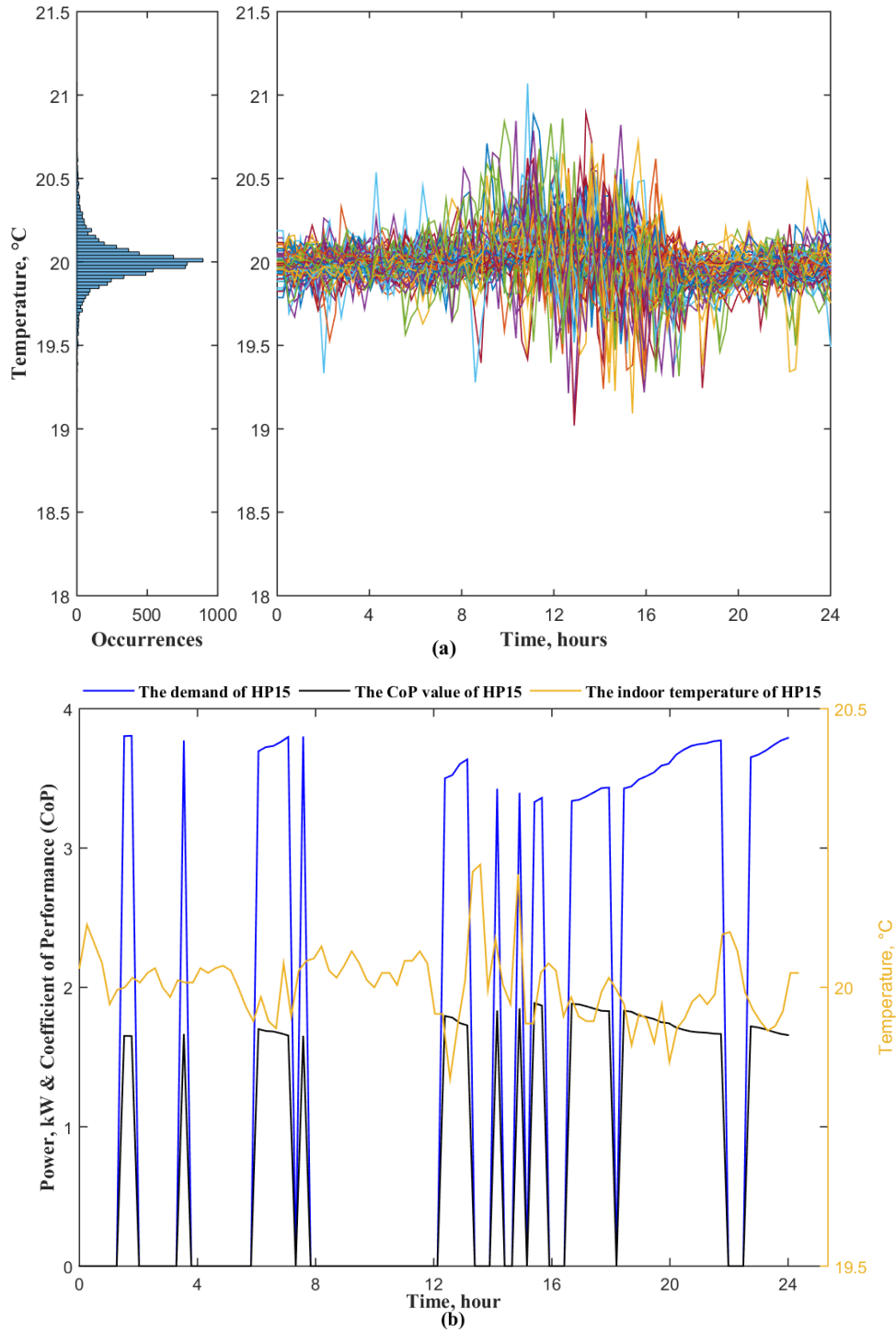


Figure 6.5: (a) Daily indoor temperatures of 82 HP houses and their histogram. (b) A sample of 1 HP house daily heating demand along with its daily CoP value and its daily temperature.

With a single HP, Figure 6.5 (b) presents daily samples of the following characteristics: heating loads, CoP values, and indoor temperatures. Figure 6.6 (a) shows individual 82 EV charging loads over a day of quarter-hourly time steps, including their daily average charging demand. Individual EV loads were predicted based on the method presented in Chapter 5.

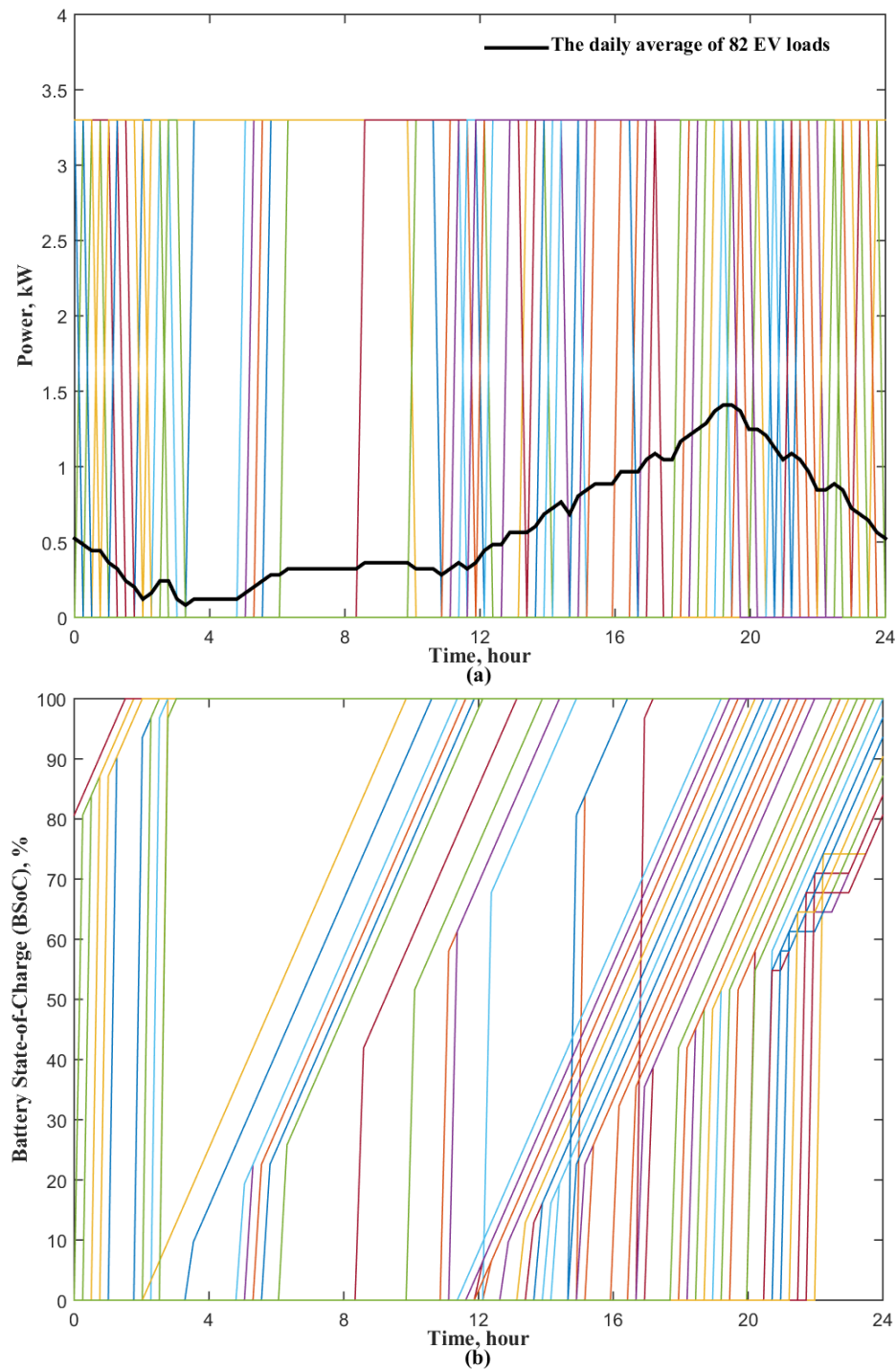


Figure 6.6: (a) Daily 82 EV charging loads. (b) BSoC levels of 82 EVs.

Daily BSoC levels of 82 EVs are calculated using Equation (6.1) based on individual EV loads, as shown in Figure 6.6 (b). Figure 6.7 shows samples of two EV charging loads over a day of quarter-hourly time steps along with their BSoC levels.

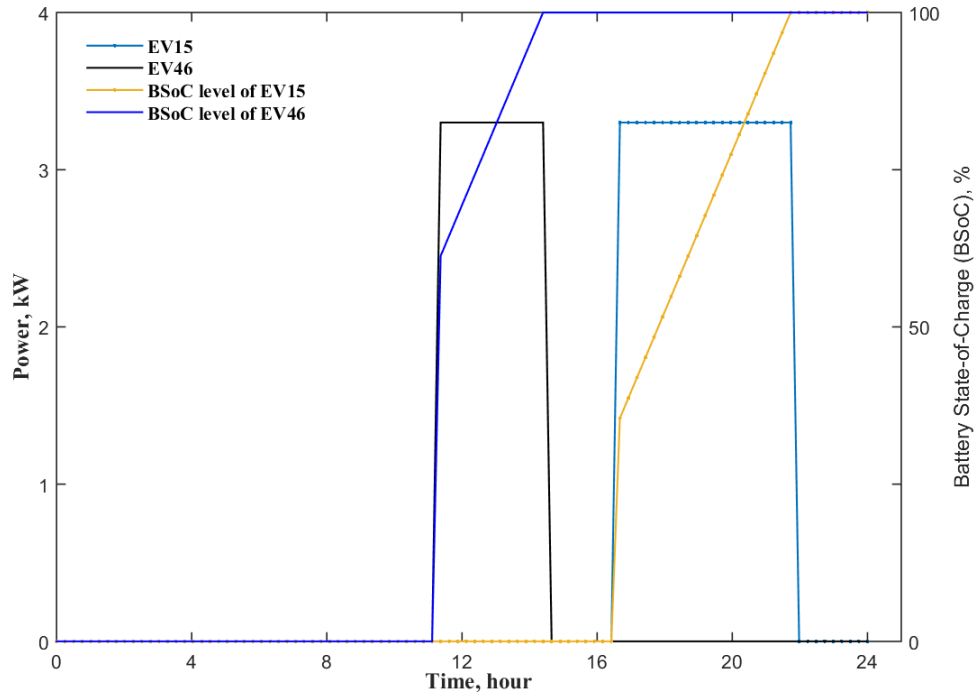


Figure 6.7: A sample of two EV charging loads along with their BSoC levels.

#### 6.4 Simulation Results

In this work, the decentralized control algorithm is presented using two case studies, as described below.

Case 1 evaluates the network under study considering the modelled 82 EVs and 82 HPs without using the decentralized control algorithm. Case 2 evaluates this network considering optimized EV/HP uses with the decentralized control algorithm.

The two case studies are presented using daily RMS voltages and daily voltage unbalance factors per each connection point of the network under study. In addition, daily RMS current flows are recorded across feeder segments.

Consumer satisfaction is monitored by presenting EV daily BSoC levels and daily indoor temperatures of HP houses. Figure 6.8 shows daily RMS voltages at each connection point of the network under study. RMS voltages are per-unitized with a base voltage of 230V per phase.

It can be seen that, these voltages are within their fluctuation tolerances, as assigned by Engineering Recommendations P28 in LV networks [117]. Figure 6.9 illustrates RMS current flows through feeder segments across adjacent connection points. RMS current flows are per-unitized using the rated currents of each underground cable (i.e.  $300\text{mm}^2$ ,  $185\text{mm}^2$ , and  $95\text{mm}^2$ ). The rated values of cable current, and the cut-out values of fuse current were extracted from another study [129].

Figure 6.9 shows that, with the considered connections of EVs and HPs, main feeder segments will be overloaded to 1.2pu during peak hours. Figure 6.10 demonstrates daily voltage unbalance fluctuations per each connection point. These fluctuations are within the limit according to Engineering Recommendations P29 [118].

For Case 1, Figure 6.5 (a) shows daily indoor temperatures of 82 HP houses. These indoor temperatures are calculated based on outdoor temperatures, thermostatic operational cycles, and other factors, as modelled in Section 6.2.2. Figure 6.6 (b) indicates 82 EV daily BSoC levels without using the decentralized control algorithm (Case 1). It can be seen that, all EVs have achieved the 100% BSoC level in different timings based on their initial BSoC levels and their initial charging times.

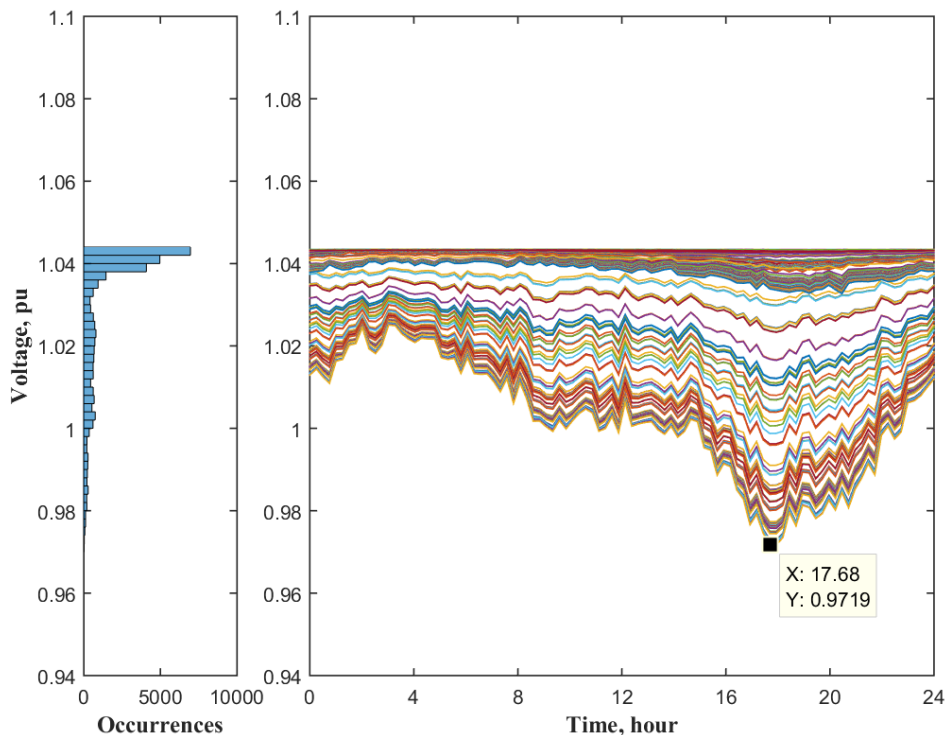


Figure 6.8: Daily 330 RMS voltages at each connection point of the network under study along with their histogram (Case 1).

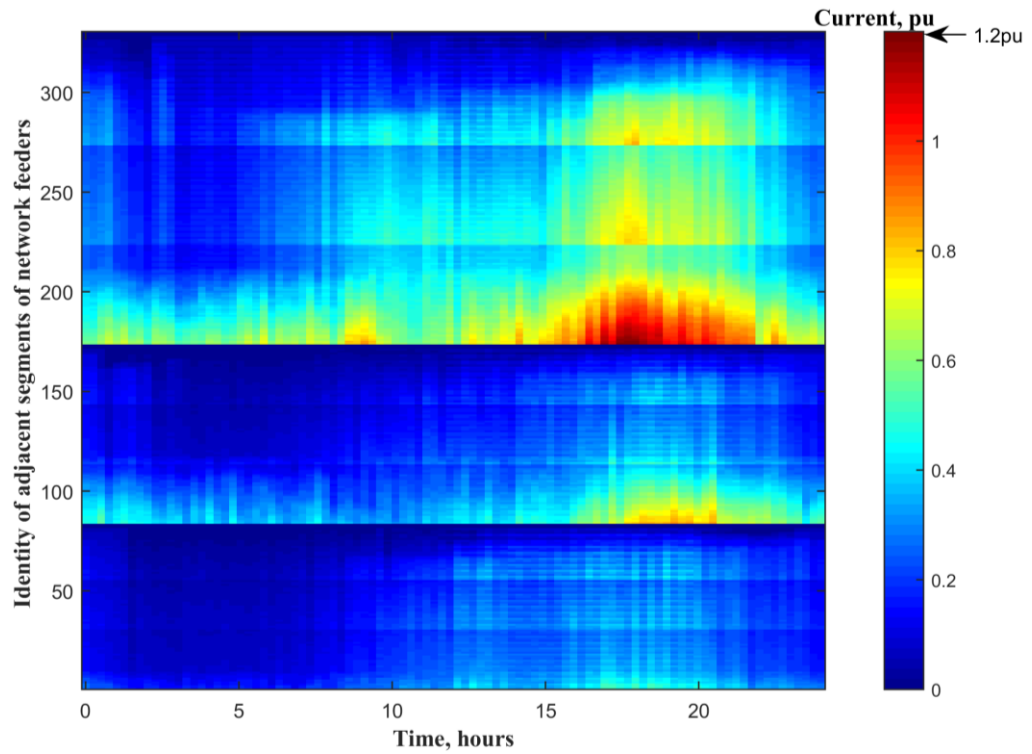


Figure 6.9: Heat map of daily 330 RMS current flows through feeder segments across adjacent connection points (Case 1).

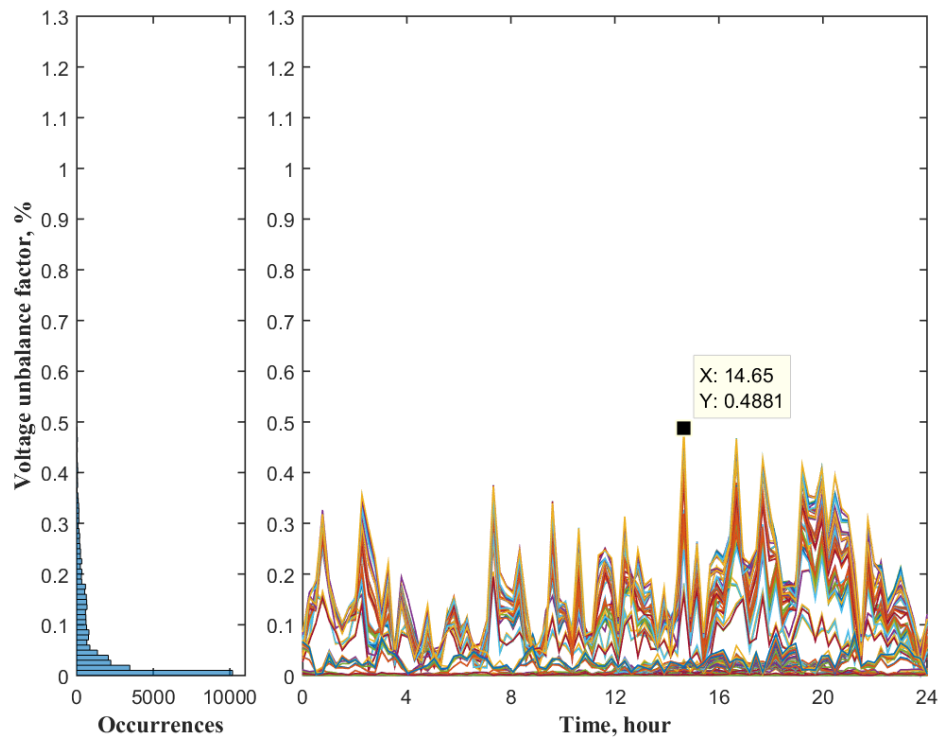


Figure 6.10: Daily 330 voltage unbalance factors at each connection point of the network under study along with their histogram (Case 1).

In Case 2, the decentralized control algorithm is used to optimize the use of EVs and HPs. The day-ahead time-varying tariff is firstly synthesized using Equations (6.9) and (6.10). Then, all the objective functions of EVs and HPs are solved in a matter of seconds (3.783s) using MATLAB R2015a (see Appendix E).

Simulation results of Case 2 are presented as follows. Figure 6.11 demonstrates RMS voltages at each connection point of the network under study over a day of quarter-hourly time steps. RMS current through feeders was reduced from 1.2pu to 1.028pu using the decentralized control algorithm, as shown in Figure 6.12. The cut-out value of fuse current is 1.047pu for the main feeder, as presented in Ref. [129]. Voltage unbalance factors were maintained within their limit, while using the decentralized control algorithm (see Figure 6.13).

Figure 6.14 demonstrates the optimized EV charging loads and their average charging loads over a day. The decentralized control algorithm interrupts EVs from being charged only if they reach  $\mathcal{F}_{Mn} \times 100\%$  of their complete BSoC level or more, as shown in Equations (6.11) and (6.14). Figure 6.15 shows that, all EVs achieve more than 87% of the complete BSoC levels using the proposed algorithm. This percentage means that the value of  $\mathcal{F}_{Mn}$  is 0.87 for these 82 EVs.

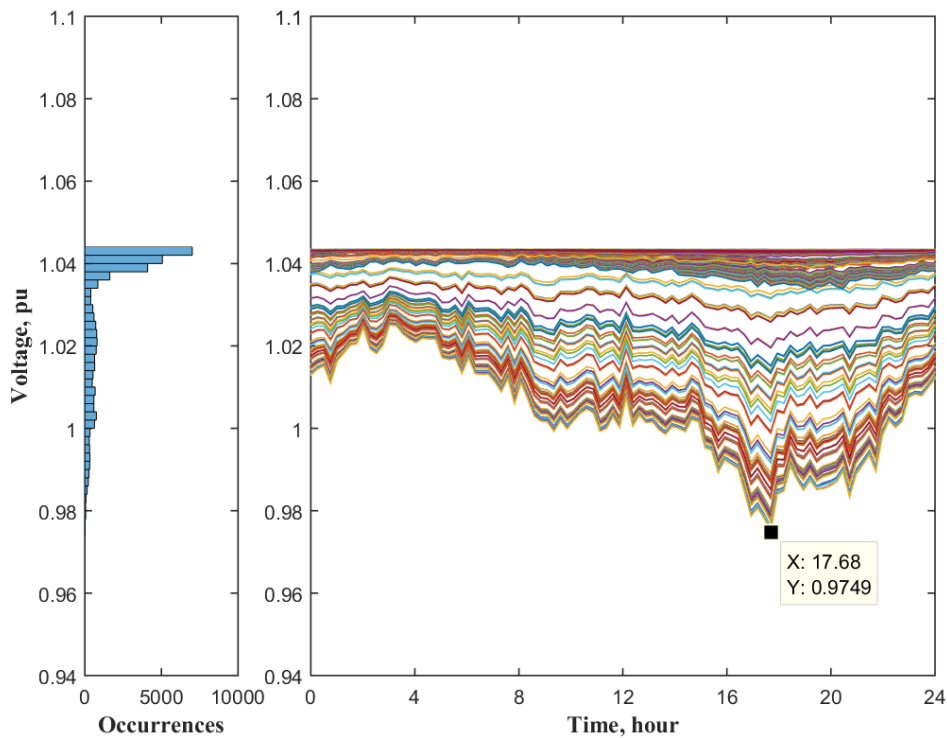


Figure 6.11: Daily 330 RMS voltages at each connection point of the network under study along with their histogram (Case 2).

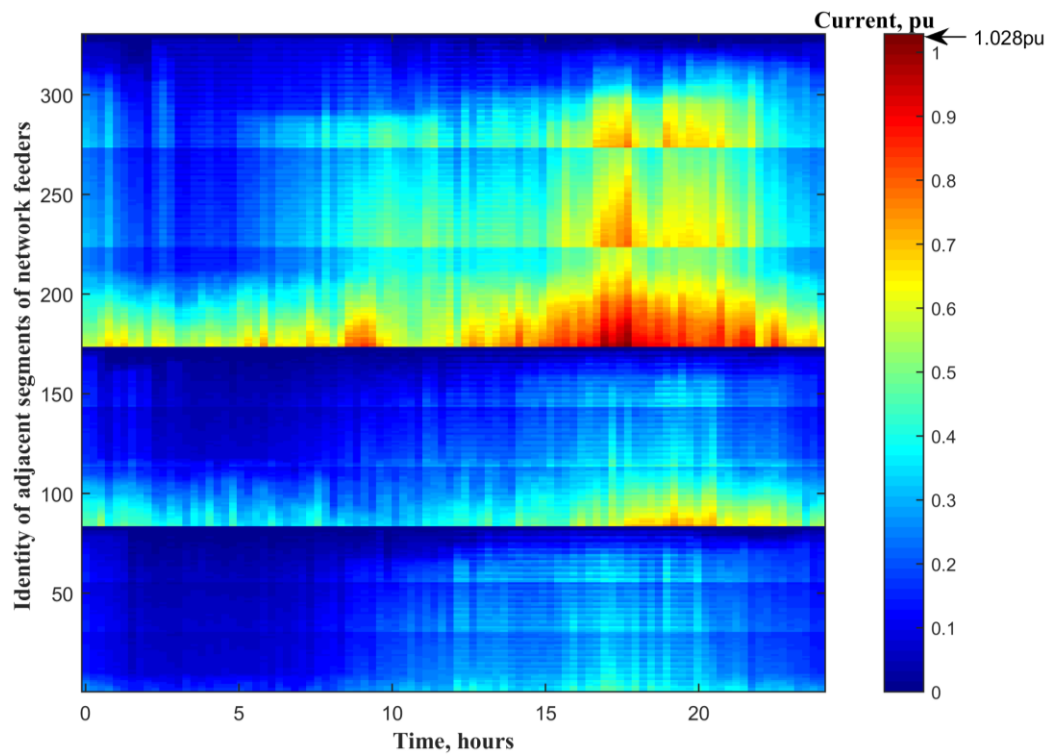


Figure 6.12: Heat map of daily 330 RMS current flows through feeder segments across adjacent connection points (Case 2).

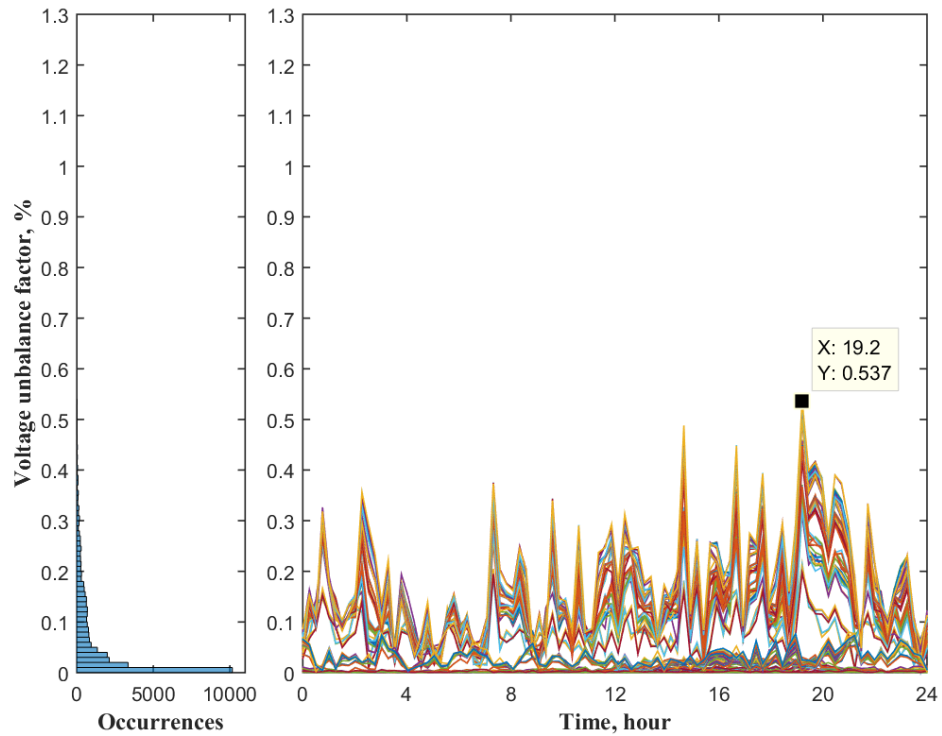


Figure 6.13: Daily 330 voltage unbalance factors at each connection point of the network under study along with their histogram (Case 2).

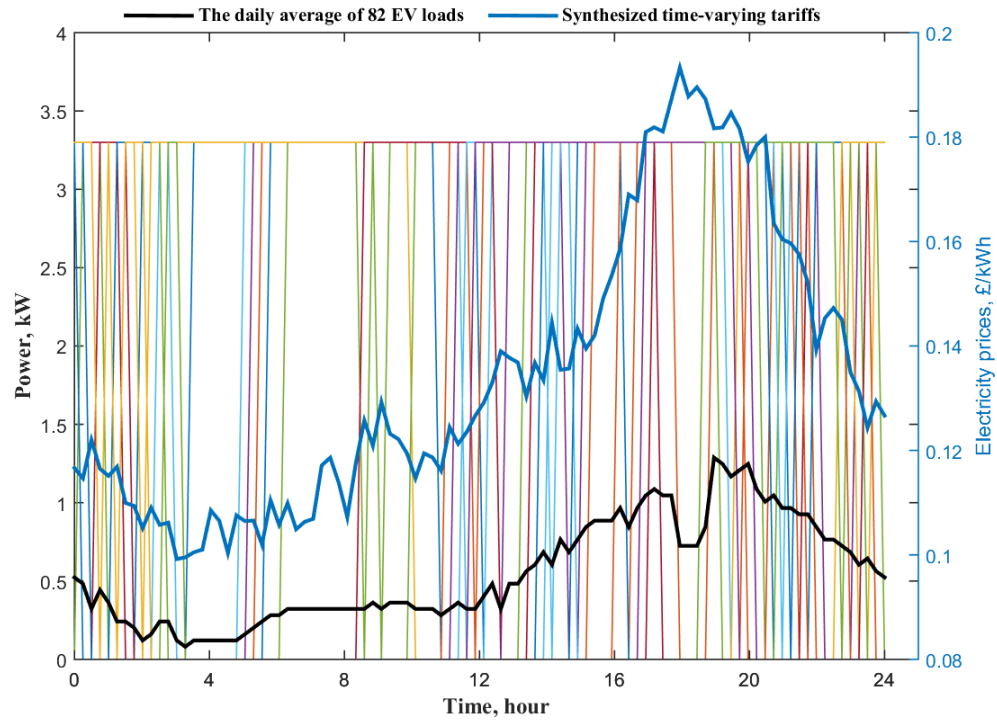


Figure 6.14: Optimized 82 EV daily charging loads and their average charging loads (Case 2).

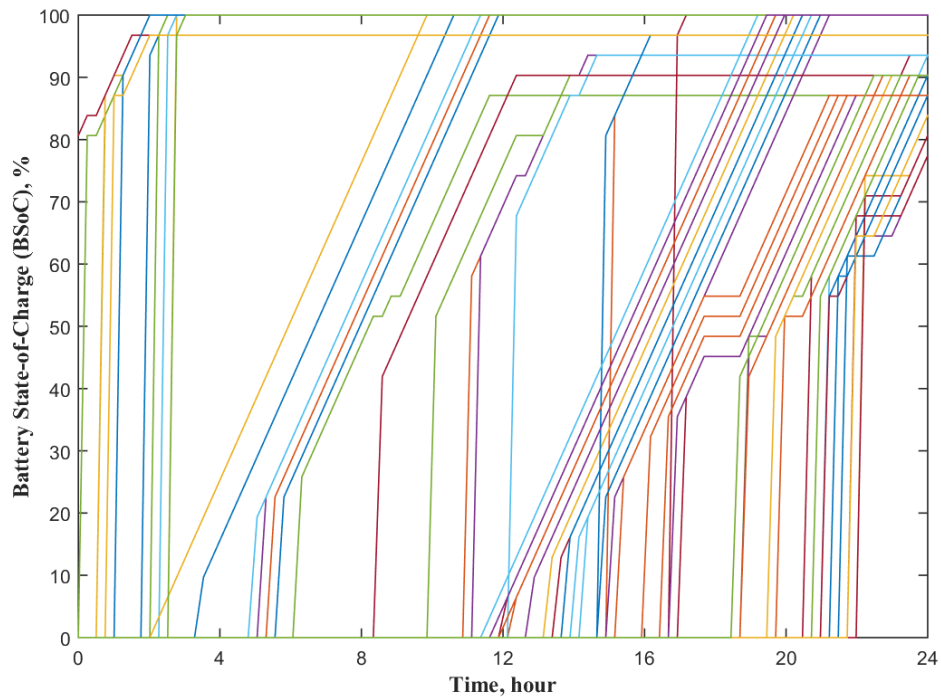


Figure 6.15: The daily BSoC levels of the optimized 82 EVs (Case 2).

Figure 6.16 presents the adjusted HP heating loads and their average heating demand over a day of quarter-hourly time steps. Percentages of adjusted energy relative to typical energy were calculated over a day for each individual HP load using Figure 6.16 (Case 2) and Figure 6.4 (a) (Case 1). The minimum percentage was determined to be 78%. Therefore, the value of  $F_{Mn}$  was 0.78 for these 82 HPs. Figure 6.17 shows that the decentralized control algorithm is able to maintain the daily indoor temperatures of HP houses between 18°C and 21.5°C.

Figure 6.18 compares between Case 1 and Case 2 in terms of daily electricity bills considering quarter-hourly time steps for 82 EV users. Electricity bills of EV users were reduced by an average of 10% (i.e. from £2.18 in Case 1 to just £1.96 in Case 2), as shown in Figure 6.18. Electricity bills of HP users were decreased by an average of 12% (i.e. from £7.18 in Case 1 to £6.32 in Case 2), as illustrated in Figure 6.19. Therefore, the decentralized control algorithm reduced the electricity bills of EV/HP users by an average of 11% over a day.

The decentralized controller enables network operators to serve these EVs and HPs using existing infrastructure. Consequently, additional network reinforcement can be deferred without extensive requirement for communication systems.

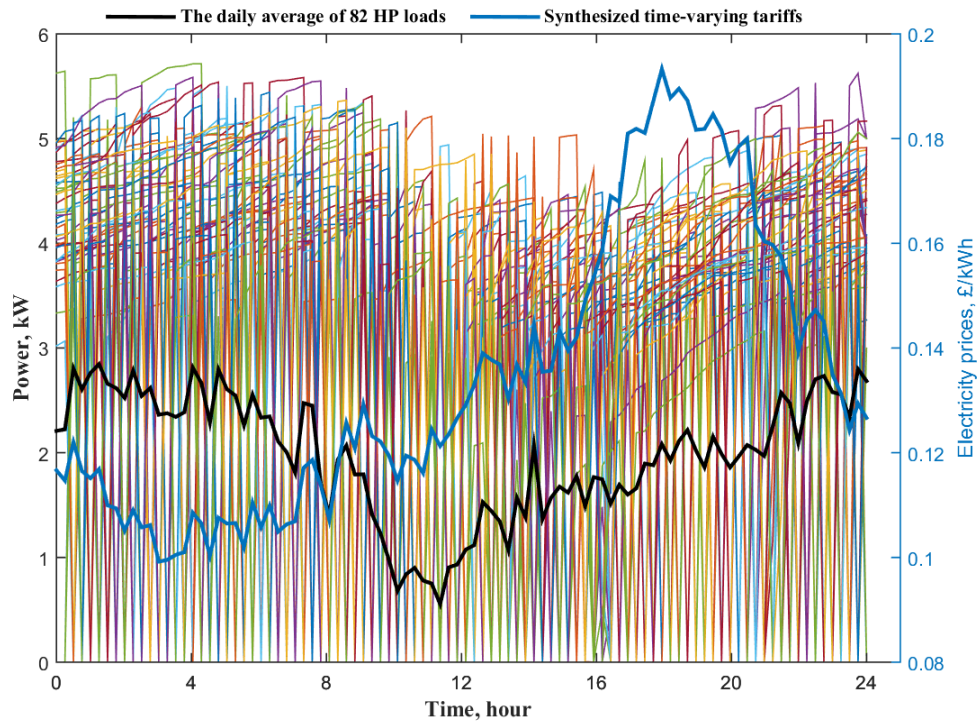


Figure 6.16: Optimized 82 HP daily heating loads and their average heating demands (Case 2).

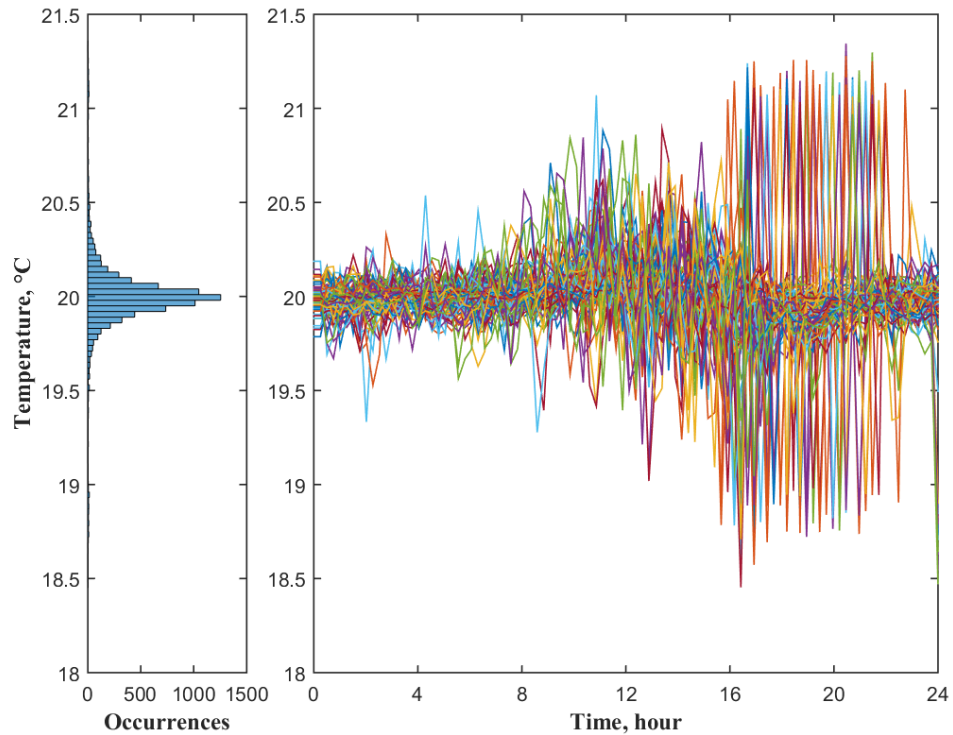


Figure 6.17: The indoor temperatures of 82 HP houses optimized along with their histogram (Case 2).

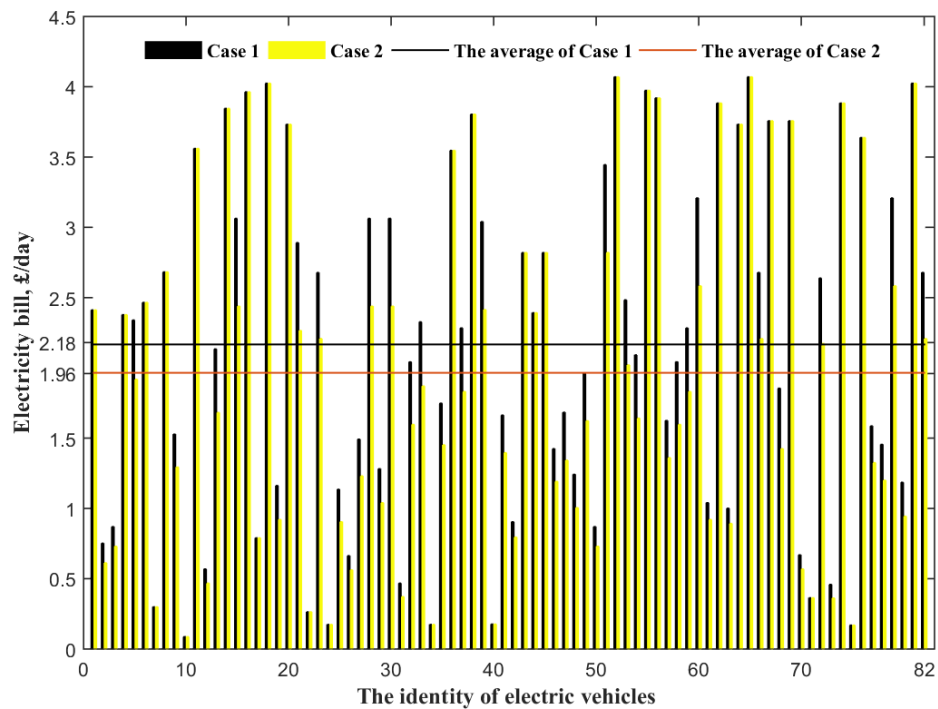


Figure 6.18: The electricity bill reduction of EV users in Case 2 relative to Case 1.

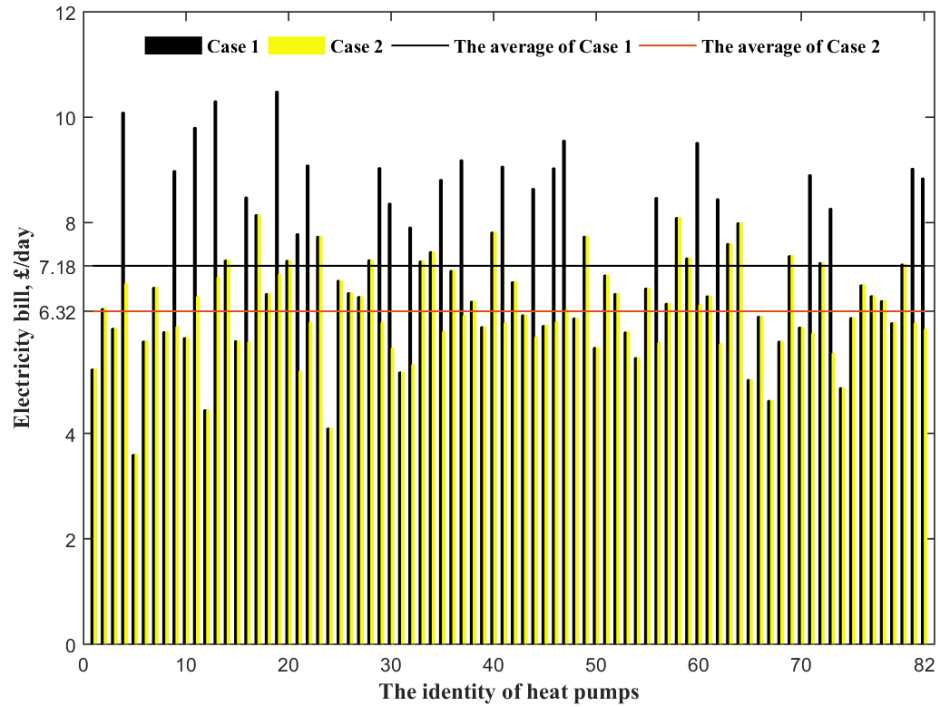


Figure 6.19: The electricity bill reduction of HP users in Case 2 relative to Case 1.

## 6.5 Conclusions

The decentralized control algorithm was developed to adjust EV and HP loads using a synthesized time-varying tariff based on mixed integer linear programming. The levels of consumer satisfaction were evaluated using mathematical models of the BSoC levels of EVs and the indoor temperatures of HP houses.

A convenient use of an EV was considered by achieving at least 87% of its complete BSoC level. A comfortable use of an HP was considered by keeping the indoor temperature of its house between 18-21.5°C.

Without the decentralized control algorithm, the RMS current exceeded their rated value by 20%, serving 82 EVs and other 82 HPs using a real network of 330 residential customers. With the control algorithm, the RMS current exceeded their rated value by just 2.8% while serving these EVs and HPs. Moreover, the controller decreased electricity bills of EV and HP users by an average of 11% over a day.

Therefore, the decentralized control algorithm is able to accommodate additional EV and HP loads without network reinforcement using an automated load shedding, while overcoming the need for third parties (e.g. aggregators) and extensive communication systems.

# CHAPTER 7

## 7. Conclusions and Recommendations for Further Work

### 7.1 Conclusions

Small-scale, residential, and distributed energy resources (DER) were studied to investigate their impact on electric power systems. The considered DER units were electric vehicles (EVs), heat pumps (HPs), and photovoltaic (PV) arrays. The objectives of this study were outlined as follows: predicting the UK residential demand considering DER power, evaluating distribution network parameters with the DER units, coordinating EV charging loads, and controlling EV and HP loads together.

To meet these objectives, a prediction technique was developed to incorporate DER power into the UK residential demand. Two modelling tools were implemented in MATLAB to simulate real and test networks considering different case studies of DER integration. A centralized control algorithm was designed to coordinate EV charging loads according to network constraints. A decentralized control algorithm was planned to control EV and HP loads based on consumer satisfaction, network constraints, and electricity prices. The results of the studies are summarized as follows.

#### 7.1.1 Impacts of Distributed Energy Resources on Future Demand

In Chapter 3, the UK residential demand in 2035 was predicted considering residential EVs, HPs, and PV arrays.

The UK overall demand of 2014, which was collected at 5-minute time steps, was read from GridWatch databases. The demand was then averaged into half-hourly time steps. The UK residential demand was calculated using its percentage of contribution relative to the UK overall demand, as reported by National Grid.

Customer-Led Network Revolution (CLNR) trials were used to provide daily mean values of power for each month of the year between 2012 and 2014. Mean values of the active power of 133 EVs, 336 HPs, and 151 PV arrays were gathered over a day of half-hourly time steps.

The annual power of DER units was synthesized using a normal probability distribution and median filter. The annual power was scaled and combined using Future Energy Scenarios by National Grid, predicting the UK residential demand at half-hourly time steps in 2035.

Residential PV generation was predicted to exceed the UK residential demand by an average of 2GW over summer mid days. An average increase of 10GW in the UK residential demand was expected between 4:00-7:00 pm, because of the decrease in PV power generation during that time interval.

Therefore, National Grid should incentivise the use of residential energy storage systems (ESS) to store the surplus of PV power generation. In this way, demand increase can be managed using the energy stored in local ESS units. Further, fast flexible generation plants can accommodate demand increase.

### **7.1.2 Impacts of Distributed Energy Resources on Distribution Networks**

In Chapter 3, the impact of residential EVs, HPs and PV arrays upon the future residential demand was studied. In Chapter 4, the impact of DER units on distribution networks was assessed based on voltage magnitudes, voltage unbalance factors, and power flows. Two networks, a low voltage section of the UK generic distribution network (UKGDN) and a real low voltage network of Electricity North West, were used in this chapter.

A low voltage section of the UKGDN was modelled using three-phase four-wire connections in MATLAB/Simulink/Simscape/SimPowerSystems. The mean values of the active power of 8,000 residential customers and 133 EVs over a day of half-hourly time steps were read from CLNR trials. The daily mean values were used to model 384 residential customers, while connecting 96, 192, and 288 EVs.

A real network of Electricity North West was studied using a MATLAB function of unbalanced load flow that was developed in this research. This network serves 135 residential customers. The network was studied by connecting different combinations of EVs, HPs, and PV arrays to existing residential customers.

Over a day of minute-by-minute time steps, individual residential loads were synthesized using normal probability distribution, while individual EV charging loads

were generated using uniform probability distribution. Mean values of residential and EV loads, which were read from CLNR trials, were used.

Using mathematical models over a day of minute-by-minute time steps, individual HP loads were modelled based on ambient temperature, whereas individual PV generation was modelled using solar irradiance.

In the UKGDN case study, unbalanced voltages were detected even if the numbers of similar EVs were equally distributed across the three phases. This is a result of different EV charging time durations. Transformers and cables exceeded their rated values with EV connections. It was noticed that, the low voltage section of the UKGDN can tolerate a maximum connection of 96 EVs without further reinforcement.

In the real network case study, a bi-directional unbalanced power flow was observed with PV arrays, causing an increase in voltage magnitude. With separate and simultaneous connections of EVs, HPs, and PV arrays, voltage unbalance factors exceeded their limits.

A conclusion is therefore made that a combination of EV/PV or HP/PV mitigates the impact of these low carbon loads, because PV generation partially compensates the consumption of EVs and HPs.

### **7.1.3 Centralized Load Allocation of Electric Vehicles in Distribution Networks**

The results of Chapter 4 showed that uncoordinated EV charging loads lead to the violation of network constraints. In Chapter 5, a central controller was introduced to coordinate high EV charging loads using nonlinear optimization considering voltage magnitudes, voltage unbalance factors, and other network constraints.

The controller, which was installed at the secondary side of 11/0.4kV distribution transformer, employs two-way communications to collect and send information from and to residential and EV loads.

The UKGDN was extended to include the medium voltage section of 19-bus network. Voltage magnitudes, voltage unbalance factors, and other network constraints were calculated using unbalanced load flow over a day of minute-by-minute time steps.

Without the controller, the medium voltage section of the UKGDN tolerated the uncoordinated charging loads of 384 EVs. However, the low voltage section of the UKGDN requires further reinforcement, because voltage magnitudes, voltage unbalance factors, and network components exceeded their limits.

With the controller, voltage magnitudes, voltage unbalance factors, and network components were maintained within their limits, while providing all EVs with enough energy to be fully charged. The limits of voltage magnitudes were  $-6/+10\%$  at the low voltage level and  $-6/+6\%$  at the medium voltage level. The limit of maximum voltage unbalance factor was 1.3%.

A conclusion is made that the centralized controller has the ability to assist the network operator to coordinate high EV charging loads without the need for additional network reinforcement. However, the costs of information and communication technologies need to be considered when a centralized controller is used.

#### **7.1.4 Decentralized Load Adjustment of Electric Vehicles and Heat Pumps**

It was shown in Chapter 5 that a centralized controller requires two-way communications between the controller and EV premises. To overcome this requirement, a decentralized controller was implemented in Chapter 6.

The decentralized controller was tested using a real low voltage distribution network of Electricity North West. The network, which serves 330 residential customers, is different from the one used in Chapter 4.

The decentralized control algorithm was used to control 82 EVs and 82 HPs in different premises considering consumer satisfaction. Consumer satisfaction was monitored using mathematical models of EV battery state-of-charge (BSoC) levels and the indoor temperatures of HP premises.

The objective of the decentralized control algorithm is to minimize electricity bills over a day, achieving at least 87% of EV complete BSoC level, and maintaining the indoor temperatures of HP premises between 18-21.5°C. Mixed integer linear programming is used to adjust EV and HP loads based on a synthesized time-varying tariff.

The uncontrolled loads of EVs and HPs and the individual loads of residential customers were combined to monitor voltage magnitudes, voltage unbalance factors, and current flows using unbalanced load flow over a day of quarter-hourly time steps. Current flows through the cables exceeded their rated values by 20% without the decentralized controller.

With the controlled EV and HP loads, current flows through the cables exceeded their rated values by only 2.8%, while maintaining EV final BSoC levels and the indoor temperatures of HP premises within their boundaries. Electricity bills of residential premises with EVs and HPs were reduced by an average of 11% over a day. The network constraints of voltage magnitudes and voltage unbalance factors did not exceed their limits.

Therefore, the decentralized controller is capable to control EV and HP loads, so that, consumer electricity bills are reduced, consumer satisfaction is guaranteed, and network constraints are not violated. At the same time, the decentralized controller can defer distribution network reinforcement, overcoming the need for extensive communications between the controller and residential premises.

## **7.2 Recommendations for Further Work**

The following recommendations were distinguished to extend the work of this thesis.

### **7.2.1 Demand Predictions**

In Chapter 3, a surplus of residential PV power generation was predicted over residential demand. Prediction results showed that the generation of PV arrays will exceed the residential demand over summer mid-days. Therefore, it is recommended that the size of residential ESS units is investigated to store the surplus of residential PV power generation. Moreover, it is suggested that trials of more than 133 EVs, 336 HPs, and 151 PVs are included in the prediction model to acquire a diverse representation of these DER units. Weather data can be embedded in the prediction model to increase the accuracy of prediction results.

### **7.2.2 Impact Assessments**

In Chapter 4, the impact of residential EVs, HPs, and PV arrays on distribution networks was studied. Voltage magnitudes, voltage unbalance factors, and power flows were considered. Therefore, a suggestion is made that harmonics and flicker should be studied to evaluate other power quality aspects. A risk assessment of various uneven distributions of residential customers across the three phases of distribution networks is recommended. This impact assessment on distribution networks can be investigated using Monte Carlo Simulation of sequential unbalanced power flow.

### **7.2.3 Centralized Controller**

In Chapter 5, a centralized controller was implemented to mitigate the impact of EV charging loads on distribution networks. Residential loads, EV loads, and network constraints were considered with the central controller. To evaluate the feasibility of the central controller, a revised control algorithm should include BSoC levels and battery degradation costs. In addition, it is recommended that the central controller is extended to control some other smart appliances.

### **7.2.4 Decentralized Controller**

In Chapter 6, a decentralized controller was used to adjust EV and HP loads considering electricity prices, consumer satisfaction, and network constraints. It is recommended that the performance of the decentralized control algorithm is evaluated in the laboratory. Thereafter, the algorithm can be scaled into a real-world application using smart switches, which control the EV and HP loads autonomously.

---

**References**

- [1] European Commission, “Flexible Electricity Networks to Integrate the expected Energy Evolution Results,” 2009. [Online]. Available: <http://www.fenix-project.org>. [Accessed: 18-Aug-2016].
- [2] New York Independent System Operator, “A Review of Distributed Energy Resources,” Energy Advisory, Arlington, 2014.
- [3] J. A. P. Lopes, N. Hatzigiargyriou, J. Mutale, P. Djapic, and N. Jenkins, “Integrating distributed generation into electric power systems: A review of drivers, challenges and opportunities,” *Electr. Power Syst. Res.*, vol. 77, no. 9, pp. 1189–1203, 2007.
- [4] Electrical Power Research Institute, “Realizing the Full Value of Central and Distributed Energy Resources,” California, USA, 2014.
- [5] Department of Energy & Climate Change (DECC), “United Kingdom housing energy fact file,” England, UK, 2013.
- [6] Imperial College and Element Energy, “Infrastructure in a low-carbon energy system to 2030: Transmission and distribution for Climate Change,” Cambridge, UK, 2014.
- [7] Department of Energy & Climate Change (DECC), “UK Renewable Energy Roadmap,” London, UK, 2011.
- [8] National Grid plc, “Future Energy Scenarios,” National Grid House, Warwick Technology Park, Gallows Hill Warwick, UK, 2016.
- [9] Element Energy and Carbon Alternatives, “Heat Pumps in District Heating,” Department of Energy & Climate Change (DECC), London, UK, 2016.
- [10] Element Energy, “Pathways to high penetration of electric vehicles Final report for Element Energy,” Cambridge, UK, 2013.
- [11] Element Energy, “Further Analysis of Data from the Household Electricity Usage Study: Correlation of Consumption with Low Carbon Technologies,” Cambridge, UK, 2014.
- [12] Regulation (EC) No 443/2009 of the European Parliament and of the Council, “Setting emission performance standards for new passenger cars as part of the community’s integrated approach to reduce CO<sub>2</sub> emissions from light-duty vehicles,” 2009. [Online]. Available: <http://data.europa.eu/eli/reg/2009/443/oj>. [Accessed: 18-Feb-2015].

- 
- [13] M. Nilsson and B. Nykvist, “Governing the electric vehicle transition – Near term interventions to support a green energy economy,” *Appl. Energy*, vol. 179, pp. 1360–1371, 2016.
- [14] Office for Gas and Electricity Market, “Electricity Capacity Assessment Report 2014 Annual report,” London, UK, 2014.
- [15] T. Boßmann and I. Staffell, “The shape of future electricity demand: Exploring load curves in 2050s Germany and Britain,” *Energy*, vol. 90, pp. 1317–1333, 2015.
- [16] National Grid plc, “Electricity Ten Year Statement 2014,” National Grid House, Warwick Technology Park, Gallows Hill Warwick, UK, 2014.
- [17] B. Lunz, P. Stöcker, S. Eckstein, A. Nebel, S. Samadi, B. Erlach, M. Fishedick, P. Elsner, and D. Uwe, “Scenario-based comparative assessment of potential future electricity systems – A new methodological approach using Germany in 2050 as an example,” *Appl. Energy*, vol. 171, pp. 555–580, 2016.
- [18] B. Zakeri, S. Rinne, and S. Syri, “Wind Integration into Energy Systems with a High Share of Nuclear Power—What Are the Compromises?,” *energies*, vol. 8, pp. 2493–2527, 2015.
- [19] European Copper Institute, “Power System Flexibility Strategic Roadmap,” GmbH, Germany, 2015.
- [20] National Grid plc, “Future Energy Scenarios,” National Grid House, Warwick Technology Park, Gallows Hill Warwick, UK, 2015.
- [21] M. G. Vay’a, M. D. Galus, R. A. Waraich, and G. Andersson, “On the Interdependence of Intelligent Charging Approaches for Plug-in Electric Vehicles in Transmission and Distribution Networks,” in *3rd IEEE PES Innovation Smart Grid Technologies Europe (ISGT Europe)*, 2012, pp. 1–8.
- [22] Y. Mu, J. Wu, N. Jenkins, H. Jia, and C. Wang, “A Spatial – Temporal model for grid impact analysis of plug-in electric vehicles,” *Appl. Energy*, vol. 114, pp. 456–465, 2014.
- [23] G. Strbac, N. Jenkins, M. Hird, P. Djapic, and G. Nicholson, “Integration of operation of embedded generation and distribution networks,” Manchester, UK, 2002.
- [24] A. Navarro-espinosa and L. F. Ochoa, “Probabilistic Impact Assessment of Low Carbon Technologies in LV Distribution Systems,” *IEEE Trans. Power Systems*, vol. 31, no. 3, pp. 2192–2203, 2016.
- [25] P. Richardson, “Integration of Distributed Energy Resources in Low Voltage Electricity Networks,” PhD thesis, School of Electrical, Electronic and Communications Engineering, College of Engineering and Architecture, Dublin, 2012.

- 
- [26] E. Valseira-Naranjo, D. Mart, A. Sumper, R. Villaf, and A. Sudri, "Deterministic and Probabilistic Assessment of the Impact of the Electrical Vehicles on the Power Grid," in *IEEE Power and Energy Society General Meeting*, 2011, pp. 1–8.
- [27] R. Leou, C. Su, and C. Lu, "Stochastic Analyses of Electric Vehicle Charging Impacts on Distribution Network," *IEEE Trans. Power Systems*, vol. 29, no. 3, pp. 1055–1063, 2014.
- [28] P. Richardson, D. Flynn, and A. Keane, "Impact Assessment of Varying Penetrations of Electric Vehicles on Low Voltage Distribution Systems," in *IEEE Power and Energy Society General Meeting*, 2010, pp. 1–6.
- [29] M. Bilton, N. E. Chike, M. Woolf, P. Djapic, M. Wilcox, and G. Strbac, "Impact of Low Voltage - Connected low carbon technologies on network utilisation," Reprt B4 for the "Low Carbon London" LCNF project: Imperial College London, 2014.
- [30] The Institute of Electrical and Electronics Engineers, "IEEE Application Guide for IEEE Std 1547.2-2008, IEEE Standard for Interconnecting Distributed Resources with Electric Power Systems," New York, USA, 2009.
- [31] Y. Li and P. A. Crossley, "Voltage balancing in low-voltage radial feeders using Scott transformers," *IET Gener. Transm. Distrib.*, vol. 8, no. 8, pp. 1489–1498, 2014.
- [32] S. Lee, J. Kim, D. Kim, H. Go, C. Kim, E. Kim, and S. Kim, "Evaluation of Voltage Sag and Unbalance due to the System Connection of Electric Vehicles on Distribution System," *J Electr Eng Technol*, vol. 9, no. 2, pp. 452–460, 2014.
- [33] P. G.A., S. P., E. C. Bentley, and M. Narayana, "Impact of Electric Vehicles on Power Distribution Networks," in *Vehicle Power and Propulsion Conference (VPPC)*, 2009, pp. 827–831.
- [34] A. Jiménez and N. García, "Unbalanced Three-Phase Power Flow Studies of Distribution Systems with Plug-in Electric Vehicles," in *North American Power Symposium (NAPS)*, 2012, no. 1, pp. 1–6.
- [35] A. M. A. Haidar, K. M. Muttaqi, and D. Sutanto, "Technical challenges for electric power industries due to grid-integrated electric vehicles in low voltage distributions: A review," *Energy Convers. Manag.*, vol. 86, pp. 689–700, 2014.
- [36] X. Han, C. Sandels, K. Zhu, L. Nordström, and P. Söderström, "Empirical Analysis for Distributed Energy Resources' Impact on Future Distribution Network," in *IEEE EnergyCon Conference & Exhibition*, 2012, pp. 731–737.
- [37] P. Papadopoulos, S. Skarvelis-Kazakos, I. Grau, L. M. Cipcigan, and N. Jenkins, "Electric vehicles' impact on British distribution networks," *IET Electr. Syst. Transp.*, vol. 2, no. 3, pp. 91–102, 2011.

- 
- [38] K. Qian, C. Zhou, and Y. Yuan, "Electrical Power and Energy Systems Impacts of high penetration level of fully electric vehicles charging loads on the thermal ageing of power transformers," *Int. J. Electr. Power Energy Syst.*, vol. 65, pp. 102–112, 2015.
- [39] L. P. Fernández, T. Gómez, S. Román, R. Cossent, C. M. Domingo, and P. Frías, "Assessment of the Impact of Plug-in Electric Vehicles on Distribution Networks," *IEEE Trans. Power Systems*, vol. 26, no. 1, pp. 206–213, 2011.
- [40] M. Thomson and D. G. Infield, "Impact of widespread photovoltaics generation on distribution systems," *IET Renew. Power Gener.*, vol. 1, no. 1, pp. 33–40, 2007.
- [41] A. Toliyat, A. Kwasinski, and F. M. Uriarte, "Effects of high penetration levels of residential photovoltaic generation," in *IEEE conference on Renewable Energy Research and Applications (ICRERA)*, 2012, pp. 1 – 6.
- [42] S. Ali, N. Pearsall, and G. Putrus, "Using Electric Vehicles to Mitigate Imbalance Requirements Associated with High Penetration Level of Grid-connected Photovoltaic Systems," in *22nd International Conference on Electricity Distribution Stockholm (CIRED)*, 2013, pp. 1–4.
- [43] R. C. G. Li, L. Wang, and M. Alam, "The impact of plug-in hybrid electric vehicles on distribution networks: A review and outlook," *Renew. Sustain. Energy Rev.*, vol. 15, no. 1, pp. 544–553, 2011.
- [44] G. Razeghi, L. Zhang, T. Brown, and S. Samuelson, "Impacts of plug-in hybrid electric vehicles on a residential transformer using stochastic and empirical analysis," *J. Power Sources*, vol. 252, pp. 277–285, 2014.
- [45] M. F. Shaaban, A. A. Eajal, and E. F. El-Saadany, "Coordinated charging of plug-in hybrid electric vehicles in smart hybrid AC/DC distribution systems," *Renew. Energy*, vol. 82, pp. 92–99, 2015.
- [46] Maigha and M. L. Crow, "Economic Scheduling of Residential Plug-In (Hybrid) Electric Vehicle (PHEV) Charging," *energies*, vol. 7, pp. 1876–1898, 2014.
- [47] J. Yu, W. Gu, and Z. Wu, "Intelligent PHEV Charging and Discharging Strategy in Smart Grid," in *IEEE fifth International Conference on Advanced Computational Intelligence (ICACI)*, 2012, pp. 1107–1112.
- [48] Z. Fan, "A Distributed Demand Response Algorithm and Its Application to PHEV Charging in Smart Grids," *IEEE Trans. Smart Grid*, vol. 3, no. 3, pp. 1280–1290, 2012.
- [49] P. Richardson, J. Taylor, D. Flynn, and A. Keane, "Stochastic analysis of the impact of electric vehicles on distribution networks," in *21st International Conference on Electricity Distribution (CIRED)*, 2011, pp. 1–5.

- 
- [50] P. Papadopoulos, I. Grau, B. Awad, L. M. Cipcigan, and N. Jenkins, "Impact of Residential Charging of Electric Vehicles on Distribution Networks, a Probabilistic Approach," in *Universities Power Engineering Conference (UPEC)*, 2010, pp. 1–5.
- [51] M. Neaimeh, R. Wardle, A. M. Jenkins, J. Yi, G. Hill, P. F. Lyons, Y. Hübner, P. T. Blythe, and P. C. Taylor, "A probabilistic approach to combining smart meter and electric vehicle charging data to investigate distribution network impacts," *Appl. Energy*, vol. 157, pp. 688–698, 2015.
- [52] S. F. Abdelsamad, W. G. Morsi, and T. S. Sidhu, "Probabilistic Impact of Transportation Electrification on the Loss-of-Life of Distribution Transformers in the Presence of Rooftop Solar Photovoltaic," *IEEE Trans. Sustain. Energy*, vol. 6, no. 4, pp. 1565–1573, 2015.
- [53] A. Navarro and L. Ochoa, "What - if Scenario Impact Studies based on real LV networks," The University of Manchester, 2014.
- [54] H. Liang and W. Zhuang, "Stochastic Modeling and Optimization in a Microgrid: A Survey," *energies*, vol. 7, pp. 2027–2050, 2014.
- [55] Energy Network Association Technology, "Assessing the Impact of Low Carbon Technologies on Great Britain's Power Distribution Networks," Capenhurst Technology Park, Chester, England, 2012.
- [56] H. Bulkeley, S. Bell, S. Lyon, G. Powells, E. Judson, and D. Lynch, "Customer-Led Network Revolution Durham University Social Science Research," Northern Powergrid, British Gas Trading, and University of Durham, UK, 2014.
- [57] W. Robin and D. Peter, "Initial Load and Generation Profiles from CLNR Monitoring Trials," Customer-Led Network Revolution (CLNR) Project, UK, 2012.
- [58] Commission for Energy Regulation, "Electricity Smart Metering Customer Behaviour Trials (CBT) Findings Report CER/11/080a," Belgard Square North, Tallaght, Dublin 24, Ireland, 2011.
- [59] UK Power Networks, "DNO Guide to Future Smart Management of Distribution Networks Summary Report," Summary Report for the "Low Carbon London" LCNF project, London, UK, 2014.
- [60] G. Ye, Y. Xiang, and J. F. G. Cobben, "Assessment of the Voltage Level and Losses with Photovoltaic and Electric Vehicle in Low Voltage Network," in *IEEE 14th International Conference on Environment and Electrical Engineering (EEEIC)*, 2014, pp. 431 – 436.
- [61] S. Babaei, D. Steen, L. A. Tuan, O. Carlson, and L. Bertling, "Effects of Plug-in Electric Vehicles on Distribution Systems: A Real Case of Gothenburg," in *Innovative Smart Grid Technologies Conference Europe (ISGT Europe)*, 2010, pp. 1–8.

- 
- [62] R. Garcia-Valle and J. A. P. Lopes, Eds., *Electric Vehicle Integration into Modern Power Networks*. Springer Science+Business Media New York, 2013, pp. 158–163.
- [63] Z. Liu, C. Chen, and J. Yuan, “Hybrid Energy Scheduling in a Renewable Micro Grid,” *Appl. Sci.*, vol. 5, pp. 516–531, 2015.
- [64] M. Honarmand, A. Zakariazadeh, and S. Jadid, “Self-scheduling of electric vehicles in an intelligent parking lot using stochastic optimization,” *J. Franklin Inst.*, vol. 352, no. 2, pp. 449–467, 2014.
- [65] A. Zakariazadeh, S. Jadid, and P. Siano, “Multi-objective scheduling of electric vehicles in smart distribution system,” *Energy Convers. Manag.*, vol. 79, pp. 43–53, 2014.
- [66] M. A. Ortega-vazquez, “Optimal scheduling of electric vehicle charging and vehicle-to-grid services at household level including battery degradation and price uncertainty,” *IET Gener. Transm. Distrib.*, vol. 8, no. 6, pp. 1007–1016, 2014.
- [67] Z. Yang, K. Li, A. Foley, and C. Zhang, “Optimal Scheduling Methods to Integrate Plug-in Electric Vehicles with the Power System: A Review,” in *Proceedings of the 19th IFAC World Congress*, 2014, pp. 8594–8603.
- [68] Z. Yang, K. Li, and A. Foley, “Computational scheduling methods for integrating plug-in electric vehicles with power systems: A review,” *Renew. Sustain. Energy Rev.*, vol. 51, pp. 396–416, 2015.
- [69] L. Hua, J. Wang, and C. Zhou, “Adaptive Electric Vehicle Charging Coordination on Distribution Network,” *IEEE Trans. Smart Grid*, vol. 5, no. 6, pp. 2666 – 2675, 2014.
- [70] S. Deilami, A. S. Masoum, P. S. Moses, and M. A. S. Masoum, “Real-Time Coordination of Plug-In Electric Vehicle Charging in Smart Grids to Minimize Power Losses and Improve Voltage Profile,” *IEEE Trans. Smart Grid*, vol. 2, no. 3, pp. 456–467, 2011.
- [71] A. S. Masoum, S. Deilami, A. Abu-Siada, and M. A. S. Masoum, “Fuzzy Approach for Online Coordination of Plug-In Electric Vehicle Charging in Smart Grid,” *IEEE Trans. Sustain. Energy*, vol. 6, no. 3, pp. 1112–1121, 2015.
- [72] J. De Hoog, T. Alpcan, M. Brazil, D. A. Thomas, and I. Mareels, “Optimal Charging of Electric Vehicles Taking Distribution Network Constraints Into Account,” *IEEE Trans. Power Systems*, vol. 30, no. 1, pp. 365–375, 2015.
- [73] I. Sharma, C. A. Cañizares, and K. Bhattacharya, “Modeling and Impacts of Smart Charging PEVs in Residential Distribution Systems,” in *IEEE PES General Meeting*, 2012, pp. 1–8.

- 
- [74] M. Alonso, H. Amaris, J. G. Germain, and J. M. Galan, "Optimal Charging Scheduling of Electric Vehicles in Smart Grids by Heuristic Algorithms," *energies*, vol. 7, pp. 2449–2475, 2014.
- [75] S. Rahim, N. Javaid, A. Ahmad, S. Ahmed, Z. Ali, N. Alrajeh, and U. Qasim, "Exploiting heuristic algorithms to efficiently utilize energy management controllers with renewable energy sources," *Energy Build.*, vol. 129, pp. 452–470, 2016.
- [76] M. F. Shaaban and E. F. El-Saadany, "Accommodating high penetration of PEV in distribution networks," in *IEEE Electrical Power & Energy Conference (EPEC)*, 2013, pp. 1–6.
- [77] M. F. Shaaban and E. F. El-Saadany, "Accommodating High Penetrations of PEVs and Renewable DG Considering Uncertainties in Distribution Systems," *IEEE Trans. Smart Grid*, vol. 29, no. 1, pp. 259–270, 2014.
- [78] J. Xiong, D. Wu, H. Zeng, S. Liu, and X. Wang, "Impact Assessment of Electric Vehicle Charging on Hydro Ottawa Distribution Networks at Neighborhood Levels," in *the IEEE 28th Canadian Conference on Electrical and Computer Engineering*, 2015, pp. 1072–1077.
- [79] P. Papadopoulos, N. Jenkins, L. M. Cipcigan, I. Grau, and E. Zabala, "Coordination of the Charging of Electric Vehicles Using a Multi-Agent System," *IEEE Trans. Smart Grid*, vol. 4, no. 4, pp. 1802–1809, 2013.
- [80] S. Mocci, N. Natale, F. Pilo, and S. Ruggeri, "Demand side integration in LV smart grids with multi-agent control system," *Electr. Power Syst. Res.*, vol. 125, pp. 23–33, 2015.
- [81] G. Unda, P. Papadopoulos, S. Skarvelis-kazakos, L. M. Cipcigan, N. Jenkins, and E. Zabala, "Management of electric vehicle battery charging in distribution networks with multi-agent systems," *Electr. Power Syst. Res.*, vol. 110, pp. 172–179, 2014.
- [82] F. H. Malik and M. Lehtonen, "A review: Agents in smart grids," *Electr. Power Syst. Res.*, vol. 131, pp. 71–79, 2016.
- [83] K. Mahmud and G. E. Town, "A review of computer tools for modeling electric vehicle energy requirements and their impact on power distribution networks," *Appl. Energy*, vol. 172, pp. 337–359, 2016.
- [84] A. Barbato and A. Capone, "Optimization Models and Methods for Demand-Side Management of Residential Users: A Survey," *energies*, vol. 7, pp. 5787–5824, 2014.
- [85] G. Strbac, "Demand side management: Benefits and challenges," *Energy Policy*, vol. 36, pp. 4419–4426, 2008.

- 
- [86] Parliamentary Office of Science & Technology (POSTNOTE), “Electricity Demand-Side Response,” Parliamentary Office of Science & Technology, UK, 2014.
- [87] Frontier Economics and Sustainability First, “Demand Side Response in the domestic sector- a literature review of major trials,” Department of Energy & Climate Change, London, UK, 2012.
- [88] B. Zhou, W. Li, K. Wing, Y. Cao, Y. Kuang, X. Liu, and X. Wang, “Smart home energy management systems: Concept, configurations, and scheduling strategies,” *Renew. Sustain. Energy Rev.*, vol. 61, pp. 30–40, 2016.
- [89] M. Iqbal, M. Azam, M. Naeem, A. S. Khwaja, and A. Anpalagan, “Optimization classification, algorithms and tools for renewable energy: A review,” *Renew. Sustain. Energy Rev.*, vol. 39, pp. 640–654, 2014.
- [90] P. van Zoest, Z. Lukszo, E. Veldman, and P. M. Herder, “Analysis of future electricity demand and supply in the low voltage distribution grid,” in *IEEE 11th International Conference on Networking, Sensing and Control (ICNSC)*, 2014, pp. 619–624.
- [91] G. Angrisani, M. Canelli, C. Roselli, and M. Sasso, “Integration between electric vehicle charging and micro-cogeneration system,” *Energy Convers. Manag.*, vol. 98, pp. 115–126, 2015.
- [92] J. D. McDonald, B. Wojszczyk, B. Flynn, and I. Voloh, “Distribution Systems, Substations, and Integration of Distributed Generation,” in *Encyclopedia of Sustainability Science and Technology*, R. A. Meyers, Ed. Springer Science+Business Media, New York, 2013.
- [93] P. Siano, “Demand response and smart grids — A survey,” *Renew. Sustain. Energy Rev.*, vol. 30, pp. 461–478, 2014.
- [94] M. Negnevitsky, “Demand Response Under the Smart Grid Paradigm,” in *The 31st International Symposium on Automation and Robotics in Construction and Mining (ISARC)*, 2014, pp. 58–71.
- [95] M. Moretti, S. N. Djomo, H. Azadi, K. May, K. De Vos, S. Van Passel, and N. Witters, “A systematic review of environmental and economic impacts of smart grids,” *Renew. Sustain. Energy Rev.*, vol. 68, pp. 888–898, 2017.
- [96] B. Smets, “Investigation on Demand Side Management Techniques in the Smart Grid using Game Theory and ICT Concepts,” University of Antwerp, 2014.
- [97] F. J. Soares, P. M. R. Almeida, and J. A. Pec, “Quasi-real-time management of Electric Vehicles charging,” *Electr. Power Syst. Res.*, vol. 108, pp. 293–303, 2014.

- 
- [98] E. Karfopoulos, L. Tena, A. Torres, P. Salas, J. G. Jorda, A. Dimeas, and N. Hatziaargyriou, "A multi-agent system providing demand response services from residential consumers," *Electr. Power Syst. Res.*, vol. 120, pp. 163–176, 2015.
- [99] Y. Iwafune, Y. Yagita, T. Ikegami, and K. Ogimoto, "Short-term Forecasting of Residential Building Load for Distributed Energy Management," in *EnergyCon, Dubrovnik*, 2014, pp. 1197–1204.
- [100] M. Mazidi, A. Zakariazadeh, S. Jadid, and P. Siano, "Integrated scheduling of renewable generation and demand response programs in a microgrid," *Energy Convers. Manag.*, vol. 86, pp. 1118–1127, 2014.
- [101] N. Bassamzadeh, R. Ghanem, S. Lu, and S. J. Kazemitabar, "Robust Scheduling of Smart Appliances with Uncertain Electricity Prices in a Heterogeneous Population," *Energy Build.*, vol. 84, pp. 537–547, 2014.
- [102] W. Gu, H. Yu, W. Liu, J. Zhu, and X. Xu, "Demand Response and Economic Dispatch of Power Systems Considering Large-Scale Plug-in Hybrid Electric Vehicles/Electric Vehicles (PHEVs/EVs): A Review," *energies*, vol. 6, pp. 4394–4417, 2013.
- [103] N. O. Connell, P. Pinson, H. Madsen, and M. O. Malley, "Benefits and challenges of electrical demand response: A critical review," *Renew. Sustain. Energy Rev.*, vol. 39, pp. 686–699, 2014.
- [104] P. Warren, "A review of demand-side management policy in the UK," *Renew. Sustain. Energy Rev.*, vol. 29, pp. 941–951, 2014.
- [105] M. C. Falvo and G. Graditi, "Electric Vehicles Integration in Demand Response Programs," in *International Symposium on Power Electronics, Electrical Drives, Automation and Motion*, 2014, pp. 548–553.
- [106] E. Parry and M. Redfern, "Load Management of the Electricity Supply Network using Plug-in Vehicles," in *Universities Power Engineering Conference (UPEC)*, 2010, pp. 1–6.
- [107] KEMA Consulting GmbH in cooperation with Imperial College and NERA Economic Consulting, "Integration of Renewable Energy in Europe," European Commission, Directorate-General Energy, Kurt-Schumacher-Str, Germany, 2014.
- [108] Z. Tan, P. Yang, and A. Nehorai, "An Optimal and Distributed Demand Response Strategy with Electric Vehicles in the Smart Grid," *IEEE Trans. Smart Grid*, vol. 5, no. 2, pp. 861–869, 2014.
- [109] L. Gan, U. Topcu, and S. H. Low, "Optimal Decentralized Protocol for Electric Vehicle Charging," *IEEE Trans. Power Systems*, vol. 28, no. 2, pp. 940–951, 2013.

- 
- [110] D. Papadaskalopoulos and G. Strbac, “Decentralized Participation of Flexible Demand in Electricity Markets — Part I: Market Mechanism,” *IEEE Trans. Power Systems*, vol. 28, no. 4, pp. 3658–3666, 2013.
- [111] D. Papadaskalopoulos, G. Strbac, and P. Mancarella, “Decentralized Participation of Flexible Demand in Electricity Markets — Part II: Application With Electric Vehicles and Heat Pump Systems,” *IEEE Trans. Power Systems*, vol. 28, no. 4, pp. 3667–3674, 2013.
- [112] D. Papadaskalopoulos, D. Pudjianto, and G. Strbac, “Decentralized Coordination of Microgrids With Flexible Demand and Energy Storage,” *IEEE Trans. Sustain. Energy*, vol. 5, no. 4, pp. 1406–1414, 2014.
- [113] D. Papadaskalopoulos and G. Strbac, “Nonlinear and Randomized Pricing for Distributed Management of Flexible Loads,” *IEEE Trans. Smart Grid*, vol. 7, no. 2, pp. 1137–1146, 2016.
- [114] GridWatch, “Download Data Sets from the GridWatch Database.” [Online]. Available: [www.gridwatch.templar.co.uk/download.php](http://www.gridwatch.templar.co.uk/download.php). [Accessed: 08-Jan-2016].
- [115] Customer-Led Network Revolution (CLNR) Project, “Project Trails.” [Online]. Available: <http://www.networkrevolution.co.uk/customer-trials/>. [Accessed: 28-Jan-2015].
- [116] S. Ingram, S. Probert, and K. Jackson, “The Impact of Small Scale Embedded Generation on the Operating Parameters of Distribution Networks,” England, UK, 2003.
- [117] Department of Trade and Industry, *The electricity safety, quality and continuity regulations. Stationary Office, London, UK*, 2002, pp. 1–47.
- [118] Engineering Recommendation P29, *Planning limits for voltage unbalance in the United Kingdom*. 1990.
- [119] P. Pillay and M. Manyage, “Definitions of Voltage Unbalance,” in *IEEE Power Engineering Review.*, 2001, pp. 50–51.
- [120] Electricity North West, “Low Voltage Network Solutions,” 2015. [Online]. Available: <http://www.enwl.co.uk/about-us/the-future/lcnf-tier-1-projects/low-voltage-network-solutions>. [Accessed: 28-Jun-2015].
- [121] Bristol City Council, “Bristol City Council Air Quality Monitoring.” [Online]. Available: <http://www.bristol.airqualitydata.com/cgi-bin/currentreadings.cgi>. [Accessed: 08-Jun-2015].
- [122] European Commission, “Driving and parking patterns of European car drivers—a mobility survey,” Joint Research Centre, Institute for Energy and Transport, ZG Petten, The Netherlands, 2012.

- 
- [123] M. E. Baster, “Modelling the performance of Air Source Heat Pump Systems,” MSc. Thesis, Mechanical Engineering, Strathclyde, 2011.
- [124] R.K. Johnson, “Measured Performance of a Low Temperature Air Source Heat Pump,” U.S. Department of Energy Office of Scientific and Technical Information, 2013.
- [125] S. Derek, “Real-Time Mobile Communication of Power Requirements for Electric Vehicles,” *Technol. Innov. Management Rev.*, pp. 22–27, 2012.
- [126] International Energy Agency, “How 2 Guide for Smart Grids in Distribution Networks Roadmap Development and Implementation,” 9 rue de la Fédération 75739 Paris Cedex 15, France, 2015.
- [127] A. S. Masoum, S. Deilami, P. S. Moses, M. A. . Masoum, and A. Abu-Siada, “Smart load management of plug-in electric vehicles in distribution and residential networks with charging stations for peak shaving and loss minimisation considering voltage regulation,” *IET Gener. Transm. Distrib.*, vol. 5, no. 8, pp. 877–888, 2011.
- [128] W. H. Kersting, *Distribution System Modeling and Analysis*. CRC Press LLC, 2002, pp. 271-285.
- [129] T. Haggis, “Network Design Manual,” E.ON Central Networks, UK, 2006.
- [130] O. Beaudé, S. Lasaulce, M. Hennebel, and I. Mohand-kaci, “Reducing the Impact of EV Charging Operations on the Distribution Network,” *IEEE Trans. Smart Grid*, vol. 7, no. 6, pp. 2666–2679, 2016.
- [131] Energy Saving Trust, “Detailed analysis from the first phase of the Energy Saving Trust’s heat pump field trial,” Department of Energy & Climate Change (DECC), London, UK, 2012.
- [132] Energy Saving Trust, “Detailed analysis from the second phase of the Energy Saving Trust’s heat pump field trial,” Department of Energy & Climate Change (DECC), London, UK, 2013.
- [133] MathWorks, “Model a Dynamic System.” [Online]. Available: <http://uk.mathworks.com/help/simulink/gs/define-system.html>. [Accessed: 01-May-2016].
- [134] M. J. Fell, M. Nicolson, G. M. Huebner, and D. Shipworth, “Is it time? Consumers and time of use tariffs,” UCL Energy Institute, 2015.
- [135] Centre for Sustainable Energy, “Investigating the potential impacts of Time of Use (TOU) tariffs on domestic electricity customers Report to Ofgem,” Report to Office for gas and electricity market (Ofgem), 2014.

- [136] J. Schofield, R. Carmichael, S. Tindemans, M. Woolf, M. Bilton, and G. Strbac, "Residential consumer responsiveness to time-varying pricing," Report A3 for the "Low Carbon London" LCNF project: Imperial College London, 2014.
- [137] R. Hledik and J. Lazar, "Distribution System Pricing with Distributed Energy Resources," Future Electric Utility Regulation, Lawrence Berkeley National Laboratory, US, 2016.
- [138] Frontline Systems, "FrontlineSolvers." [Online]. Available: <http://www.frontsys.com/>. [Accessed: 01-Feb-2016].
- [139] MathWorks, "Mixed-Integer Linear Programming." [Online]. Available: <http://uk.mathworks.com/products/optimization/features.html>. [Accessed: 08-Jun-2016].
- [140] Electricity North West Limited (ENWL) and the University of Manchester, "Low Voltage Networks Models and Low Carbon Technology Profiles," Dissemination Document, Electricity North West Limited, UK, 2015.

## Appendix A: The Top-Level Code of Future Demand Predictions

The prediction tool of the UK residential demand, which considers the power of electric vehicles (EVs), heat pumps (HPs), and photovoltaic (PV) arrays, was written using MATLAB, as shown below. The UK future residential demand was predicted between the years of 2016 to 2035 at half-hourly time steps.

```
% Load the prepared data of the matrix [fes1] into the workspace
load fes1
% Create power means of EV, HP, and PV units over a year of half-hourly time steps
[yhp, yev, ypv]=disagg(hp,ev,pv);
% Concatenate these yearly data into a one matrix called [norm]
norm=[ntyd nwyg medfilt1(yev,5)./max(medfilt1(yev,5))
medfilt1(yhp,5)./max(medfilt1(yhp,5)) medfilt1(yhp,5)./max(medfilt1(yhp,5))
medfilt1(ypv,5)./max(medfilt1(ypv,5)) ntyd.*rpc ntyd.*(1-rpc)];
createfigure(1inspace(0,365,17520),[52*norm(:,1) 52*norm(:,7)]);
createfigure1(1inspace(0,24,48),100*pers(:,1:2));
createfigure2(1inspace(0,24,48),[52*norm(14*48:(14*48)+47,1)
52*norm(14*48:(14*48)+47,7)], [52*norm(104*48:(104*48)+47,1)
52*norm(104*48:(104*48)+47,7)], [52*norm(193*48:(193*48)+47,1)
52*norm(193*48:(193*48)+47,7)], [52*norm(299*48:(299*48)+47,1)
52*norm(299*48:(299*48)+47,7)]);
createfigure3(1inspace(0,24,48), ev(:,[1 4 7 10]));
createfigure4(1inspace(0,24,48), pv(:,[1 4 7 10]));
createfigure5(1inspace(0,24,48),ev(:,1),1inspace(0,31,31*48),
yev(1:31*48),medfilt1(yev(1:31*48),5),[ev(:,1)
mean(reshape(medfilt1(yev(1:31*48),5),48,31),2)]);
createfigure6(1inspace(0,24,48),[ev(:,1)
mean(reshape(medfilt1(yev(1:31*48),5),48,31),2)]);
createfigure7(1inspace(0,365,365*48), medfilt1(yev,5));
figure
plot(1inspace(0,365,365*48), medfilt1(yev,5));
figure
plot(1inspace(0,365,365*48), medfilt1(ypv,5));
[x16,~]=evaluation1(16,fes1,norm);
[x18,~]=evaluation1(18,fes1,norm);
[x20,~]=evaluation1(20,fes1,norm);
[x22,~]=evaluation1(22,fes1,norm);
[x24,~]=evaluation1(24,fes1,norm);
[x26,~]=evaluation1(26,fes1,norm);
[x28,~]=evaluation1(28,fes1,norm);
[x30,~]=evaluation1(30,fes1,norm);
[x32,~]=evaluation1(32,fes1,norm);
[x34,~]=evaluation1(34,fes1,norm);
[x35,~]=evaluation1(35,fes1,norm);
createfigure8(1inspace(0,365,365*48),x35(:,1),x35(:,2),x35(:,3),x35(:,4));
createfigure9(1inspace(0,24,48),x35(14*48:(14*48)+47,:),x35(104*48:(104*48)+47,:),x35
(193*48:(193*48)+47,:),x35(299*48:(299*48)+47,:));
figure
boxplot([x16(:,1) x18(:,1) x20(:,1) x22(:,1) x24(:,1) x26(:,1) x28(:,1) x30(:,1)
x32(:,1) x34(:,1)
x35(:,1)], 'notch', 'on', 'labels', {'2016', '2018', '2020', '2022', '2024', '2026', '2028',
'2030', '2032', '2034', '2035'});
figure
```

```

boxplot([x16(:,3) x18(:,3) x20(:,3) x22(:,3) x24(:,3) x26(:,3) x28(:,3) x30(:,3)
x32(:,3) x34(:,3)
x35(:,3)], 'notch', 'on', 'labels', {'2016', '2018', '2020', '2022', '2024', '2026', '2028',
'2030', '2032', '2034', '2035'});
Tx=[min(x16) max(x16); min(x18) max(x18); min(x20) max(x20); min(x22) max(x22);
min(x24) max(x24); min(x26) max(x26); min(x28) max(x28); min(x30) max(x30); min(x32)
max(x32); min(x34) max(x34); min(x35) max(x35)];
xlswrite('Table.xlsx',Tx);

```

### Appendix B: The Model of the UK Generic Distribution Network

Figure B.1 shows the model of the low voltage section of the UK generic distribution network (UKGDN) in MATLAB/Simulink/Simscape/SimPowerSystems. The “SimPowerSystems” components of “Simscape” libraries are used to construct the UKGDN in MATLAB/Simulink environment as follows. A “Three-Phase Source” is adjusted to model the power source of 100MVA. A “Three-Phase Transformer” is modified to model the Delta/Star, 500kVA, 11/0.433kV distribution transformer. A “Three-Phase PI Section Line” and “Single-Phase Series RLC Branch” are used to model 4-core underground cables (i.e. a three-phase line and neutral line), whereas a “PI Section Line” is used to model other 2-core cables. Residential loads and EV loads are modelled as data driven objects using “Controlled Voltage Source” and “Controlled Current Source”.

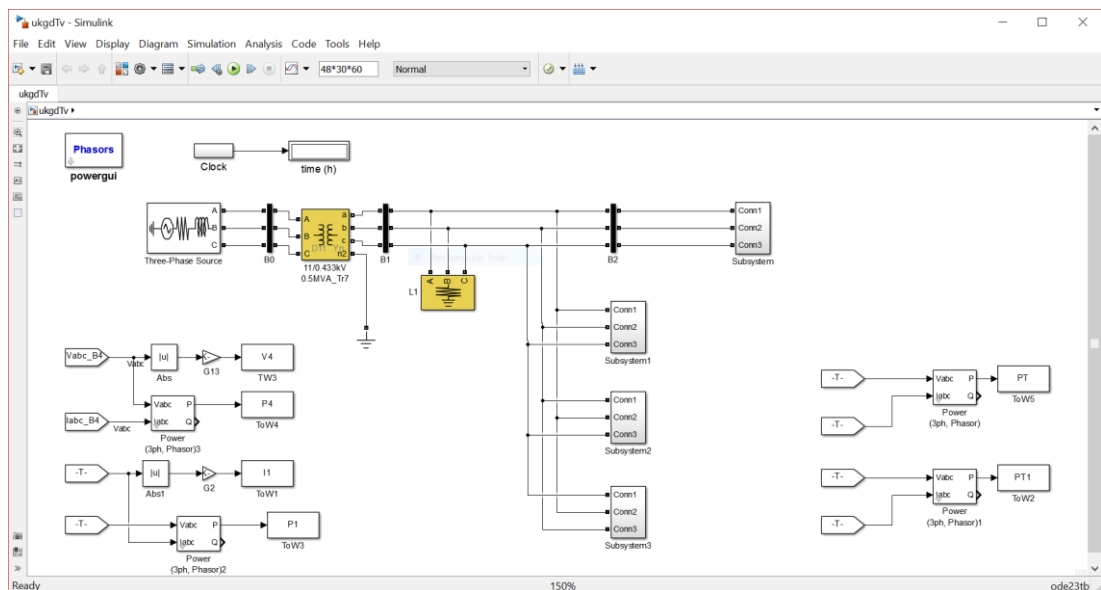


Figure B.1: The high level of the UK generic distribution network (UKGDN) model (i.e. low voltage section) using Matlab/Simulink/SimPowerSystem.

Figure B.2 shows the components of each feeder with 96 residential customers, which were distributed across four segments of main underground cables.

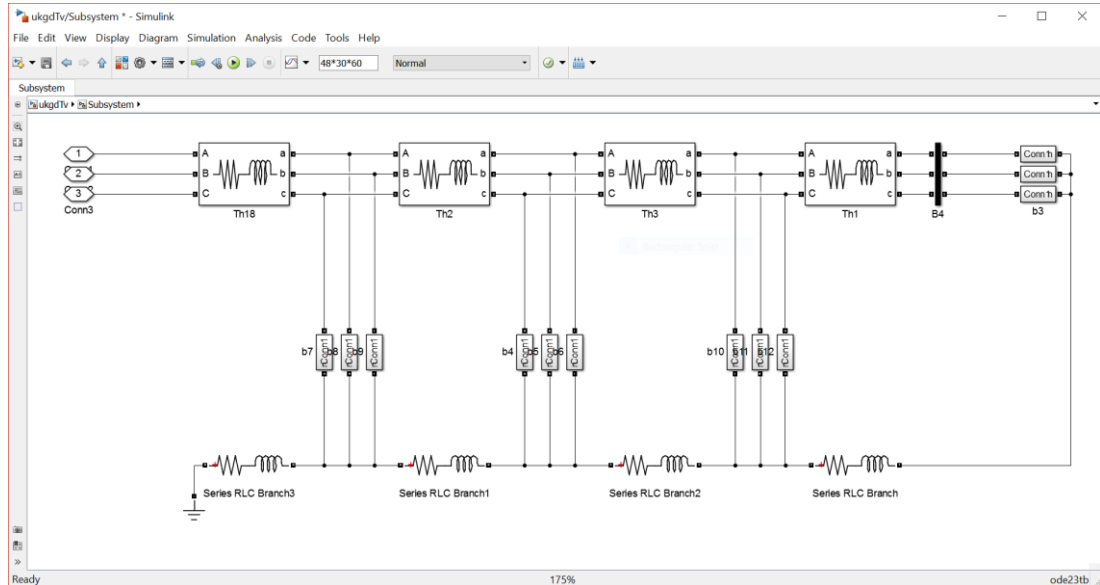


Figure B.2: The components of the UKGDN Subsystems.

## Appendix C: The Top-Level Code of Stochastic Studies

The real network of Electricity North West, which was used to demonstrate stochastic studies, was modelled in MATLAB R2015a, as shown in the following M-file.

```
clear
close all
clc
load p1x
load phps
p=getp(px,135);
pevs=getev(135,1);
S=p;
S1=S-pvs;
S2=S+pevs;
S3=S+phps;
S5=S-pvs+pevs+phps;
[V, VUF, T1, I1]=call(S);
% Histogram figures are visualized for the first case study, as illustrated below
figure
subplot(2,2,1);
hist(V);
xlabel({'Voltage, pu','(a)'},'Fontweight','bold','FontName','Times New Roman');
ylabel('Occurrences','Fontweight','bold','FontName','Times New Roman');
subplot(2,2,2);
hist(VUF);
xlabel({'Voltage Unbalance Factor, %','(b)'},'Fontweight','bold','FontName','Times
```

```

New Roman');
ylabel('Occurrences','FontWeight','bold','FontName','Times New Roman');
subplot(2,2,3);
hist(abs(T1));
xlabel({'Power, pu','(C)'},'FontWeight','bold','FontName','Times New Roman');
ylabel('Occurrences','FontWeight','bold','FontName','Times New Roman');
subplot(2,2,4);
hist(abs(I1));
xlabel({'Current, pu','(d)'},'FontWeight','bold','FontName','Times New Roman');
ylabel('Occurrences','FontWeight','bold','FontName','Times New Roman');
% S1, S2, S3, S4, and S5 are then analysed using the function developed of call().
% Meanwhile, histogram figures are visualized for other case studies, as illustrated
previously.
% Comparing figure of real and synthesized loads (residential loads) is visualized,
as illustrated below
figure
plot(linspace(0,1440,1440), [mean(p); interp1(linspace(0,24,48), px(:,1),
linspace(0,24,1440))]);
xlabel('Time, minute','FontWeight','bold','FontName','Times New Roman');
ylabel('Power, kw','FontWeight','bold','FontName','Times New Roman');
legend('Modelled', 'Real');
% Comparing figure of real and synthesized loads (EV charging loads) is visualized,
as illustrated below
figure
plot(linspace(0,1440,1440), mean(pevs));
xlabel('Time, minute','FontWeight','bold','FontName','Times New Roman');
ylabel('Power, kw','FontWeight','bold','FontName','Times New Roman');
% 3D figure of HP loads
[x,y]=meshgrid(linspace(0,1440,1440),linspace(1,135,135));
figure
mesh(x,y,phps);
xlabel('Time, minute','FontWeight','bold','FontName','Times New Roman');
ylabel('Days','FontWeight','bold','FontName','Times New Roman');
zlabel('Power,kw','FontWeight','bold','FontName','Times New Roman');
% 3D figure of PV power generation
figure
mesh(x,y,pvs);
xlabel('Time, minute','FontWeight','bold','FontName','Times New Roman');
ylabel('Days','FontWeight','bold','FontName','Times New Roman');
zlabel('Power,kw','FontWeight','bold','FontName','Times New Roman');

```

## Appendix D: The Top-Level Codes of the Centralized Controller

EV charging loads were re-allocated using a Macro in Visual Basic Application (VBA) based on Generalised Reduced Gradient (GRG) solver in Microsoft Excel. Meanwhile, power flows and simulation results of low voltage and medium voltage sections of the UKGDN was visualized using MATLAB.

### D.1 Optimization Code

```

Sub Centrallized_Controller()
    ActiveWindow.SmallScroll Down:=12
    Range("H28:J30").Select
    Selection.Copy
    Sheets("Sheet1").Select
    ActiveWindow.SmallScroll Down:=15
    Range("H28").Select
    SolverOk SetCell:="$J$30", MaxMinVal:=3, ValueOf:=1913, ByChange:="$H$2:$J$25" _
        , Engine:=1, EngineDesc:="GRG Nonlinear"
    SolverAdd CellRef:="$AH$2:$AH$25", Relation:=3, FormulaText:="216.2"
    SolverAdd CellRef:="$AJ$2:$AJ$25", Relation:=1, FormulaText:="1.3"
    SolverAdd CellRef:="$AL$2:$AL$25", Relation:=1, FormulaText:="292"
    SolverAdd CellRef:="$AP$2:$AP$25", Relation:=1, FormulaText:="1"
    SolverOk SetCell:="$J$30", MaxMinVal:=3, ValueOf:=1913, ByChange:="$H$2:$J$25" _
        , Engine:=1, EngineDesc:="GRG Nonlinear"
    SolverOk SetCell:="$J$30", MaxMinVal:=3, ValueOf:=1913, ByChange:="$H$2:$J$25" _
        , Engine:=1, EngineDesc:="GRG Nonlinear"
    SolverSolve
    Sheets ("Answer Report").Select
    ActiveWindow.SmallScroll Down:=3
End Sub

```

Table D.1: Answer report of centralized controller using generalized reduced gradient.

Answer Report					
Result: Solver found a solution. All Constraints and optimality conditions are satisfied.					
Cell	Name	Original Value	Final Value		
\$J\$30	PcEV	1913.882604	1913		
Variable Cells					
Cell	Name	Original Value	Final Value	Integer	
\$H\$2:\$J\$25					
Constraints					
Cell	Name	Cell Value	Formula	Status	Slack
\$AH\$2:\$AH\$25			>= 216.2		
\$AJ\$2:\$AJ\$25			<= 1.3		
\$AL\$2:\$AL\$25			<= 292		
\$AP\$2:\$AP\$25			<= 1		
\$J\$30	PEVs	1913	\$J\$30=1913	Binding	

## D.2 Visualization Code

```

load pxcs
createfigure1([mean(pev);
interp1(linspace(0,1440,48),M93eJ14,linspace(0,1440,1440))]');
createfigure1([mean(p);
interp1(linspace(0,1440,48),must(:,1)',linspace(0,1440,1440))]');
createfigure2(R1.VoltageUnbalance');
createfigure2([R1.VoltageUnbalance(:,1) R1.VoltageUnbalance(:,1)
R1.VoltageUnbalance(:,2) R1.VoltageUnbalance(:,2) R1.VoltageUnbalance(:,3)
R1.VoltageUnbalance(:,3) R1.VoltageUnbalance(:,4) R1.VoltageUnbalance(:,4)
R1.VoltageUnbalance(:,5) R1.VoltageUnbalance(:,5) R1.VoltageUnbalance(:,6)
R1.VoltageUnbalance(:,6) R1.VoltageUnbalance(:,7) R1.VoltageUnbalance(:,7)
R1.VoltageUnbalance(:,8) R1.VoltageUnbalance(:,8)]');
createfigure2([rms(abs(R1.PhaseVoltages(:,1:3)),2)
rms(abs(R1.PhaseVoltages(:,1:3)),2) rms(abs(R1.Phasevoltages(:,4:6)),2)
rms(abs(R1.PhaseVoltages(:,4:6)),2) rms(abs(R1.Phasevoltages(:,7:9)),2)
rms(abs(R1.PhaseVoltages(:,7:9)),2) rms(abs(R1.Phasevoltages(:,10:12)),2)
rms(abs(R1.PhaseVoltages(:,10:12)),2) rms(abs(R1.PhaseVoltages(:,13:15)),2)
rms(abs(R1.PhaseVoltages(:,13:15)),2) rms(abs(R1.PhaseVoltages(:,16:18)),2)
rms(abs(R1.PhaseVoltages(:,16:18)),2) rms(abs(R1.PhaseVoltages(:,19:21)),2)
rms(abs(R1.PhaseVoltages(:,19:21)),2) rms(abs(R1.PhaseVoltages(:,22:24)),2)
rms(abs(R1.PhaseVoltages(:,22:24)),2)]'./(11000/sqrt(3)));
createfigure7(pxcs);
figure
contour(pev);
createfigure3(linspace(0,1440,1440), abs(R2.PhaseVoltages)./230);
createfigure4(linspace(0,1440,1440), R3.voltageUnbalance);
createfigure4(linspace(0,1440,1440), R2.voltageUnbalance);
createfigure3(linspace(0,1440,1440), abs(R3.PhaseVoltages)./ 230);
createfigure8(30*[R1.TransformerLoading1 R5.TransformerLoading1]);
createfigure3(linspace(0,1440,1440), abs(R2.PhaseCurrents)./292);
createfigure4(linspace(0,1440,1440), R2.TransformerLoading2);
createfigure4(linspace(0,1440,1440), R3.TransformerLoading2);
createfigure3(linspace(0,1440,1440), abs(R3.PhaseCurrents)./292);

```

## Appendix E: The Top-Level Code of the Decentralized Controller

The decentralized control algorithm was written in MATLAB for adjusting the EV and HP loads, as shown below.

```

% EV charging loads are modelled based on the TS
% where TS is the arrival/departure time of daily trips
load TS
pev1=PEVs(82, TS);
% Their initial Battery State-of-Charge (BSOC) levels are calculated using the
following function
soc1=BSOC(pev1);
% HP heating loads are generated based on ambient tempratures
load temp
[php1,T,cop]=PHPs(82,temp,0.613,28,20,20,1.57);
% where temp is ambinet temprature

```

```

% 0.613 is the air denisty
% 28 is the HP supply temprature
% 20 is the HP return temprature
% 1.57 is the value of thermal resistivty
% T is the updated indoor tempratures of HP houses
% php is the HP heating demand over a day
% cop is the coffeicient of performance for each HP

% Time-varying tariffs are generated using a nonlinear mathematical, which
% was solved using generalised reduced gradinet solver and stored in f
load f

% Optimization using mixed integer linear programming
% 82 EV charging loads are adjusted using the following script
tic
ph=sum(pev1,2);
intcon=96;
pevs=pev1;
[n1,n2]=size(pevs);
pes1=sum(pevs,2);
pev2=zeros(n1,96);
lb=zeros(1,96);
for i=1:n1
    pev2(i,:)=optmfun(intcon,lb,pevs(i,:));
end
toc
soc2=BSOC(pev2);
% HP heating loads are also adjusted using mixed integer linear
% programming and the results of optimization were saved in php2 and T2
load php2
load T2
% Unbalnced Power Flows are evaluted with and without optimization
% p is the residential loads of 330 customers
% z is the impedance matrix of the network under study
load p
load z
[vrt1, vuf1, Itx1]=NetConst(z,p,pev1,php1);
[vrt2, vuf2, Itx2]=NetConst(z,p,pev2,php2);

% Figures
figure
[hAx,~,~]=plotyy(linspace(0,24,96), pev1([15 46],:),linspace(0,24,96), soc1([15
46],:));
ylabel(hAx(2),'Battery State-of-Charge (BSOC), %');
figure
[hAx1,~,~]=plotyy(linspace(0,24,96), [php1(:,15) cop(:,15)],linspace(0,24,96),
T(:,15));
ylabel(hAx1(2),'Temperature, °C');
figure
[hAx2,~,~]=plotyy(linspace(0,24,96),php2,linspace(0,24,96),f);
createfigure1(linspace(0,24,96),[pev2; mean(pev2)], f);

```